THE EFFECTS OF OCEAN ACIDIFICATION ON GROWTH, PHOTOSYNTHESIS, AND DOMOIC ACID PRODUCTION BY THE TOXIGENIC DIATOM *PSEUDO-NITZSCHIA AUSTRALIS*

A thesis submitted to the faculty of
San Francisco State University
In partial fulfillment of
the requirements for
the Degree

Master of Science

In

Biology: Marine Biology

by

Charles Johann Wingert

San Francisco, California

May 2017

CERTIFICATION OF APPROVAL

I certify that I have read *The Effects of Ocean Acidification on Growth, Photosynthesis, and Domoic Acid Production by the Toxigenic Diatom Pseudo-nitzschia australis* by Charles Johann Wingert, and that in my opinion this work meets the criteria for approving a thesis submitted in partial fulfillment of the requirement for the degree Master of Science in Biology: Marine Biology at San Francisco State University.

William P. Cochlan, Ph.D.
Senior Research Scientist, RTC
Research Professor of Biology, SFSU

Tomoko Komada, Ph.D.
Senior Research Scientist, RTC
Professor of Chemistry, SFSU

Vera L. Trainer, Ph.D.
Supervisory Research Oceanographer
NOAA Northwest Fisheries Science Center

THE EFFECTS OF OCEAN ACIDIFICATION ON GROWTH, PHOTOSYNTHESIS, AND DOMOIC ACID PRODUCTION BY THE TOXIGENIC DIATOM *PSEUDO-NITZSCHIA AUSTRALIS*

Charles Johann Wingert
San Francisco, California
2017

A northern California strain of *Pseudo-nitzschia australis* was examined using non-axenic, batch cultures to examine the effects of more acidic conditions (reduced pH due to increased pCO_2) on the growth, photosynthesis, and domoic acid production of this toxigenic diatom. Specific growth rates at the lowest pH tested (7.8) were 30 percent lower than the other three pH treatments (8.1, 8.0, 7.9). Macronutrient drawdown ratios of Si:N and Si:P decreased linearly with declining pH. Maximum rates of photosynthesis per cell were significantly elevated in the two lowest pH treatments relative to the control pH of 8.1. Domoic acid (DA) was detected in all pH treatments during both the nutrient-replete exponential growth phase and the nutrient-deplete stationary growth phase. Total cellular DA did not significantly differ among pH treatments during exponential growth, but increased with decreasing pH and reached a maximum of 3.61 pg DA $\cdot$ $cell^{-1}$ during the stationary phase of growth.

I certify that the Abstract is a correct representation of the content of this thesis

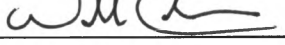

Chair, Thesis Committee

May 19, 2017

Date

ACKNOWLEDGEMENTS

The following thesis would never have come to fruition without the collective support and effort of many individuals. The patience, encouragement, and mentorship of my advisor, Dr. William Cochlan, was the backbone of this research project and I am eternally grateful and honored for the opportunity to have worked as a part of his laboratory. I would also like to thank my committee members Drs. Tomoko Komada and Vera Trainer for their insight and efforts provided while assisting me in my research, and reviewing this dissertation. I am extremely appreciative for the patient tutelage of Christopher Ikeda, Julian Herndon, and Brian Bill, who graciously taught me the laboratory skills and techniques that were utilized in the present work. A special thanks goes out to my lab mate, Bridget Hansen, who offered constant encouragement through the most difficult moments of this project. I would also like to thank Dr. Vera Trainer and Brian Bill for the time and resources they invested to help me analyze my domoic acid samples at the NOAA Northwest Fisheries Science Center, Drs. Raphael Kudela and Misty Peacock at the University of California Santa Cruz (UCSC) for their assistance running my DIC samples, and Dr. Mark Wells and Kathleen Thornton at the University of Maine for processing my POC/PON samples. Lastly, I would especially like to thank my entire family for their unwavering love and wisdom that supported me through my tenure as a graduate student—without you, none of this would have been possible. This research was supported by U.S. National Science Foundation (NSF).

TABLE OF CONTENTS

LIST OF TABLES

Table Page

Table Page

LIST OF FIGURES

Figures Page

Figures Page

Introduction

Changes in the Earth's climate are having profound effects on the chemistry and biology of the ocean. While the primary force is the anthropogenic release of atmospheric greenhouse gases and the resulting changes in global temperatures, critical secondary effects are the perturbations driven by increased absorption of CO_2 by the surface ocean (e.g., Feely et al. 2004; Jackson 2008; Hauri et al. 2013). Since the industrial revolution, the ocean has absorbed roughly 30 percent of the anthropogenically emitted CO_2, and currently CO_2 is dissolving into the World's ocean at rate of approximately 20-25 million tons per day (e.g., Doney et al. 2009, 2012; IPCC 2014). This process is driving a steady increase in the partial pressure of CO_2 (pCO_2) and a decrease in seawater pH – collectively termed ocean acidification (OA) – at a rate unprecedented in earth's recent geological history (Caldeira and Wickett 2003; IPCC 2014). Projections suggest that by the year 2100, average atmospheric CO_2 will increase between 720-1,020 ppm with the resultant decrease in surface ocean pH by 0.14-0.32 pH units (IPCC 2014). However, eastern boundary upwelling systems (EBUS), where CO_2-rich and nutrient-replete waters upwell to the surface, are already experiencing levels of OA not predicted for most surface waters until the end of the century; the accelerated decline in seawater pH has been unambiguously demonstrated in the upwelling regions off the coast of California (Feely et al. 2008, 2016).

Such coastal upwelling regions, representative of the classical short food chain, are generally based on the transfer of primary production to large copepods and finally to fish (Cushing 1971), and are assumed to be efficient in the transfer of 'new' nitrate-based primary production (*sensu* Dugdale and Goering 1967; Eppley and Peterson 1979) to higher trophic levels owing to the relative direct transfer of biomass (Parsons et al. 1984). The potential outcome of ocean acidification in these upwelling regions is magnified due to the key role they play in supporting the bulk of the world's fisheries, although how OA will impact the diatoms that make up the base of these efficient food chains is still unclear. Diatoms are particularly important not only in upwelling systems, but collectively ca. 40 percent of the World's oceanic primary production is the result of the photosynthetic activity of these microorganisms (Yang and Gao 2012). These photoautotrophs, through their assimilation of CO_2 and subsequent export of fixed carbon to deeper water play a critical role in in the global carbon cycle (Berner 2003; Riebesell et al. 2009). Given that CO_2 is a critical component of the photosynthetic process, the study of OA effects on phytoplankton has focused mainly on carbon acquisition. However, decreasing pH resulting from increased absorption of CO_2 also will directly affect cellular membrane potential, enzyme activity, and energy partitioning (Beardall and Raven 2004; Giordano et al. 2005), all of which will influence cell metabolism. The physiological impacts of OA on these primary producers will undoubtedly be reflected in the success of higher

trophic levels, and possibly commercially important marine fisheries needed to support humankind.

In an increasingly acidic ocean, it is likely that the biodiversity and species composition of phytoplankton communities will change, and certain species will be better adapted to thrive than others (Herve et al. 2012). Therefore, to understand the resultant effects on coastal ecosystems, it is imperative to investigate the impacts of OA, on the phytoplankton species that normally thrive in such environments, such as diatoms, and determine how or if OA will influence their growth and competitive success.

Today, marine diatoms are living in an ocean that contains relatively low concentrations of dissolved CO_2 compared to when they first evolved, 150-250 million years ago (Beardall and Raven 2004). As the biological availability of CO_2 has declined over time, many groups of phytoplankton, including diatoms, developed inorganic carbon concentrating mechanisms (CCMs) to support their photosynthetic requirements (Reinfelder 2011). For example, CCMs in most marine diatoms allow them to acquire and utilize bicarbonate (HCO_3^-) for photosynthesis, which, relative to CO_2, is the more prevalent source of dissolved inorganic carbon (DIC) in the modern ocean (e.g., Tortell et al. 2000, 2002, 2006). However, operating and maintaining CCMs requires cellular energy (ATP) and because of this, it has been suggested that many diatoms may theoretically benefit from an increase in the availability of dissolved CO_2, since this will likely free

additional energy for other cellular processes (e.g., Raven and Johnston 1991). To date, diatom studies have observed a mix of positive, neutral, and negative growth and photosynthetic responses for diatoms when cultured under elevated CO_2 concentrations; physiological responses that vary as a function of species and even strain. For example *Phaeodactylum tricornutum* (Wu et al. 2010), *Pseudo-nitzschia multiseries* (Sun et al. 2011), *P. fraudulenta* (Tatters et al. 2012) and *Thalassiosira pseudonana* (McCarthy et al. 2012; Yang and Gao 2012) all increased their specific growth rates when maintained at elevated CO_2 concentrations (low pH), and different strains of *T. pseudonana* increased their maximum photosynthetic rates by 17 to 25% (Sobrino et al. 2008; Yang and Gao 2012). Neutral physiological responses to increased CO_2 have been observed for two *Chaetoceros* species including *C. muelleri* (Ihnken et al. 2011), *C. brevis* (Boelen et al. 2011), and a different strain of *T. pseudonana* (Crawfurd et al. 2011), whereas, decreased rates of growth and/or photosynthesis have been measured for cultures of *Skeletonema costatum* (Chen and Gao 2004), *T. pseudonana* (Sobrino et al. 2008), and *P. tricornutum* (Wu et al. 2010) when maintained at elevated pCO_2.

Some phytoplankton, including certain pennate diatoms, are capable of producing potent neurotoxic compounds, which when generated in sufficient concentrations can impact entire marine ecosystems. Such toxin-producing phytoplankton are commonly referred to as harmful algal bloom (HAB) species,

since they often pose a potentially serious risk to the health humans, wildlife, and economically important fisheries supported by these marine ecosystems. In the last few decades, reports on the occurrence and intensity of such HAB events have increased around the globe (e.g., Anderson et al. 2008; Hallegraeff 2010). Although the reasons for these observed trends are not clear, environmental factors such as eutrophication, warming sea surface temperatures, and other anthropogenic influences, such as OA, have been suggested as contributing factors (e.g., Fu et al. 2012; Wells et al. 2015).

Diatoms of the globally distributed genus *Pseudo-nitzschia* Pergallo (Heterokonta, Bacillariophycea) are capable of generating domoic acid (DA), a potent neurotoxic amino acid, which is responsible for amnesic shellfish poisoning (ASP) in humans, and can impact both marine mammals and birds (Bates et al. 1989; Wright et al. 1989). In California, thousands marine mammal and seabird deaths have been attributed to DA, as a consequence of their consumption of DA-contaminated prey. Along the entire west coast of the United States, seasonal closures of commercial and recreational fisheries have become more common due to the increased frequency of these DA toxic events (Lelong et al. 2012; Trainer et al. 2012). In the spring and summer of 2015, an unprecedented HAB of toxigenic *Pseudo-nitzschia* stretched from Santa Barbara, California to southeastern Alaska. This HAB impacted major commercial and recreational fisheries in California, Oregon and Washington in 2015 and 2016, including Dungeness crab and rock

crab, and led to multiple prolonged fishery closures and health advisories, resulting in severe economic losses in all three states (e.g., California Ocean Science Trust 2016; Du et al. 2016; McCabe et al. 2016).

Of the 37 described species within the *Pseudo-nitzschia* genus, only 14-15 species have been confirmed to produce DA, but blooms of these particular species do not always result in significant DA production (cf. reviews by Lelong et al. 2012; Trainer et al. 2012). Due to the potential harm that these diatoms can impose on coastal marine ecosystems and their resultant impact on commercial fisheries and human health, there has been considerable interest in elucidating the environmental factors responsible for stimulating or enhancing DA production in these toxigenic species.

The trophic transfer of DA begins with its accumulation within the digestive tract of filter-feeding bivalves (e.g., clams, mussels, oysters) and/or planktivorous fin fish, such as anchovies or sardines, when they consume *Pseudo-nitzschia* cells containing DA. Most of the toxin is concentrated in the viscera of these filter-feeders but does not get absorbed to their surrounding tissues because DA is a water-soluble, hydrophilic molecule. As a result, DA can be expelled from many of these organisms rather quickly, once a toxic bloom has subsided in a process termed depuration (Trainer et al. 2012). However, these primary consumers do not appear to collect DA that is dissolved within the surrounding seawater. Thus, the trophic transfer of DA occurs when toxic *Pseudo-nitzschia*

cells are first concentrated in the digestive systems of primary filter-feeding consumers, which are then eaten by secondary consumers. It is interesting to note that in general, the physiology of bivalves is not negatively impacted by ingesting toxic *Pseudo-nitzschia,* and this lack of susceptibility is most likely due to the simplicity of their nervous systems, relative to both mammals and birds (Lelong et al. 2012).

Since the first documented ASP event in 1987 off Prince Edward Island, Canada, which resulted in the deaths of three people and the illness of hundreds more, monitoring programs for *Pseudo-nitzschia* and DA have been successfully implemented around the globe (e.g., Trainer et al. 2012). However, the environmental factors responsible for stimulating DA production in *Pseudo-nitzschia* are still not fully understood. Field and laboratory studies have identified a variety of possible toxin promoters, including the phase of cellular growth (cf. reviews by Bates 1998; Pan et al. 1998), macronutrient limitation (e.g., Bates et al. 1991, 1996, 1998), high (Lundholm et al. 2004; Trimborn et al. 2008) and low pH (Sun et al. 2011; Tatters et al. 2012), the bioavailability of important trace metals such as iron (Fe) (e.g., Maldonado et al. 2002; Wells et al. 2005; Trick et al. 2010), and the different nitrogen substrates used to support growth (e.g., Howard et al. 2007; Cochlan et al. 2008; Thessen et al. 2009; Auro and Cochlan 2013). Despite these important findings, until the full biosynthetic pathway of DA is mapped, it

will be difficult to conclusively determine the most influential environmental factors responsible for enhancing DA production in *Pseudo-nitzschia*.

As anthropogenic CO_2 emissions continue to fuel OA, it is critically important for the scientific community to understand how the physiology of HAB-forming species such as *Pseudo-nitzschia,* which can dominate coastal phytoplankton communities, may shift in response to the ongoing changes within their environment – specifically, the increase in CO_2 availability and the resultant reduction in seawater pH. Presently, there are only a few published studies that have examined these factors with respect to either the growth or toxicity of the various species of *Pseudo-nitzschia*. Some experiments show 2-3 fold increases in cellular DA concentrations under elevated pCO_2 (reduced pH levels) when cultures were either P- (*P. multiseries*; Sun et al. 2011) or Si-limited (*P. fraudulenta*; Tatters et al. 2012), and these authors suggest that increased availability of inorganic carbon may be mechanistically responsible. However, other studies using different methodologies and strains of *P. multiseries*, found that cellular toxicity increased up to 70-fold at elevated, not reduced pH levels (Lundholm et al. 2004; Trimborn et al. 2008). The relationship between seawater pH and exponential growth rate is equally confusing, where culture studies have shown that reduced pH resulted in increased (Sun et al. 2011; Tatters et al. 2012), decreased (Lundholm et al. 2004) or no change in specific growth rate (Cho et al. 2001) depending on the species of *Pseudo-nitzschia* and the experimental

conditions employed. With respect to photosynthesis, Sun et al. (2011) found that increased pCO_2 resulted in significantly higher carbon fixation rates in *P. multiseries* for both P-limited and P-replete cultures. These few studies represent the only research conducted to date, which have examined the effects of pH/pCO_2 on the physiology and DA toxin production of *Pseudo-nitzschia*. Clearly, there is a need for additional research if we are to gain a better understanding of how these toxigenic organisms may respond to a future, more acidic ocean, and their resultant effects on the health of impacted marine ecosystems.

The research presented here examines the effects of reduced pH, resulting from increased availability of dissolved CO_2, on the rates of cellular growth, photosynthesis and nutrient (nitrate [NO_3^-], silicate [$Si(OH)_4$], and orthophosphate [PO_4^{3-}]) utilization, as well as cellular elemental (carbon and nitrogen) composition, and DA production by the pennate diatom *Pseudo-nitzschia australis*. The aim of this study is to obtain this basic physiological information, in order to contribute towards a better understanding of how this HAB species responds to present and future pH conditions in the coastal ocean. This is the first study to assess the physiological performance of this toxigenic diatom to potential future conditions of ocean acidification.

Methods

In this laboratory study of *Pseudo-nitzschia australis*, culturing conditions were first optimized during preliminary experiments performed at present day CO_2 concentrations, and *in vivo* measures were employed to estimate growth as a function of time. Following these initial experiments, a series of more complex batch culture experiments were conducted where growth, photosynthesis and toxin production were measured at current and elevated CO_2 concentrations.

I. *Preliminary Experiment*:

A preliminary experiment was performed to determine the saturating photosynthetic photon flux density (PPFD) for the growth of *P. australis* (i.e., the PPFD where growth is no longer limited by its availability) when maintained under the desired experimental conditions. A toxigenic strain of *P. australis* (HAB 327b, isolated in April, 2014 from offshore of San Pedro, CA, USA by H.A. Bowers) was grown in enriched filter-sterilized (0.2-µm, PolyCap® TC filter, Whatman Corp.) natural coastal seawater (obtained from Bodega Marine Laboratory, Bodega Bay, CA, USA). The seawater was enriched with ESNW medium (Harrison et al. 1980; Berges et al. 2001 and subsequent Corrigendum 2004) as outlined by Cochlan et al. (2008) with the following modifications: silicic acid, nitrate, and orthophosphate were added at initial concentrations of 100, 200, and 20 µmol $\cdot$ L^{-1}, respectively. Cultures were unialgal, but not axenic and were

grown in duplicate (n = 2), 50-mL borosilicate round-bottom test tubes (equipped with polytetrafluoroethylene [PTFE] caps), at eight PPFDs: 25, 37, 60, 90, 110, 140, 190, 265 μmol photons $\cdot$ m^{-2} $\cdot$ s^{-1}). The PPFDs were chosen based on previous research performed with this species (Cochlan et al. 2008; Auro and Cochlan 2013; Bill 2011), and were measured using a 4π collector (QSL-100 quantum scalar irradiance meter, Biospherical Instruments Inc.) immersed within medium-filled culture tubes, which were wrapped in various combinations of neutral density plastic film (LEE Filters, Burbank, CA, USA) to achieve the desired range of experimental PPFD conditions. All cultures were arranged in pre-determined positions within a temperature-controlled environmental test chamber (Sanyo MLR-352H) maintained at an ambient temperature of 13°C (± 0.5°C). Light within the chamber was provided on a 14:10 h L:D cycle from banks of white fluorescent bulbs (Mitsubishi FL40SS-W/37). Stock cultures used for inoculations were grown at 13°C in 50-mL sterile, polystyrene tissue culture flasks (BD Falcon™, Becton Dickinson Bioscience) equipped with vented caps and provided a PPFD of 125 μmol photons m^{-2} s^{-1} on a 14:10 L:D cycle. All glassware and tubing used for culturing were initially soaked in deionized (DI) water with a mild detergent (Contrad® 70, Decon Labs Inc.), then soaked in weak HCl acid (10% v/v), rinsed thoroughly with ultra-pure water (18.2 MΩ-cm Milli-Q®, Millipore Inc.), and autoclaved prior to use.

The specific growth rates at each PPFD were determined from twice daily (10:00 and 18:00) measurements of *in vivo* fluorescence (Tuner AU-10 fluorometer) until fluorescence values began to peak, indicating the cells were no longer growing exponentially and had entered their stationary growth phase. Each culture tube was mixed by gentle inversion immediately before *in vivo* fluorescence was measured by inserting the tube directly into the fluorometer (Brand and Guillard 1981). Cultures were allowed to acclimate to the experimental conditions for one batch cycle (ca. 6 days) at each PPFD before being transferred to fresh media and subsequently grown for one additional batch cycle (ca. 6 days). Specific growth rates were calculated from a least-squares linear regression analysis of the exponential growth phase, determined from plots of the natural log of *in vivo* fluorescence versus time, and using the exponential growth equation (Guillard 1973):

$$\mu = \frac{\ln(N_1 / N_0)}{t_1 - t_0} \tag{1.1}$$

where μ is the exponential growth rate (d^{-1}), and N_1 and N_0 are the relative fluorescence units (RFU) from *in vivo* fluorescence measurements at time 1 (t_1) and time 0 (t_0), respectively. During the primary experiment, samples were collected for determination of cell densities, which were used for determination of specific growth rates reported in this study (see below).

II. Primary Experiment—*Cultures and Growth Conditions*:

A toxigenic strain of *P. australis* (HAB 200, isolated in April, 2015 from Santa Cruz Wharf, CA, USA by H.A. Bowers) was grown under controlled laboratory conditions to quantify the effects of pH on the rates of growth and photosynthesis, as well as DA production. Unialgal, but not axenic batch cultures were grown in 4.0 L of filter-sterilized (0.2-µm, PolyCap® TC filter, Whatman Corp.) natural coastal seawater enriched with nutrients, vitamins and metals as described above. Macronutrient concentrations were chosen in order to achieve culture biomass levels closely resembling those commonly observed during intense blooms in the natural environment. Media was prepared at least two days prior to use, and pH and temperature adjusted (see below for details) prior to sterile filtration and cellular inoculation. Cultures were maintained in acid-cleaned, autoclaved 6.0-L Pyrex® glass boiler flasks, equipped with custom-made silicon stoppers to accommodate gas lines and sampling ports. Each culture was continuously mixed using a magnetic stir bar assembly (ca. 60 rpm) to facilitate the suspension of cells within the medium. Temperature-controlled environmental test chambers (Sanyo MLR-352H) maintained the culture vessels at an ambient temperature of 13°C (± 0.5°C), and provided light on a 14:10 h light:dark cycle using banks of white fluorescent bulbs (Mitsubishi FL40SS-W/37) at a saturating PPFD of 240 µmol photons $\cdot$ m^{-2} $\cdot$ s^{-1}.

III. *Experimental Outline and Growth Rate Measurements*:

A series of batch culture experiments were conducted to assess the physiological response of *P. australis* (HAB 200) at current and reduced pH levels controlled by CO_2 concentration. *Pseudo-nitzschia australis* was grown under four pH levels, each conducted in triplicate (n = 3): ambient pH = 8.1 (current global average at the sea surface) and low pH = 8.0, 7.9, 7.8 (currently observed in some regions of the California EBUS), using a pH/CO_2 monitoring and control system (Loligo® Systems) that uses bubbled CO_2 (15% mixture with ambient air; Praxair, USA) to maintain the desired pH conditions (see below for details). Whole culture samples were collected for estimation of exponential growth rates at daily intervals, and also at specific times within the cellular growth phase for determination of photosynthetic performance, elemental composition, and toxicity. These sampling periods (hereafter referred to as 'major sampling' times) correspond to the nutrient-replete, exponential growth phase (where cellular growth is maximal, but toxicity is expected to be low), and the nutrient-depleted, stationary phase (where growth is minimal, but cellular toxicity is expected to be maximal). Major sampling during the exponential growth phase occurred on days 4 (pH 8.1 and 7.9) and 5 (pH 8.0 and 7.8) of each treatment's batch cycle, while major sampling during the stationary growth phase occurred on days 7 (pH 8.1), 8 (pH 8.0 and 7.9), and 9 (pH 7.8). The major sampling periods in the stationary

phase were always two days after the peak RFU values measured during the late exponential growth phase.

Individual 'starter' cultures (n = 1) were acclimated to each pH condition for a minimum of three consecutive batch cycles (15-16 d in duration and equivalent to 25-30 generations) before being split into triplicate (n = 3) cultures for the fourth experimental batch cycle where detailed sampling and measurements were performed. Prior to initiation of the fourth experimental culturing phase, it was confirmed that the exponential growth rates of the individual acclimation cultures for each pH treatment did not vary (< 10% variation) for three consecutive batch cycles. Growth rates were estimated from daily sampling of *in vivo* fluorescence (Turner Designs 10-AU fluorometer) and microscopic cell counts using a 1-mL gridded Sedgewick-Rafter chamber and an inverted microscope (Olympus model IX83) equipped with a differential interference contrast system. A minimum of 1,000 cells were counted for each sample to ensure reliable abundance estimates; 1,000 counts per sample yields estimates of total cell abundance with an accuracy (95% confidence limit) between ± 5 and ± 10% (Guillard and Sieracki 2005). For cell counts, whole culture samples (1.5 mL) from each treatment were preserved with acidic Lugol's solution (2.5% v/v final concentration) and stored in the dark at ca. 5°C until analyzed. Specific growth rates were calculated as described above, however, only cell-specific growth rates

were reported since *in vivo* fluorescence measurements were used primarily as a means to quickly monitor cultures during the primary experiment.

IV. *Seawater Carbonate System Measurements*:

In order to maintain the desired experimental pH levels, each culture was gently bubbled with 0.2-µm filtered 15% CO_2/air gas mixture using a computer controlled pH/pCO_2 STAT regulation system (Loligo® Systems). This automatic feed-back system consists of a pH probe (Sentix® 41-3; Wissenschaftlich-Technische Werkstatten [WTW]) within each culture flask connected to a pH meter (model 3310, WTW), and monitored by a PC computer (equipped with CapCTRL software, version 1.3.2) interfaced with a 4-channel gas control instrument (DAQ-M) that controls solenoid valves to inject commercially prepared compressed CO_2/air mixture (15% v/v; Praxair Gas) directly into the media of the individual culture flasks through a Pyrex® course-fritted, glass dispersion tube (part 39533-12EC; Corning Inc.). Using this system (illustrated in Figure 1), the pH in each culture vessel was continuously monitored throughout the experiment. When pH increased above 0.05 pH units from the desired experimental level, due to biological activity such as photosynthesis, the automated system opened an associated solenoid valve in the air-line, allowing the filtered CO_2 to be gently bubbled into the culture via a submerged glass diffuser, suspended from the vessel's silicone stopper. Once pH dropped to the desired experimental level, the

automated system would then close the associated solenoid valve and cease the flow of CO_2. The air-line of each culture was also equipped with a dedicated flow meter set at a rate of ca. 5.3 mL min^{-1} (Cole-Parmer®), which provided greater control of CO_2 injection. All pH measurements in this study are presented on the National Bureau of Standards (NBS)/National Institute of Standards and Technology (NIST) scale. The glass pH probes were calibrated (3-point calibration) at the beginning of every batch cycle using NBS/NIST-traceable buffer solutions (Fisher color-coded certified standard buffer solutions; pH 4.00, 7.00, and 10.00; Catalog No. SB105).

Samples (60 mL) for total dissolved inorganic carbon (DIC) were taken by syringe filtering of culture through pre-combusted (5 hours, 450°C) 25-mm diameter, glass-fiber filters (GF/F, Whatman®), into pre-combusted 20-mL borosilicate scintillation vials (Fisher Scientific), freed of air bubbles, and preserved with 0.20 mL of 5% mercuric chloride ($HgCl_2$). Samples were sealed and stored at ca. 5°C until analyzed for total DIC using a Shimadzu TOC-Vcsh analyzer equipped with auto sampler (ASI-V). Using this instrument, samples were acidified and sparged with a carrier gas (purified air), which converted the DIC pool in the sample to CO_2, where the gas was quantified by a non-dispersive infrared detector. Carbonate chemistry parameters were calculated from DIC, pH, silicate, orthophosphate, temperature, and salinity measurements using the software program CO2Sys (Lewis and Wallace 1998) with dissociation constants

for carbonic acid refitted by Dickson and Millero (1987). Measured and calculated parameters are provided in Tables 2 and 3.

V. *Analysis of Macronutrient Drawdowns*:

Samples (12 mL) for nitrate plus nitrite (NO_3^- + NO_2^-), orthophosphate (PO_4^{3-}), and silicate ($Si[OH]_4$) were collected at the same time (ca. 12:00 h) each day and gently filtered through Whatman® GF/F filters into 15-mL polypropylene conical tubes (BD Falcon™, Becton Dickinson Bioscience), previously soaked in Milli-Q® ultra-pure water for at least 24 h, and stored frozen (-10°C) until analysis. Samples were allowed to thaw overnight before being analyzed using a Lachat Instruments automated ion analyzer (8000 series; Hach Co.), following the colorimetric methods of Smith and Bogren (2001) for NO_3^- + NO_2^- (hereafter referred to as simply nitrate [NO_3^-]), Knepel and Bogren (2002) for PO_4^{3-}, and Wolters (2002) for $Si(OH)_4$. Macronutrient drawdown rates, determined from their disappearance in the culture media over time, were calculated by dividing the difference in nutrient concentration in successive samples by the length of the time interval (ca. 1 day). Daily drawdown ratios of the three macronutrients were then quantified and averaged for every biological replicate within a pH treatment (n = 3). Additional macronutrient samples were collected from each culture at the time of major sampling during both the nutrient-replete, exponential growth phase, and the nutrient-depleted, stationary growth phase. These additional samples were

used, in conjunction with DIC, pH, temperature, and salinity measurements, to calculate the parameters of the seawater carbonate system.

VI. *Photosynthesis vs. Irradiance (P-E) Curves and Cellular Fluorescence Capacity (F_v/F_m):*

Photosynthetic rates were determined by the ability of *P. australis* to incorporate inorganic ^{14}C isotope into organic C as a function of PPFD. These photosynthesis versus irradiance (P-E) measurements were conducted with samples collected during the nutrient-replete, exponential growth phase, and quantified using a temperature-controlled photosynthetron, equipped with white (halogen) light at 16 PPFDs between 0 and 1,000 μmol photons $\cdot$ m^{-2} $\cdot$ s^{-1}. Whole culture samples (5 mL per sub-sample at each PPFD) were inoculated with 4.5 μCi of $NaH^{14}CO_3$ (72 μCi total per triplicate), and incubated for 30 min within 25-mL glass scintillation vials (Fisher Scientific). The $NaH^{14}CO_3$ (PerkinElmer; initial concentration = 1 mCi $\cdot$ mL^{-1}) was pre-mixed with un-enriched sterile-filtered artificial seawater prior to inoculations (working stock = 0.11 mCi $\cdot$ mL^{-1}). Thirty-minute incubations were terminated by acidification of each sub-sample with 0.5 mL of 10% HCl (v/v), and allowed to degas for ca. 24 hours prior to the addition of 15 mL of scintillation fluid (EcoLume™, MP Biomedicals LLC). Samples were subsequently mixed by gentle inversion, allowed to sit undisturbed overnight for >12 hours, and radio-assayed using a Wallac 1414 liquid scintillation

counter (PerkinElmer Guardian™). All ^{14}C uptake rates were corrected for dark uptake. P-E curves were generated using a non-linear, least-squares regression technique (KaleidaGraph©; Synergy Software) and rate estimates of photosynthesis, normalized to cell number, chlorophyll *a* (Chl *a*), particulate carbon (PC), were fitted to the three-parameter P-E model of Platt and Gallegos (1980), as follows:

$$P^B = P_s^B(1 - e^{\frac{-\alpha \cdot E}{P_s^B}})(e^{\frac{-\beta \cdot E}{P_s^B}}) \quad (1.2)$$

where P^B is the biomass-specific rate of photosynthesis (i.e., inorganic carbon uptake rate) at irradiance E, α is the light-limited initial slope (i.e., photosynthetic efficiency), β describes the effects of photoinhibition at high PPFD, and P_s^B is the maximum theoretical photosynthetic rate in the absence of photoinhibition (i.e., $\beta = 0$). The maximum carbon uptake rate observed (P_m^B) is equivalent to P_s^B when $\beta = 0$. Otherwise:

$$P_m^B = P_s^B \left(\frac{\alpha}{\alpha+\beta}\right)\left(\frac{\beta}{\alpha+\beta}\right)^{\frac{\beta}{\alpha}} \quad (1.3)$$

The light saturation coefficient, or index of photoadaptaion (E_k), was calculated as P_m^B/α and is defined as the PPFD where the extrapolation of α and P_m^B intersect. A summary of the photosynthetic parameters is given in Table 1.

The *in vivo* cellular fluorescence capacity (F_v/F_m) of cultures was measured in 8-mL sub-samples using a Turner AU-10 fluorometer, and calculated as the ratio of variable (F_v) to maximum (F_m) fluorescence for dark-adapted (10 min.) cells using the 3-[3,4-dichlorophenyl]-1,1-dimethylurea (DCMU) technique (Vincent 1980; Parkhill et al. 2001).

VII. *Domoic Acid (DA) Analysis*:

Samples for particulate (pDA) and dissolved (dDA) DA concentrations were collected during the exponential growth phase and nutrient-deplete stationary growth phase for all cultures. These samples were analyzed using an indirect, competitive enzyme-linked immunosorbent assay (cELISA; Garthwaite et al. 1998), which uses flat-bottomed, 96-well polystyrene microtiter plates, pre-coated with DA-carboxy-linked BSA conjugate (Beacon Analytical Systems Inc., item # 20-0249). The DA antibody used for cELISA analysis was produced by NOAA-Northwest Fisheries Science Center via rabbit immunizations with DA-amine linked conjugate. Triplicate samples were filtered from each of the biological triplicate cultures conducted for the four pH treatments (i.e., 4 pH treatments x 3 replicate cultures x 3 pDA and 3 dDA samples) at each of the two major sampling

times. Samples (2.5, 5, and/or 10-mL) collected for pDA were filtered onto 0.45-μm pore size, 25-mm diameter, MF Millipore™ membrane filters (HAWP025), which were stored in 15-mL polypropylene centrifuge tubes (BD Falcon™, Becton Dickinson Bioscience) and frozen (-20°C) until analysis. For pDA extraction, 4 mL of Milli-Q® water was added to each sample tube, which was vortexed for 10 seconds (to release cells from the filter), placed in a bath sonicator (Branson, model #5510) for 1 hour (to lyse cells), vortexed again, and refrigerated overnight (4°C). The following morning, samples were centrifuged at 8,500xg for 15 minutes before aliquots were taken for cELISA analysis. For dDA collection, a 1.5-mL sub-sample of filtrate from each major sampling event was collected in a 2-mL polypropylene micro-centrifuge tubes (Fisher Scientific) and stored frozen (-20°C) until assayed. Absorbance was read at 450 nm using a microplate reader (Versamax™, Molecular Devices Inc.) and DA concentrations of experimental samples were calculated based on the interpolation from a standard curve with known concentrations of DA (Beacon Analytical Systems Inc.) ranging from 0.001 ng mL^{-1} to 10.000 ng mL^{-1} using a non-linear four parameter logistic curve fit model (limit of quantification = 0.02 ng mL^{-1}).

The terminology for describing DA production can be confusing. Here both particulate and dissolved DA concentrations are routinely normalized to the cell density (cells · mL^{-1}) of *P. australis* at the time of sampling, and are referred to as DA (or toxin) cell quotas for consistency with previously published studies.

Total DA quotas refer to the sum of particulate DA and dissolved DA (pDA + dDA). However, it should be noted that only particulate DA, when normalized to cell abundance, is truly cellular DA (or cellular toxicity) since dissolved DA is, by definition, found outside of the cell and is located within the surrounding medium.

VIII. *Analysis of Particulate Carbon and Nitrogen (PC, PN) and Chlorophyll a (Chl a):*

For analysis of particulate carbon and nitrogen (PC, PN) concentrations, 10 mL of whole culture samples were filtered onto pre-combusted (5 hours, 450°C) Whatman® 25-mm diameter glass microfiber filters (GF/F), placed onto pre-combusted aluminum foil, and stored inside acid-cleaned, plastic petri-dishes (Millipore, USA), which were then frozen (-20°C) until analyzed using a CHN elemental analyzer (PerkinElmer 2400 series II CHNS/O).

Chlorophyll *a* (Chl *a*) concentrations were determined from 10 mL of filtered culture samples (Whatman® 25-mm diameter GF/Fs) using *in vitro* fluorometry. Samples were extracted in 90% (v/v) acetone for approximately 24 h in the dark at -20°C and then analyzed with a Turner Designs Trilogy fluorometer, equipped with optical kit #7200-046) and following the non-acidification method of Welschmeyer (1994).

For both PC, PN and Chl *a*, triplicate samples were filtered from each of the biological triplicate cultures maintained at the four pH treatments, at the two

major sampling times during the exponential and stationary phases of cellular growth.

IX. *Statistical Analysis*:

To ensure statistical differences were detectable, biological replicates (minimum of triplicates) were conducted at each of the four pH treatments. Statistical differences between cell growth rates, the estimated photosynthetic parameters, nutrient-drawdown rates, elemental composition, and toxin production at current and elevated dissolved CO_2 concentrations were determined using a one-way analysis of variance (ANOVA). Differences between pH treatments were determined using Tukey's HSD multiple comparisons test and the resulting *q*- and *p*-values, for particular physiological measurements, can be found in Tables 11-20. Data were normally distributed, as determined by the Shapiro-Wilk test, thus permitting the use of parametric statistical analyses. The level of significance (α) was set to 0.05 for all statistical tests employed in this study. All statistical analyses were conducted using KaleidaGraph© (Synergy Software, Reading, PA, USA).

Results

I. *Preliminary Experiment*:

Specific growth rates (μ) for non-axenic cultures of *P. australis* (HAB 327B), maintained at 13°C, began to plateau at the PPFD of 140 μmol photons • m^{-2} • s^{-1} (0.72 ± 0.03 d^{-1}), but reached a maximum specific growth rate of 0.74 ± 0.02 d^{-1} at the optimal PPFD of 190 μmol photons • m^{-2} • s^{-1} (Figure. 2). At the lowest PPFD tested (25 μmol photons • m^{-2} • s^{-1}), the growth rates were ca. 46% lower than the maximum specific growth rate.

II. *Primary Experiment —Exponential Growth Rates*:

The specific growth rates of non-axenic cultures of *P. australis* (strain HAB 200) during the nutrient-replete exponential phase did not differ significantly from each other at the three higher pH levels tested. Cultures maintained at pH 8.1, 8.0 and 7.9 supported average specific growth rates of 1.33 ± 0.02 d^{-1}, 1.26 ± 0.03 d^{-1}, and 1.30 ± 0.02 d^{-1} respectively, and were not significantly different from each other (Figure 3; 8.1 vs. 8.0: $p = 0.12$; 8.1 vs. 7.9: $p = 0.70$; 8.0 vs. 7.9: $p = 0.48$). However, the average growth rate of cultures maintained at pH 7.8 (μ = 0.95 ± 0.04 d^{-1}) was ca. 30% lower than the growth rates experienced at the three higher pH treatments, and statistically different from them based on one-way analysis of variance and Tukey's HSD test (Figure 3; 8.1 vs. 7.8: $p < 0.0001$; 8.0 vs. 7.8: $p < 0.0001$; 7.9 vs 7.8: $p < 0.0001$).

III. *Macronutrient Drawdown Rates and Ratios*:

Ambient concentrations of $Si(OH)_4$. (34.0 µmol L^{-1}) and NO_3^- (21.4 µmol L^{-1}) in the un-enriched seawater used for making the culture medium were greater than expected, which resulted in greater initial concentrations of both nutrients in the medium used for culturing *P. australis* (Figure 4). However, concentrations of both $Si(OH)_4$ and NO_3^- were depleted from the cultures for ca. 2 days before the final sampling in all pH treatments during the stationary period (Figure 4). Conversely, PO_4^{3-} was never depleted from cultures in any of the pH treatments, since the drawdown of PO_4^{3-} essentially ceased once cultures entered stationary growth induced by $Si(OH)_4$ and/or NO_3^- depletion (Figure 4-5).

Linear regression analysis of the average ratio of $Si(OH)_4$ to NO_3^- (Si:N) drawdown rates reveal a significant linear relationship with decreasing pH (Figure 6A; $r^2 = 0.99$, $p = 0.007$). Cultures grown at pH 8.1 have a significantly higher Si:N drawdown rate compared to those maintained at both pH 7.9 and 7.8 (Figure 6A; 8.1 vs. 7.9: $p = 0.03$; 8.1 vs. 7.8: $p = 0.004$), but no significant differences were found in the Si:N drawdown rates between the three lower pH treatments of 8.0, 7.9, and 7.8. Average drawdown rates of $Si(OH)_4$ and NO_3^-, normalized to cell density (nM · $cell^{-1}$ · d^{-1}; Figure 7A-B), illustrate that $Si(OH)_4$ uptake decreased slightly as pH declined whereas NO_3^- uptake increased, although there was a slight drop in NO_3^- uptake at pH 7.8. However, there were no statistically

significant differences detected for cell-normalized daily drawdown rates of either $Si(OH)_4$ or NO_3^- (Figure 7A-B), between pH treatments. The average Si:P drawdown rate also decreased linearly with decreasing pH and although the observed regression was not as strong, it was still statistically significant (Figure 6B; $r^2 = 0.94$, $p = 0.03$). Average Si:P drawdown rates determined from the pH 8.1 cultures were significantly different from the pH 7.9 and 7.8 cultures (8.1 vs. 7.9: $p = 0.02$; 8.1 vs. 7.8: $p = 0.01$). However, no statistically significant differences were found between pH 8.0, 7.9, and 7.8 cultures. The cell-normalized drawdown rates of PO_4^{3-} did not differ among the various pH treatments (Figure 7C), and N:P drawdown ratios showed the least variability among pH treatments; no statistically significant differences were observed for either PO_4^{3-} drawdown rates or N:P drawdown ratios.

IV. *Photosynthesis vs Irradiance Curves and F_v/F_m*:

P-E curves were normalized to the concentrations of Chl *a*, *P. australis* cells, and particulate carbon (PC). Regardless of the normalization parameter, photoinhibition was observed for every pH treatment at the higher PPFDs (Figure 8A-C). When curves were normalized to cell abundance (Figure 8A; Table 4), the average maximum rate of carbon fixation (P_m^{cell}) in the pH 7.9 cultures was 32% and 22% greater than the pH 8.1 ($p = 0.002$) and pH 8.0 ($p = 0.02$) cultures, respectively, and these differences are statistically significant. Additionally, the

P_m^{cell} in the pH 7.8 cultures was 24% greater than the average rate calculated for the pH 8.1 cultures (p = 0.02), which is also a statistically significant increase. All other photosynthetic parameters when normalized to cell number (α, β, E_k, and E_m) did not differ significantly between the pH treatments, (Table 11).

When P-E curves were normalized to Chl *a* (Figure 8B; Table 5), the average maximum rate of carbon fixation (P_m^{Chl}) for cultures maintained at pH 7.9 was 19% and 17% greater than cultures maintained at pH 8.1 (p = 0.06) and pH 8.0 (p = 0.09), respectively. However, these differences are not statistically significant, nor were any differences seen among the other photosynthetic parameters (Table 12). Additionally, the Chl *a* content (pg · cell^{-1}) of *P. australis* cells did not significantly differ between pH treatments (Figure 9A; Table 17). P-E curves normalized to PC (Figure 8C; Table 6) showed the least variability in the calculated photosynthetic parameters, and none of these differed significantly as a function of pH (Table 13).

The mean cellular florescence capacity (F_v/F_m) measurements of culture treatments (Table 8-9) ranged from 0.58 ± 0.04 to 0.60 ±0.02 (mean ± 1 SD) in the nutrient-replete exponential growth phase, and 0.30 ±0.05 to 0.36 ±0.02 during the nutrient-depleted, stationary growth phase. However, differences between treatments were not statistically significant in either the exponential or stationary phases (Table 14).

V. *Carbon to Nitrogen Ratios and Cellular Quotas*

At the exponential sampling period, cellular C:N ratios of *P. australis* cultures ranged from 5.8 to 6.8, but there was no significant influence of pH/pCO_2 on these values (Figure 10A; Table 18). Conversely, during the stationary sampling period, cellular C:N ratios ranged from 7.3 to 11.4, and the ratios at pH 7.8 were significantly greater than those of the pH 8.1 ($p = 0.03$) and pH 8.0 ($p = 0.01$) treatments, as were the C:N ratios for cultures maintained at pH 7.9 compared to pH 8.0 cultures ($p = 0.04$) (Figure 10B; Table 18).

Cellular N-quotas during the exponential phase increased with decreasing pH and linear regression analysis shows this to be statistically significant (Figure 11A; $r^2 = 0.99$, $p = 0.01$), but statistically significant increases in absolute quotas were found only between the pH 7.8 and 8.1 treatments ($p = 0.04$; Table 19). Cellular C-quotas during the exponential sampling period were significantly greater at pH 7.9 compared to 8.1 ($p = 0.02$), but no other significant differences were observed among pH treatments (Figure 11B; Table 20). There were no significant differences in cellular N- or C- quotas during the stationary phase (Figure 11A-B; Table 19 and 20).

VI. *Domoic Acid Quotas*:

Particulate (pDA) and dissolved (dDA) domoic acid were detectable in all of the pH treatments during both nutrient-replete exponential growth and nutrient-

deplete stationary growth (Figure 12A-F; Table 7). In all four pH treatments, ca. 80% of total DA measured during exponential growth was pDA (Figure 12B-C). However, there were no statistically significant differences between pH treatments for pDA, dDA and total DA (pDA + dDA) during the exponential growth phase when normalized to cell density (hereafter referred to as DA quotas; Table 15).

In stationary growth, total DA quotas were greater in all pH treatments and showed a step-like increase in toxicity as pH decreased (Figure 12D-F; Table 7). This effect was particularly evident at pH 7.8 where the maximum total DA quota was observed (3.61 pg DA · $cell^{-1}$), which was significantly greater than the other three pH treatments (Table 16; 7.8 vs. 8.1: $p < 0.0001$; 7.8 vs. 8.0: $p < 0.0001$; 7.8 vs. 7.9: $p = 0.004$) and 2.7-fold greater than cultures maintained at pH 8.1 (control 'present-day' pH). Additionally, the total DA quota was significantly greater in the pH 7.9 treatment compared to pH 8.1 and 8.0 treatments (Table 16; 7.9 vs. 8.1: $p = 0.005$; 7.9 vs. 8.0: $p = 0.01$). Particulate DA quotas in the stationary growth phase comprised between 73-86% of the total DA for all four pH treatments, which is similar to the percentage observed during the exponential growth phase (Figure 12E-F; Table 7). Cultures grown at pH 7.8 had significantly greater pDA quotas compared to all other pH treatments (Table 16; 7.8 vs. 8.1: $p < 0.0001$; 7.8 vs. 8.0: $p < 0.0001$; 7.8 vs. 7.9: $p = 0.003$) and pH 7.9 cultures were also significantly greater than the pH 8.1 and 8.0 cultures (7.9 vs 8.1: $p = 0.002$; 7.9 vs. 8.0: $p = 0.01$). The pDA quotas obtained during stationary growth were 2-6 fold

greater than values measured during exponential growth (Table 7). A similar trend was observed for dDA quotas, where values were 3-4 fold greater during the stationary phase. Interestingly, dDA quotas did not significantly differ between pH treatments during either stationary or exponential growth (Tables 7 and 16).

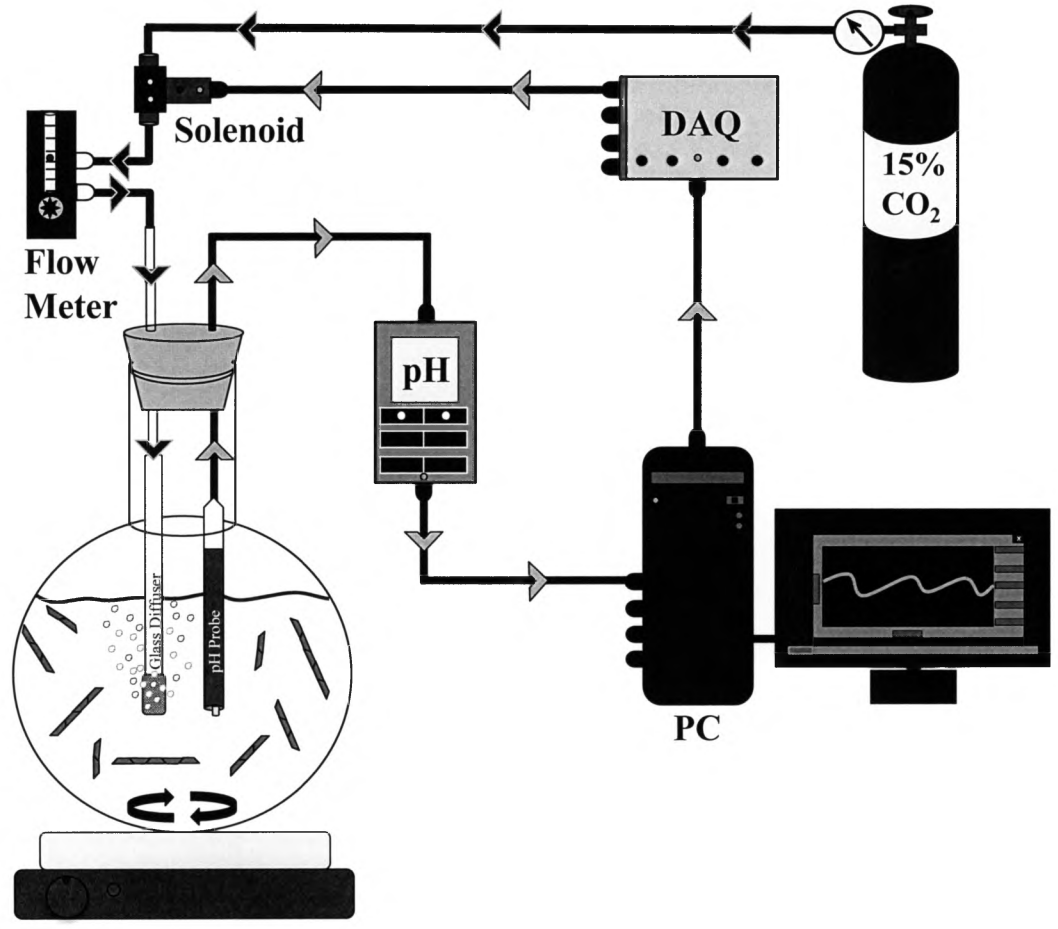

Figure 1. A schematic illustration of the computer controlled pH/pCO_2 STAT regulation system optimized to monitor and maintain the pH of the individual *P. australis* cultures. This automatic feed-back system consists of a pH probe (within each culture flask) connected to a pH meter and monitored by a PC computer (equipped with CapCTRL software), interfaced with a 4-channel gas control instrument (DAQ-M) that controls solenoid valves to inject commercially prepared compressed CO_2/air mixture (15% v/v) directly into the medium of the individual culture flask through a Pyrex® course-fritted diffuser.

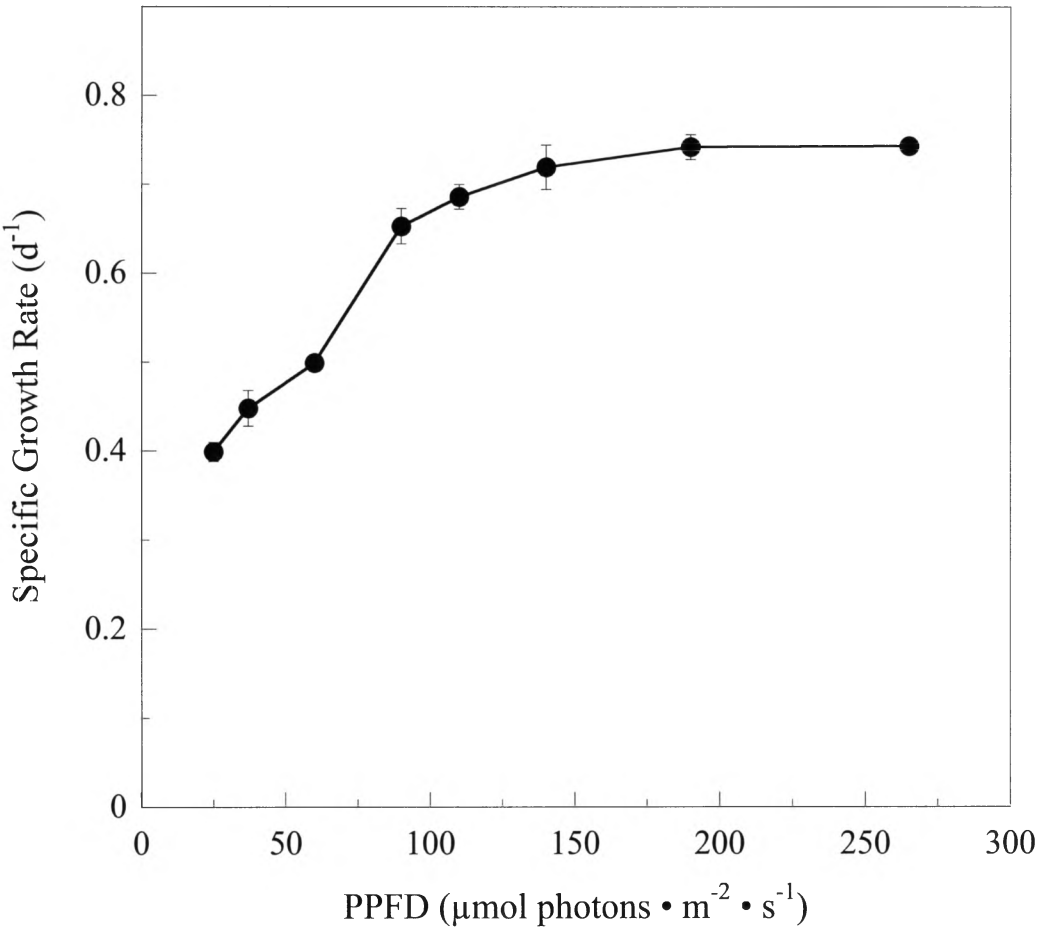

Figure 2. The average specific growth rate (μ; d^{-1}) of *P. australis* (HAB 327b) as a function of photosynthetic photon flux density (PPFD) for cells grown in sterile-filtered enriched seawater (ESNW) using nitrate as the sole N source. Values are the means of duplicate (n = 2) cultures; error bars indicate range of duplicates, and those not visible are within the size of the symbols.

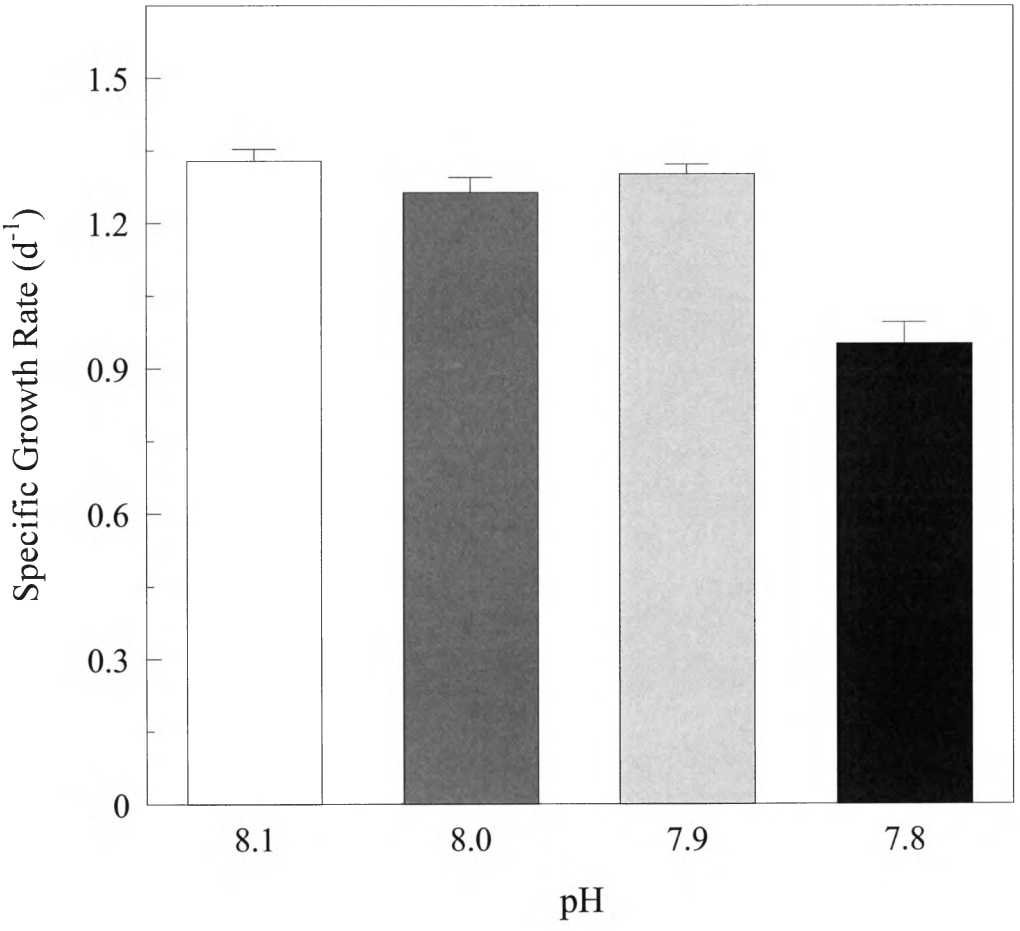

Figure 3. The average specific growth rate (μ; d^{-1}) of *P. australis* (HAB 200) cultures in the four pH treatments. Values plotted are the means of triplicate cultures ($n = 3$), and error bars represent ± 1 standard deviation (± SD).

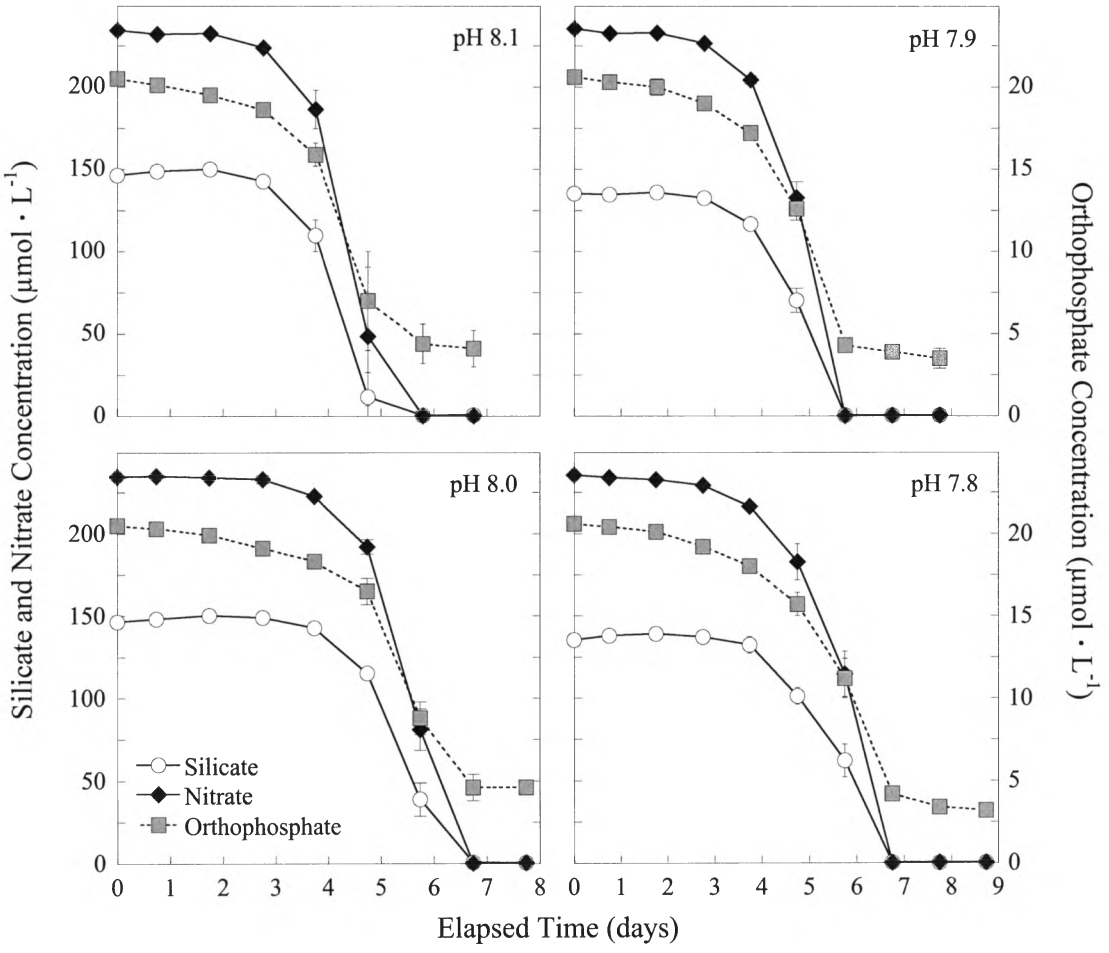

Figure 4. Mean ambient concentrations of silicate, nitrate and orthophosphate in batch cultures of *P. australis* (HAB 200) in the four pH treatments. Note the different scales of the ordinate-axes. Values plotted are the means of triplicate cultures (n = 3). Error bars represent ± 1 standard deviation (± SD) and those not visible are within the size of the symbols.

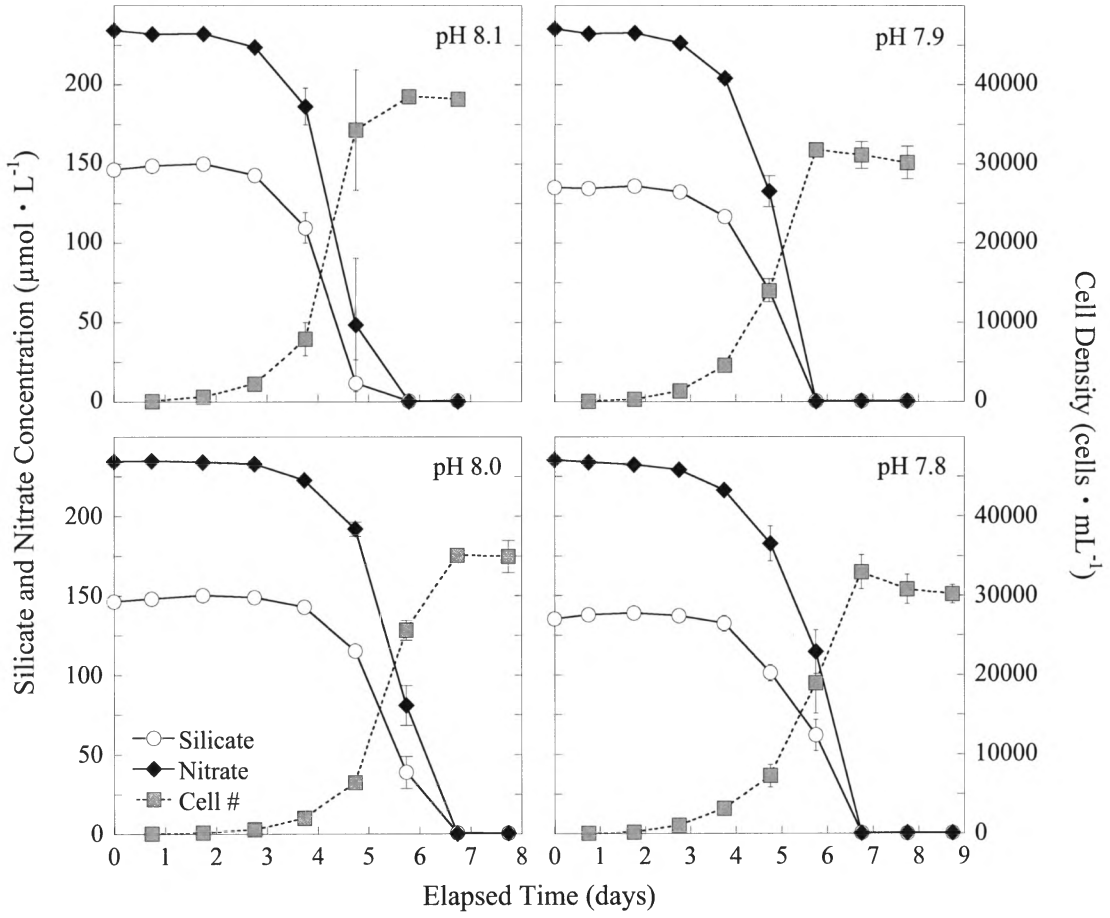

Figure 5. Mean ambient concentrations of silicate, nitrate, and *P. australis* (HAB 200) cells plotted as a function of time in the four pH treatments. Note the different scales on the ordinate axes. Values plotted are the means of triplicate cultures (n = 3). Error bars represent ± 1 standard deviation (± SD) and those not visible are within the size of the symbols.

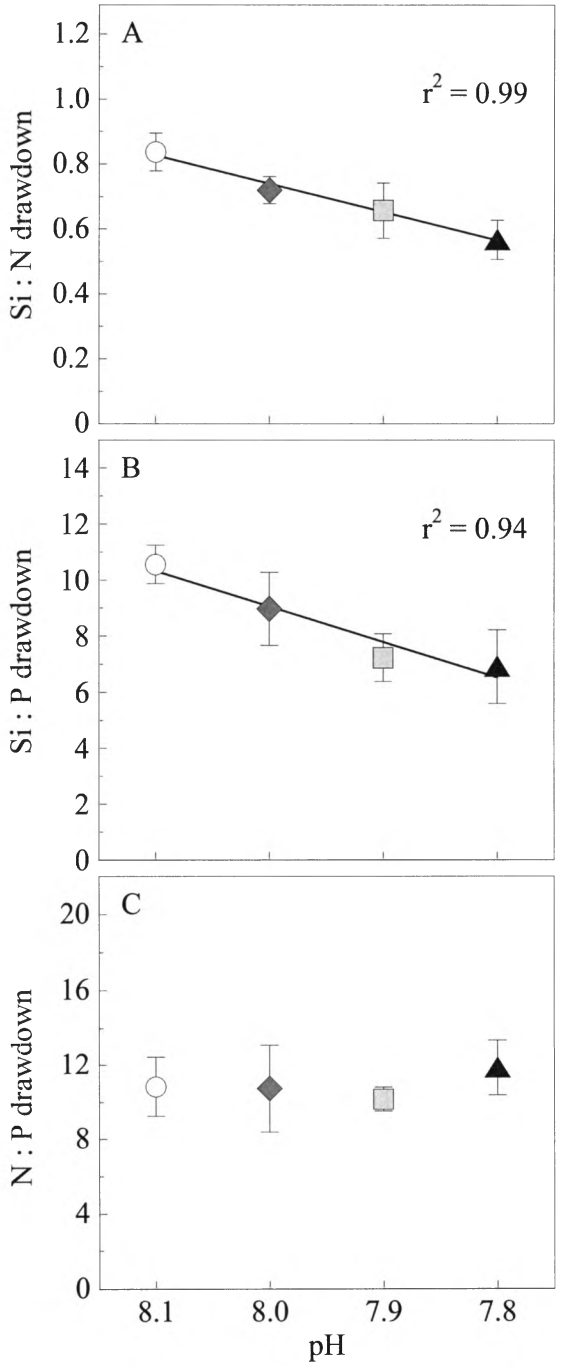

Figure 6. Mean macronutrient drawdown ratios of *P. australis* (HAB 200) cultures at the four pH treatments: (A) silicate : nitrate; (B) silicate : orthophosphate; (C) nitrate : orthophosphate. Values plotted are the means of triplicate cultures ($n = 3$). Error bars represent ± 1 standard deviation (± SD), and those not visible are within the size of the symbols.

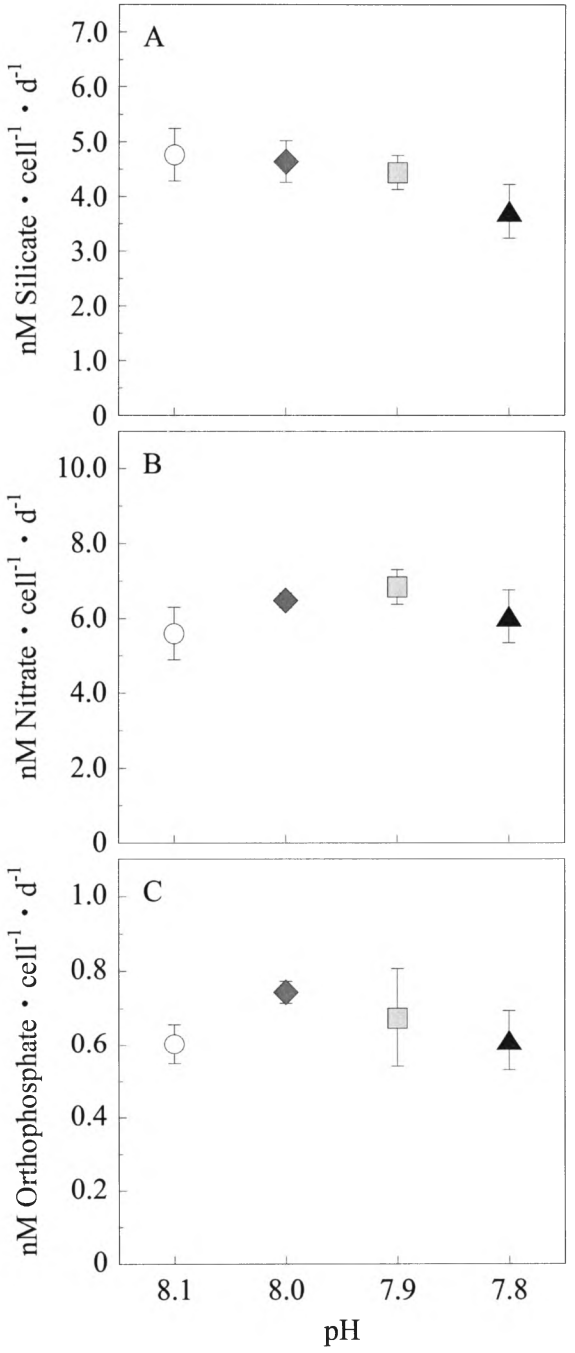

Figure 7. Mean macronutrient drawdown rates (nM • $cell^{-1}$ • day^{-1}) of (A) silicate, (B) nitrate, and (C) orthophosphate in *P. australis* (HAB 200) cultures at the four pH treatments during the exponential growth phase. Values plotted are the means of triplicate cultures (n = 3). Error bars represent ± 1 standard deviation (± SD) and those not visible are within the size of the symbols.

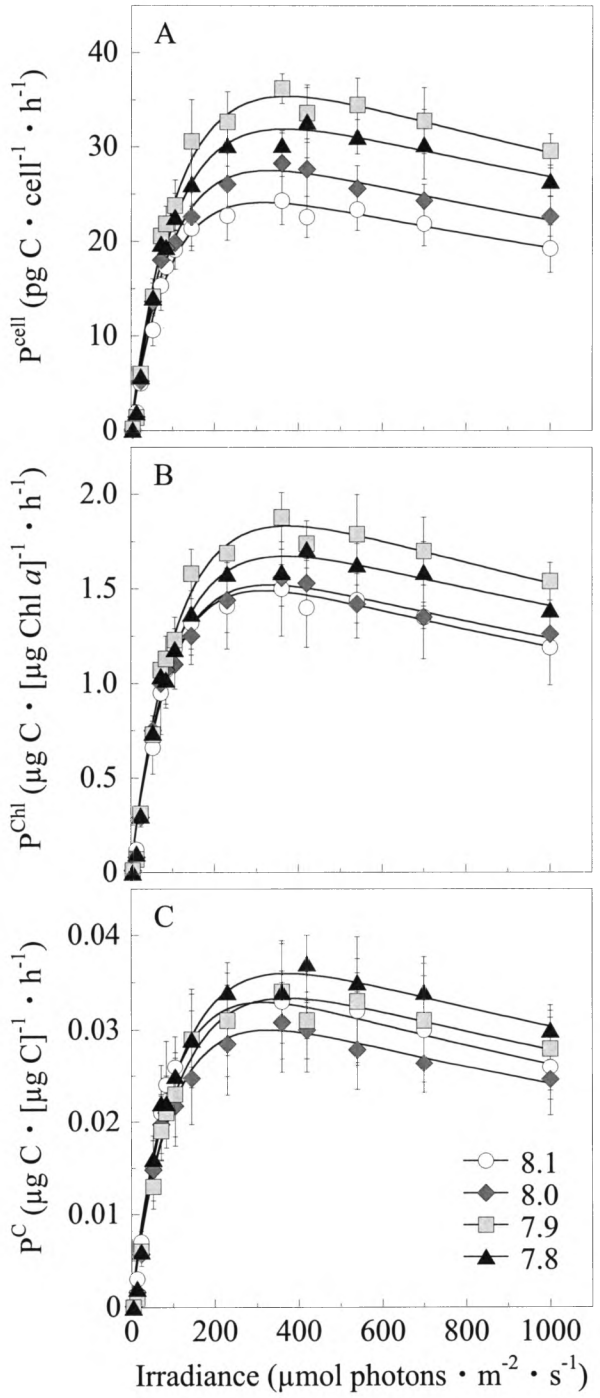

Figure 8. Photosynthesis vs. irradiance curves (P-E curves) of exponentially growing *P. australis* (HAB 200) cultures in the four pH treatments. Curves are normalized to (A) cell abundance, (B) Chl *a*, and (C) particulate carbon (PC) concentrations. Values plotted are the means of triplicate cultures (n = 3), and error bars represent ± 1 standard deviation (± SD).

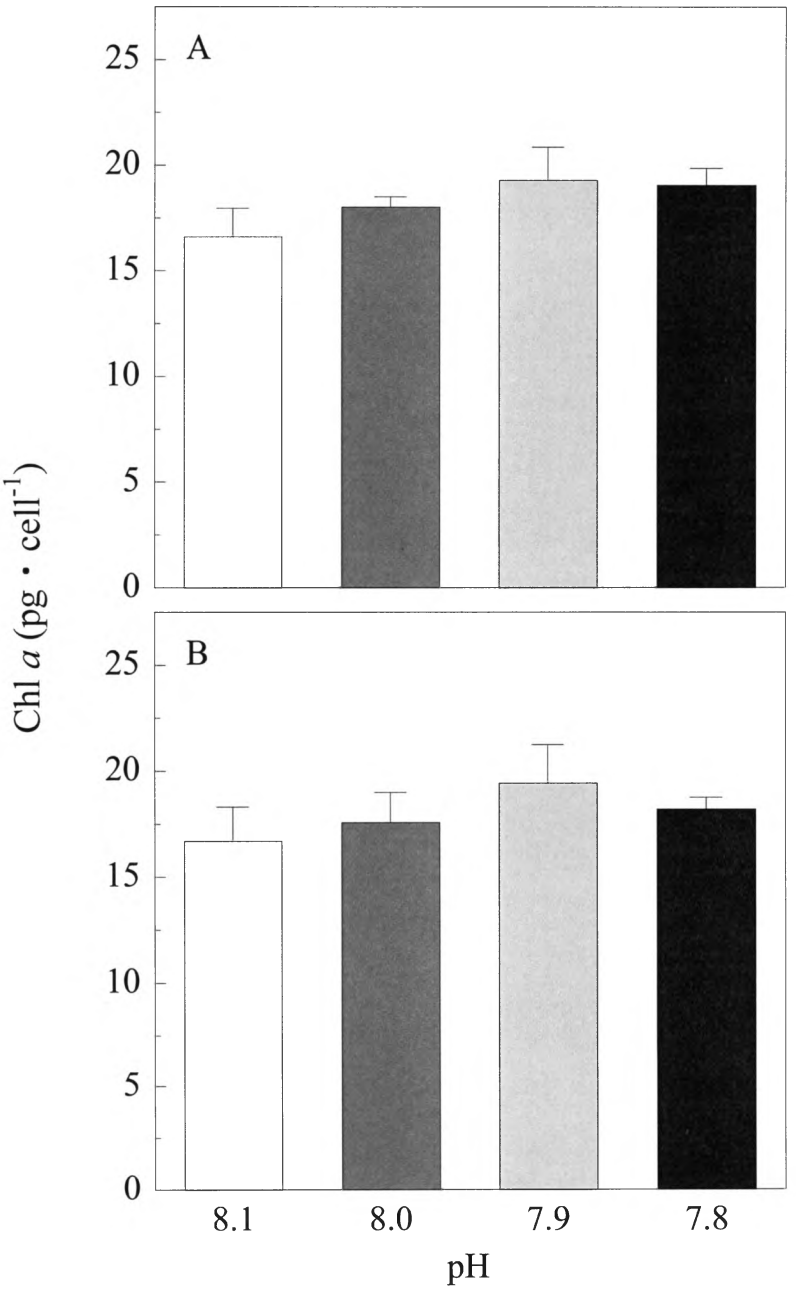

Figure 9. Cell-specific Chl *a* concentrations (pg Chl *a* • $cell^{-1}$) of *P. australis* (HAB 200) cultures in the four pH treatments during the (A) exponential and (B) stationary growth phases. Values plotted are the means of triplicate cultures (n = 3), and error bars represent ± 1 standard deviation (± SD).

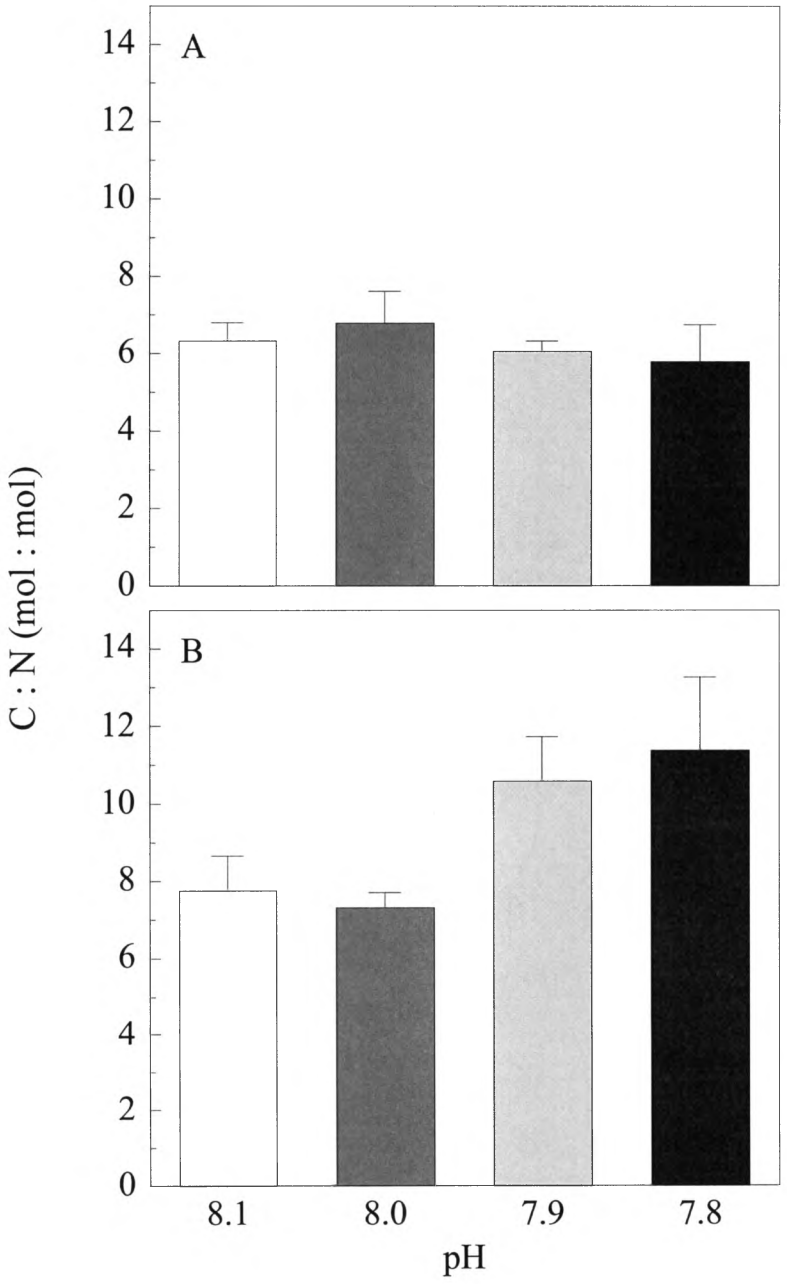

Figure 10. Cellular carbon: nitrogen molar ratios (C:N) of *P. australis* (HAB 200) cultures in the four pH treatments during the (A) exponential and (B) stationary growth phases. Values plotted are the means of triplicate cultures ($n = 3$), and error bars represent ± 1 standard deviation (± SD).

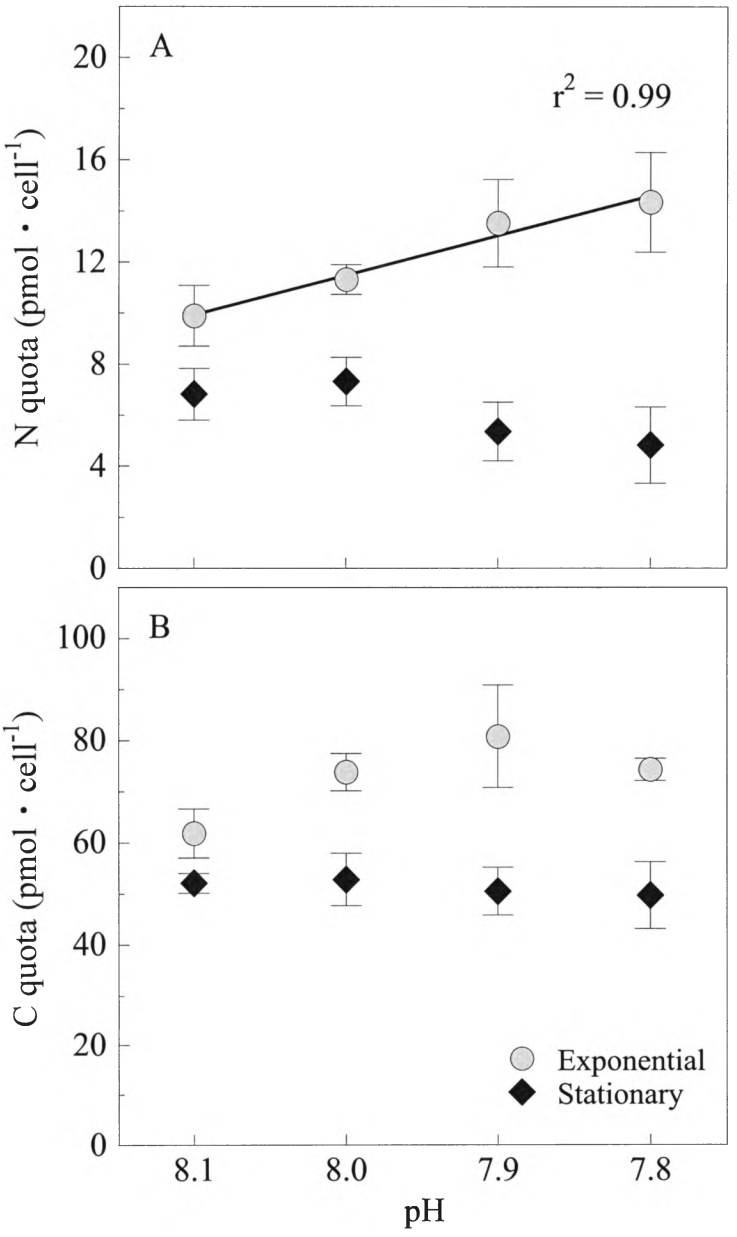

Figure 11. Cellular quotas (pmol • cell^{-1}) of (A) particulate nitrogen and (B) carbon in cultures of *P. australis* (HAB 200) during the exponential (circles) and stationary (diamonds) growth phases. Values plotted are the means of triplicate cultures ($n = 3$), and error bars represent ± 1 standard deviation (± SD).

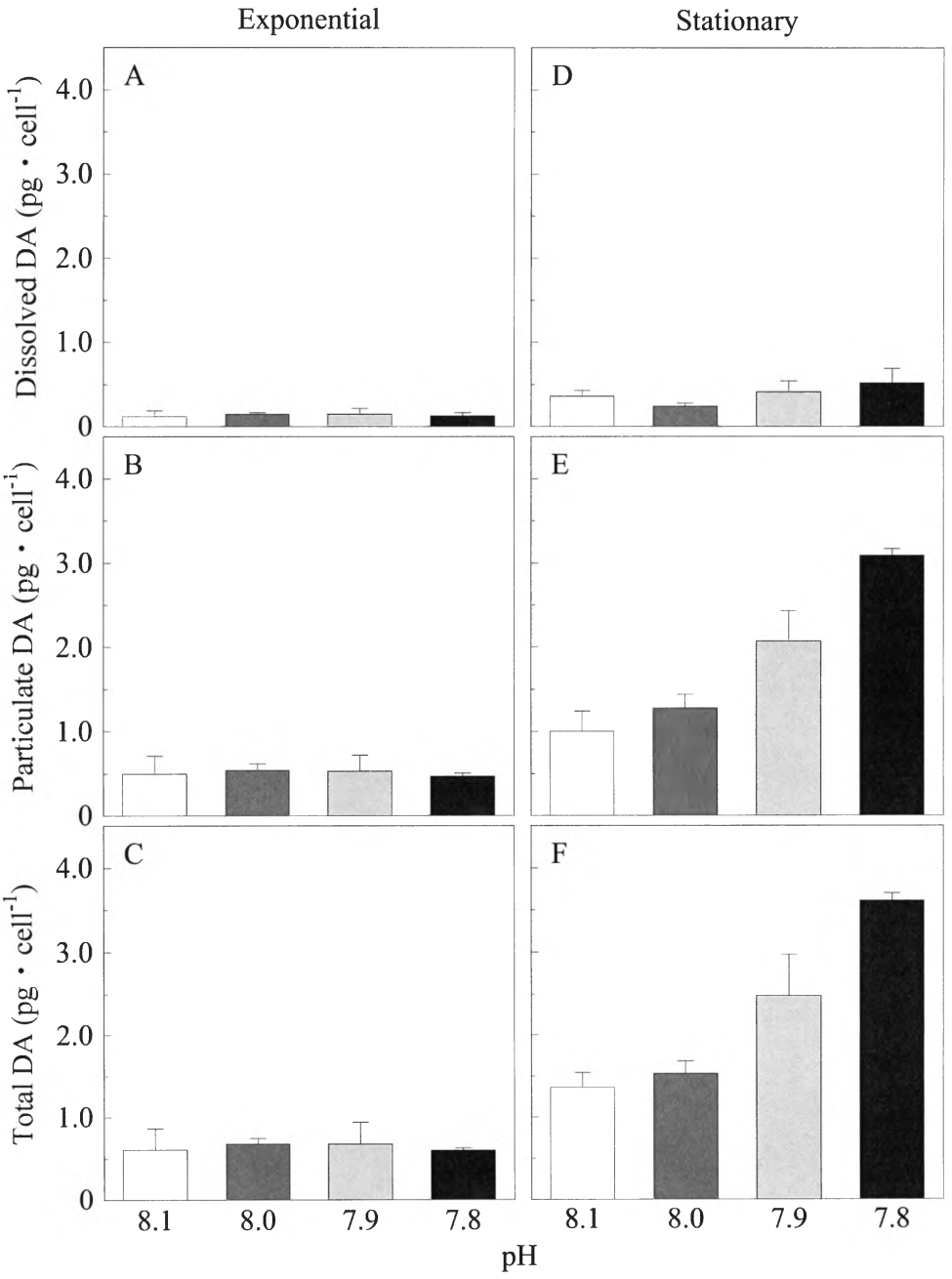

Figure 12. Domoic acid (DA) quotas (pg DA • cell^{-1}) of *P. australis* (HAB 200) cultures in the four pH treatments during the exponential (A-C) and stationary (D-F) growth phases. (A, D) dissolved DA; (B, E) particulate DA; (C, F) total DA (dissolved DA + particulate DA) all normalized to cell density. Values plotted are the means of triplicate cultures (n = 3), and error bars represent ± 1 standard deviation (± SD).

Table 1. Symbols and terminology of the photosynthetic parameters used in P versus E curves.

Symbol	Definition	Units
E	Irradiance/photosynthetic photon flux density (PPFD)	μmol photons · m^{-2} · s^{-1}
E_k	Index of photoadaptation and light-saturation point ($E_k = P_m^B / \alpha$)	μmol photons · m^{-2} · s^{-1}
E_m	PPFD where maximum carbon uptake occurs	μmol photons · m^{-2} · s^{-1}
P^B	Biomass-specific rate of photosynthesis	μg C *or* pg C · (unit biomass)$^{-1}$ · h^{-1}
P^C	Carbon-specific rate of photosynthesis	μg C · (μg C)$^{-1}$ · h^{-1} = h^{-1}
P^{cell}	Cell-specific rate of photosynthesis	pg C · (cell)$^{-1}$ · h^{-1}
P^{Chl}	Chl *a*-specific rate of photosynthesis	μg C · (μg Chl *a*)$^{-1}$ · h^{-1}
P_s^B	Theoretical maximum value of P^B in the absence of photoinhibition (i.e., $\beta = 0$)	μg C · (unit biomass)$^{-1}$ · h^{-1}
P_m^B	Observed maximum value of P^B	μg C *or* pg C · (unit biomass)$^{-1}$ · h^{-1}
P_m^C	Observed maximum value of P^C	μg C · (μg C)$^{-1}$ · h^{-1} = h^{-1}
P_m^{cell}	Observed maximum value of P^{cell}	pg C · (cell)$^{-1}$ · h^{-1}
P_m^{Chl}	Observed maximum value of P^{Chl}	μg C · (μg Chl *a*)$^{-1}$ · h^{-1}
α^B	Initial slope of the light-limited region of the P-E curve	μg C *or* pg C · (unit biomass)$^{-1}$ · h^{-1} · E^{-1}
α^C	Initial slope of the P-E curve normalized to particulate carbon (PC)	μg C · (μg C)$^{-1}$ · h^{-1} · E^{-1}
α^{cell}	Initial slope of the P-E curve normalized to cell density	pg C · (cell)$^{-1}$ · h^{-1} · E^{-1}
α^{Chl}	Initial slope of the P-E curve normalized to Chl *a* concentration	μg C · (Chl *a*)$^{-1}$ · h^{-1} · E^{-1}
β	Slope of the photoinhibited region of the P-E curve	μg C *or* pg C · (unit biomass)$^{-1}$ · h^{-1} · E^{-1}

Table 2. Parameters of the seawater carbonate system at the exponential sampling period. Concentrations of dissolved inorganic carbon (DIC), pH (NBS scale), silicate and phosphate, temperature, and salinity measurements were used to derive all of the other parameters using the software program CO2Sys (Lewis and Wallace 1998) with dissociation constants for carbonic acid as refitted by Dickson and Millero (1987). Reported values are the means of triplicate (n = 3) cultures, and parentheses indicate ± 1 standard deviation (± SD).

pH (NBS)	pCO_2 (µatm)	DIC (µmol · kg^{-1})	HCO_3^- (µmol · kg^{-1})	CO_3^{2-} (µmol · kg^{-1})	CO_2 (µmol · kg^{-1})	TA (µmol · kg^{-1})
8.14	406	2032	1882	133	16.3	2232
(0.01)	(8)	(11)	(12)	(1)	(0.3)	(9)
8.03	550	2093	1964	107	22.1	2248
(0.01)	(8)	(21)	(18)	(3)	(0.3)	(25)
7.93	719	2136	2021	87	28.8	2255
(0.02)	(34)	(25)	(25)	(2)	(1.4)	(20)
7.81	980	2213	2105	69	39.3	2292
(0.03)	(64)	(11)	(12)	(4)	(2.6)	(3)

Table 3. Parameters of the seawater carbonate system at the stationary sampling period. Concentrations of dissolved inorganic carbon (DIC), pH, silicate and phosphate, temperature, and salinity measurements were used to derive all of the other parameters using the software program CO2Sys (Lewis and Wallace 1998) with dissociation constants for carbonic acid as refitted by Dickson and Millero (1987). Reported values are the means of triplicate (n = 3) cultures and parentheses indicate ± 1 standard deviation (± SD).

pH (NBS)	pCO_2 (µatm)	DIC (µmol · kg^{-1})	HCO_3^- (µmol · kg^{-1})	CO_3^{2-} (µmol · kg^{-1})	CO_2 (µmol · kg^{-1})	TA (µmol · kg^{-1})
8.14	410	2052	1901	135	16.5	2239
(0.01)	(2)	(21)	(18)	(3)	(0.1)	(25)
8.04	537	2107	1975	111	21.5	2254
(0.01)	(19)	(17)	(18)	(2)	(0.8)	(14)
7.93	732	2175	2057	88	29.4	2279
(0.02)	(28)	(13)	(13)	(3)	(1.1)	(14)
7.84	929	2271	2157	77	37.3	2348
(0.01)	(12)	(16)	(15)	(1)	(0.5)	(17)

Table 4. Photosynthetic parameters from P-E curve fitting normalized to *P. australis* cell density. Values reported are the means of triplicate cultures (n = 3) and parentheses indicate ± 1 standard deviation (± SD). The r^2 column provides the coefficient of determination, and parentheses indicate the sample size (n). Units as in Table 1.

pH (NBS)	P_s^{cell}	P_m^{cell}	α^{cell}	β	E_k	E_m	r^2
8.14	28.38	24.14	0.299	0.0111	81	318	0.98
(0.01)	(2.39)	(2.04)	(0.039)	(0.0033)	(8)	(13)	(48)
8.03	32.28	27.54	0.327	0.0123	84	340	0.98
(0.01)	(5.03)	(2.87)	(0.037)	(0.0068)	(4)	(49)	(48)
7.93	42.35	35.41	0.365	0.0157	98	375	0.99
(0.02)	(2.31)	(1.97)	(0.044)	(0.0051)	(7)	(27)	(48)
7.81	37.48	31.92	0.342	0.0127	94	371	0.99
(0.03)	(3.76)	(2.64)	(0.048)	(0.0049)	(8)	(20)	(48)

Table 5. Photosynthetic parameters from P-E α curve fitting normalized to chlorophyll *a* (Chl *a*). Values reported are the means of triplicate cultures ($n = 3$) and parentheses indicate ± 1 standard deviation (± SD). The r^2 column provides the coefficient of determination and parentheses indicate the sample size (n). Units as in Table 1.

pH (NBS)	P_s^{Chl}	P_m^{Chl}	α^{Chl}	β	E_k	E_m	r^2
8.14	1.76	1.49	0.018	0.00069	81	318	0.99
(0.01)	(0.26)	(0.21)	(0.003)	(0.00024)	(8)	(12)	(48)
8.03	1.79	1.52	0.018	0.00068	84	340	0.98
(0.01)	(0.24)	(0.12)	(0.002)	(0.00037)	(4)	(49)	(48)
7.93	2.20	1.84	0.019	0.00081	98	375	0.99
(0.02)	(0.08)	(0.08)	(0.001)	(0.00025)	(7)	(27)	(48)
7.81	1.96	1.67	0.018	0.00066	94	371	0.99
(0.03)	(0.12)	(0.11)	(0.002)	(0.00024)	(8)	(21)	(48)

Table 6. Photosynthetic parameters from P-E curve fitting normalized to particulate carbon (PC). Values reported are the means of triplicate cultures (n = 3) and parentheses indicate ± 1 standard deviation (± SD). The r^2 column provides the coefficient of determination and parentheses indicate the sample size (n). Units as in Table 1.

pH (NBS)	P_s^C	P_m^C	α^C	β	E_k	E_m	r^2
8.14	0.039	0.033	0.00041	0.000015	81	318	0.99
(0.01)	(0.006)	(0.006)	(0.00008)	(0.000005)	(8)	(13)	(42)
8.03	0.035	0.030	0.00036	0.000014	85	340	0.98
(0.01)	(0.007)	(0.005)	(0.00006)	(0.000008)	(4)	(48)	(42)
7.93	0.040	0.033	0.00034	0.000014	98	375	0.98
(0.02)	(0.003)	(0.005)	(0.00006)	(0.000003)	(7)	(26)	(42)
7.81	0.042	0.036	0.00038	0.000014	94	371	0.99
(0.03)	(0.003)	(0.002)	(0.00004)	(0.000005)	(8)	(21)	(42)

Table 7. Domoic acid (DA) quotas of *P. australis* (HAB 200) batch cultures during the exponential and stationary growth phases. Concentrations of particulate DA (pDA), dissolved DA (dDA), and total DA (pDA + dDA) normalized to cell density (DA quotas) are provided in units of pg DA • $cell^{-1}$. Values reported are the means of triplicate cultures (n = 3), and parentheses indicate ± 1 standard deviation (± SD).

	Exponential DA (pg DA • $cell^{-1}$)			Stationary DA (pg DA • $cell^{-1}$)		
pH Treatment	dDA	pDA	Total DA	dDA	pDA	Total DA
8.10	0.12 (0.07)	0.50 (0.21)	0.61 (0.26)	0.36 (0.07)	1.00 (0.24)	1.36 (0.18)
8.00	0.15 (0.02)	0.57 (0.11)	0.68 (0.07)	0.24 (0.04)	1.28 (0.16)	1.53 (0.15)
7.90	0.14 (0.07)	0.52 (0.19)	0.68 (0.26)	0.41 (0.13)	2.07 (0.36)	2.48 (0.49)
7.80	0.13 (0.04)	0.47 (0.04)	0.60 (0.03)	0.52 (0.17)	3.09 (0.08)	3.61 (0.09)

Table 8. Measured parameters from samples taken during the nutrient-replete exponential growth phase, including macronutrient concentrations (nitrate + nitrite, silicate, and orthophosphate), cell density, particulate carbon (PC), particulate nitrogen (PN), and cellular fluorescence capacity (F_v/F_m). Values reported are the means of triplicate cultures ($n = 3$), and parentheses indicate ± 1 standard deviation (± SD).

pH (NBS)	$NO_3^- + NO_2^-$ ($\mu mol \cdot L^{-1}$)	$Si(OH)_4$ ($\mu mol \cdot L^{-1}$)	PO_4^{3-} ($\mu mol \cdot L^{-1}$)	Cell Density (mL^{-1})	PC ($\mu mol \cdot L^{-1}$)	PN ($\mu mol \cdot L^{-1}$)	F_v/F_m
8.14	173.0	107.0	15.6	9711	603.5	94.3	0.59
(0.01)	(7.2)	(5.0)	(0.8)	(1311)	(56.4)	(9.9)	(0.01)
8.03	179.7	106.0	15.9	7095	550.1	88.9	0.58
(0.01)	(8.5)	(4.4)	(0.7)	(911)	(49.9)	(14.1)	(0.04)
7.93	196.0	115.0	16.8	5054	447.5	75.3	0.60
(0.02)	(4.4)	(1.7)	(0.3)	(164)	(98.9)	(18.3)	(0.02)
7.81	174.0	99.4	15.2	7438	554.4	97.4	0.60
(0.03)	(12.3)	(8.3)	(0.7)	(1219)	(106.4)	(13.0)	(0.02)

Table 9. Measured parameters from samples taken during the nutrient-deplete stationary growth phase, including macronutrient concentrations (nitrate + nitrite, silicate, and orthophosphate), cell density, particulate carbon (PC), particulate nitrogen (PN), and cellular fluorescence capacity (F_v/F_m). Values reported are the means of triplicate cultures (n = 3), and parentheses indicate ± 1 standard deviation (± SD). Nitrate concentrations below the limit of detection (i.e. 0.02 µM) are reported as 0 µM.

pH (NBS)	$NO_3^- + NO_2^-$ (µmol · L^{-1})	$Si(OH)_4$ (µmol · L^{-1})	PO_4^{3-} (µmol · L^{-1})	Cell Density (mL^{-1})	PC (µmol · L^{-1})	PN (µmol · L^{-1})	F_v/F_m
8.14 (0.01)	0	0.58 (0.05)	4.2 (1.0)	38214 (684)	1990.2 (39.4)	260.3 (35.2)	0.35 (0.02)
8.04 (0.01)	0	0.32 (0.04)	4.2 (0.7)	36589 (2600)	1924.8 (81.0)	266.7 (23.7)	0.36 (0.02)
7.93 (0.02)	0	0.43 (0.12)	3.5 (0.5)	30180 (2049)	1518.0 (44.7)	160.9 (28.2)	0.34 (0.04)
7.84 (0.01)	0	0.30 (0.07)	3.2 (0.3)	29427 (1157)	1467.1 (235.2)	143.0 (47.2)	0.30 (0.05)

Table 10. Summary of the photosynthetic parameters for various species of *Pseudo-nitzschia* measured during nutrient-replete exponential growth. Units as in Table 1.

Species Isolate	Culture Conditions				P_m^B			α			E		Reference
	Temp (°C)	PPFD	L:D (h)	pH	P_m^C	P_m^{cell}	P_m^{Chl}	α^C	α^{cell}	α^{Chl}	E_k	E_m	
P. multiseries PEI[1], Canada	10-12	1100	24:0		2.1×10^{-2}	5.43	2.20	6.0×10^{-5}	0.017	6.06×10^{-3}	415	1272	Pan et al. (1991)
		105			4.9×10^{-2}	7.32	1.66	2.6×10^{-4}	0.039	8.69×10^{-3}	140	489	
P. multiseries PEI, Canada	0	350-	24:0		$<5.0 \times 10^{-3}$		0.08	$<1.0 \times 10^{-5}$		0.17×10^{-3}			Pan et al. (1993)[2]
	5	440			$<5.0 \times 10^{-3}$		0.20	$<1.0 \times 10^{-5}$		0.75×10^{-3}			
	10				5.0×10^{-3}		1.20	1.0×10^{-5}		2.50×10^{-3}			
	15				2.8×10^{-2}		3.42	5.0×10^{-5}		6.00×10^{-3}			
	20				3.1×10^{-2}		1.30	14.5×10^{-5}		6.50×10^{-3}			
	25				3.9×10^{-2}		2.00	9.0×10^{-5}		5.00×10^{-3}			
P. multiseries Strain NPBIO	10	53	24:0		5.5×10^{-3}		0.55	3.0×10^{-5}		3.50×10^{-3}	175	500	Pan et al. (1996d)[3]
		250			7.5×10^{-3}		1.10	2.0×10^{-5}		2.50×10^{-3}	431	900	
		410			9.0×10^{-3}		1.15	3.5×10^{-5}		4.00×10^{-3}	278	730	
		815			5.0×10^{-3}		0.75	2.5×10^{-5}		3.80×10^{-3}	231	1430	
		1100			1.4×10^{-2}		1.05	7.8×10^{-5}		5.80×10^{-3}	198	1320	
P. multiseries CCMP 2708 Canada	17	120	12:12	8.40			2.73			2.10×10^{-2}	131		Sun et al. (2011)[4]
				8.19			3.13			2.00×10^{-2}	157		
				7.96			3.30			2.40×10^{-2}	142		
P. australis HAB 200, Santa Cruz, CA, USA	13	240	14:10	8.14	3.3×10^{-2}	24.14	1.49	4.1×10^{-4}	0.299	1.80×10^{-2}	81	318	Present study
				8.03	3.0×10^{-2}	27.54	1.52	3.6×10^{-4}	0.327	1.80×10^{-2}	84	340	
				7.93	3.3×10^{-2}	35.41	1.84	3.4×10^{-4}	0.365	1.90×10^{-2}	98	375	
				7.81	3.6×10^{-2}	31.92	1.67	3.8×10^{-4}	0.342	1.80×10^{-2}	94	371	

[1] Prince Edward Island (Cardigan Bay)
[2] Values of P_m^C, P_m^{Chl}, α^C, and α^{Chl} were estimated from Figure 5A-B of Pan et al. (1993).
[3] Values of P_m^C, P_m^{Chl}, α^C, and α^{Chl} were estimated from Figures 4A-B and 5A-B of Pan et al. (1996d).
[4] Values reported from Sun et al. (2011) are for nutrient-replete cultures only.

Table 11. Q and P-values calculated by comparing the photosynthetic parameters of P-E curves normalized to cell density using one-way ANOVAs with Tukey's HSD multiple comparisons test. An asterisk indicates a significant difference ($p < 0.05$) between pH treatments.

pH Treatment (statistical value)	8.10 (q, p)	8.00 (q, p)	7.90 (q, p)	7.80 (q, p)
8.10				
P_m^{cell}	--	2.44, 0.37	8.10, 0.002 *	5.59, 0.02 *
α^{cell}	--	1.14, 0.85	2.71, 0.29	1.77, 0.62
β	--	0.41, 0.99	1.53, 0.71	0.52, 0.98
E_k	--	0.86, 0.93	4.13, 0.07	3.27, 0.17
E_m	--	1.22, 0.83	3.21, 0.18	2.96, 0.23
8.00				
P_m^{cell}	2.44, 0.37	--	5.66, 0.02 *	3.15, 0.20
α^{cell}	1.14, 0.85	--	1.57, 0.69	0.63, 0.97
β	0.41, 0.99	--	1.12, 0.86	0.11, 0.99
E_k	0.86, 0.93	--	3.27, 0.17	2.41, 0.38
E_m	1.22, 0.83	--	2.00, 0.52	1.75, 0.62
7.90				
P_m^{cell}	8.10, 0.002 *	5.66, 0.02 *	--	2.51, 0.35
α^{cell}	2.71, 0.29	1.57, 0.69	--	0.94, 0.91
β	1.53, 0.71	1.12, 0.86	--	1.01, 0.89
E_k	4.13, 0.07	3.27, 0.17	--	0.86, 0.93
E_m	3.21, 0.18	2.00, 0.52	--	0.25, 0.99
7.80				
P_m^{cell}	5.59, 0.02 *	3.15, 0.20	2.51, 0.35	--
α^{cell}	1.77, 0.62	0.63, 0.97	0.94, 0.91	--
β	0.52, 0.98	0.11, 0.99	1.01, 0.89	--
E_k	3.27, 0.17	2.41, 0.38	0.86, 0.93	--
E_m	2.96, 0.23	1.75, 0.62	0.25, 0.99	--

Table 12. Q and P-values calculated by comparing the photosynthetic parameters of P-E curves normalized to Chl *a* concentration using one-way ANOVAs with Tukey's HSD multiple comparisons test. An asterisk indicates a significant difference ($p < 0.05$) between pH treatments.

pH Treatment (statistical value)	8.10 (q, p)	8.00 (q, p)	7.90 (q, p)	7.80 (q, p)
8.10				
P_m^{Chl}	--	0.46, 0.99	4.42, 0.06	2.31, 0.41
α^{Chl}	--	0.25, 0.99	0.50, 0.98	0.25, 0.99
β	--	0.09, 0.99	0.79, 0.94	0.17, 0.99
E_k	--	0.76, 0.95	3.95, 0.09	3.11, 0.20
E_m	--	1.21, 0.83	3.22, 0.18	2.97, 0.23
8.00				
P_m^{Chl}	0.46, 0.99	--	3.95, 0.09	1.85, 0.58
α^{Chl}	0.25, 0.99	--	0.75, 0.95	1.00, 0.99
β	0.09, 0.99	--	0.70, 0.96	0.26, 0.99
E_k	0.76, 0.95	--	3.20, 0.19	2.35, 0.40
E_m	1.21, 0.83	--	2.01, 0.53	1.76, 0.62
7.90				
P_m^{Chl}	4.42, 0.06	3.95, 0.09	--	2.10, 0.49
α^{Chl}	0.50, 0.98	0.75, 0.95	--	0.75, 0.95
β	0.79, 0.94	0.70, 0.96	--	0.96, 0.90
E_k	3.95, 0.09	3.20, 0.19	--	0.84, 0.93
E_m	3.22, 0.18	2.01, 0.53	--	0.25, 0.99
7.80				
P_m^{Chl}	2.31, 0.41	1.85, 0.58	2.10, 0.49	--
α^{Chl}	0.25, 0.99	1.00, 0.99	0.75, 0.95	--
β	0.17, 0.99	0.26, 0.99	0.96, 0.90	--
E_k	3.11, 0.20	2.35, 0.40	0.84, 0.93	--
E_m	2.97, 0.23	1.76, 0.62	0.25, 0.99	--

Table 13. Q and P-values calculated by comparing the photosynthetic parameters of P-E curves normalized to particulate carbon (PC) concentration using one-way ANOVAs with Tukey's HSD multiple comparisons test. An asterisk indicates a significant difference ($p < 0.05$) between pH treatments.

pH Treatment (statistical value)	8.10 (q, p)	8.00 (q, p)	7.90 (q, p)	7.80 (q, p)
8.10				
P_m^C	--	1.10, 0.86	0.21, 0.99	1.11, 0.86
α^C	--	1.33, 0.78	1.68, 0.65	0.62, 0.97
β	--	0.42, 0.99	0.23, 0.99	0.32, 0.99
E_k	--	0.77, 0.95	4.08, 0.08	3.12, 0.20
E_m	--	1.25, 0.81	3.27, 0.18	3.02, 0.22
8.00				
P_m^C	1.10, 0.86	--	1.31, 0.79	2.21, 0.45
α^C	1.33, 0.78	--	0.34, 0.99	0.71, 0.96
β	0.42, 0.99	--	0.19, 0.99	0.10, 0.99
E_k	0.77, 0.95	--	3.31, 0.17	2.35, 0.40
E_m	1.25, 0.81	--	2.02, 0.52	1.77, 0.62
7.90				
P_m^C	0.21, 0.99	1.31, 0.79	--	0.90, 0.92
α^C	1.68, 0.65	0.34, 0.99	--	1.05, 0.88
β	0.23, 0.99	0.19, 0.99	--	0.10, 0.99
E_k	4.08, 0.08	3.31, 0.17	--	0.96, 0.90
E_m	3.27, 0.18	2.02, 0.52	--	0.25, 0.99
7.80				
P_m^C	1.11, 0.86	2.21, 0.45	0.90, 0.92	--
α^C	0.62, 0.97	0.71, 0.96	1.05, 0.88	--
β	0.32, 0.99	0.10, 0.99	0.10, 0.99	--
E_k	3.12, 0.20	2.35, 0.40	0.96, 0.90	--
E_m	3.02, 0.22	1.77, 0.62	0.25, 0.99	--

Table 14. Q and P-values calculated by comparing the cellular fluorescence capacity values (F_v/F_m) between pH treatments, during exponential and stationary growth phases, using one-way ANOVAs with Tukey's HSD multiple comparisons test. An asterisk indicates a significant difference ($p < 0.05$) between pH treatments.

pH Treatment (statistical value)	8.10 (q, p)	8.00 (q, p)	7.90 (q, p)	7.80 (q, p)
8.10				
Exponential	--	1.62, 0.68	0.27, 0.99	1.08, 0.87
Stationary	--	0.47, 0.99	0.63, 0.97	2.35, 0.40
8.00				
Exponential	1.62, 0.68	--	1.89, 0.57	2.70, 0.30
Stationary	0.47, 0.99	--	1.10, 0.86	2.82, 0.27
7.90				
Exponential	0.27, 0.99	1.89, 0.57	--	0.81, 0.94
Stationary	0.63, 0.97	1.10, 0.86	--	1.72, 0.63
7.80				
Exponential	1.08, 0.87	2.70, 0.30	0.81, 0.94	--
Stationary	2.35, 0.40	2.82, 0.27	1.72, 0.63	--

Table 15. Q and P-values calculated by comparing the domoic acid concentrations of dDA, pDA, total DA normalized to cell density (referred to as quotas in text), during the exponential growth phase, using one-way ANOVAs with Tukey's HSD multiple comparisons test. An asterisk indicates a significant difference ($p < 0.05$) between pH treatments.

pH Treatment (statistical value)	8.10 (q, p)	8.00 (q, p)	7.90 (q, p)	7.80 (q, p)
8.10				
dDA	--	1.11, 0.86	0.88, 0.92	0.44, 0.99
pDA	--	0.81, 0.94	0.23, 0.99	0.38, 0.99
Total DA	--	0.65, 0.97	0.65, 0.97	0.12, 0.99
8.00				
dDA	1.11, 0.86	--	0.22, 0.99	0.66, 0.96
pDA	0.81, 0.94	--	0.58, 0.98	1.19, 0.83
Total DA	0.65, 0.97	--	0.00, 0.99	0.77, 0.95
7.90				
dDA	0.88, 0.92	0.22, 0.99	--	0.44, 0.99
pDA	0.23, 0.99	0.58, 0.98	--	0.62, 0.97
Total DA	0.65, 0.97	0.00, 0.99	--	0.77, 0.95
7.80				
dDA	0.44, 0.99	0.66, 0.96	0.44, 0.99	--
pDA	0.38, 0.99	1.19, 0.83	0.62, 0.97	--
Total DA	0.12, 0.99	0.77, 0.95	0.77, 0.95	--

Table 16. Q and P-values calculated by comparing the domoic acid concentrations of dDA, pDA, total DA (dDA + pDA) normalized to cell density (referred to as quotas in text), during the stationary growth phase, using one-way ANOVAs with Tukey's HSD multiple comparisons test. An asterisk indicates a significant difference ($p < 0.05$) between pH treatments.

pH Treatment (statistical value)	8.10 (q, p)	8.00 (q, p)	7.90 (q, p)	7.80 (q, p)
8.10				
dDA	--	1.85, 0.59	0.72, 0.96	2.41, 0.38
pDA	--	2.06, 0.50	7.88, 0.002*	15.38, < 0.0001*
Total DA	--	1.00, 0.89	6.00, 0.005*	14.08, < 0.0001*
8.00				
dDA	1.85, 0.59	--	2.56, 0.34	4.25, 0.07
pDA	2.06, 0.50	--	5.81, 0.01*	13.32, < 0.0001*
Total DA	1.00, 0.89	--	5.99, 0.02*	13.08, < 0.0001*
7.90				
dDA	0.72, 0.96	2.56, 0.34	--	1.69, 0.65
pDA	7.88, 0.002*	5.81, 0.01 *	--	7.51, 0.003*
Total DA	6.00, 0.005*	5.99, 0.02 *	--	7.09, 0.004*
7.80				
dDA	2.41, 0.38	4.25, 0.07	1.69, 0.65	--
pDA	15.38, < 0.0001*	13.32, < 0.0001*	7.51, 0.003*	--
Total DA	14.08, < 0.0001*	13.08, < 0.0001*	7.09, 0.004*	--

Table 17. Q and P-values calculated by comparing Chl *a* concentrations normalized to cell density, during exponential and stationary growth phases, using one-way ANOVAs with Tukey's HSD multiple comparisons test. An asterisk indicates a significant difference ($p < 0.05$) between pH treatments.

pH treatment (statistical value)	8.10 (q, p)	8.00 (q, p)	7.90 (q, p)	7.80 (q, p)
8.10				
Exponential	--	2.20, 0.45	4.14, 0.07	3.79, 0.10
Stationary	--	1.04, 0.88	3.29, 0.17	1.82, 0.59
8.00				
Exponential	2.20, 0.45	--	1.94, 0.55	1.59, 0.69
Stationary	1.04, 0.88	--	2.25, 0.44	0.78, 0.94
7.90				
Exponential	4.14, 0.07	1.94, 0.55	--	0.35, 0.99
Stationary	3.29, 0.17	2.25, 0.44	--	1.47, 0.73
7.80				
Exponential	3.79, 0.10	1.59, 0.69	0.35, 0.99	--
Stationary	1.82, 0.59	0.78, 0.94	1.47, 0.73	--

Table 18. Q and P-values calculated by comparing particulate carbon:particulate nitrogen (C:N) molar ratios, during exponential and stationary growth phases, using one-way ANOVAs with Tukey's HSD multiple comparisons test. An asterisk indicates a significant difference ($p < 0.05$) between pH treatments.

pH Treatment (statistical value)	8.10 (q, p)	8.00 (q, p)	7.90 (q, p)	7.80 (q, p)
8.10				
Exponential	--	1.18, 0.84	0.68, 0.96	1.35, 0.78
Stationary	--	0.63, 0.97	4.09, 0.08	5.24, 0.03 *
8.00				
Exponential	1.18, 0.84	--	1.86, 0.58	2.53, 0.35
Stationary	0.63, 0.97	--	4.72, 0.04 *	5.87, 0.01 *
7.90				
Exponential	0.68, 0.96	1.86, 0.58	--	0.67, 0.96
Stationary	4.09, 0.08	4.72, 0.04 *	--	1.16, 0.85
7.80				
Exponential	1.35, 0.78	2.53, 0.35	0.67, 0.96	--
Stationary	5.24, 0.03 *	5.87, 0.01 *	1.16, 0.85	--

Table 19. Q and P-values calculated by comparing cellular N quotas, during exponential and stationary growth phases, using one-way ANOVAs with Tukey's HSD multiple comparisons test. An asterisk indicates a significant difference ($p < 0.05$) between pH treatments.

pH treatment (statistical value)	8.10 (q, p)	8.00 (q, p)	7.90 (q, p)	7.80 (q, p)
8.10				
Exponential	--	1.57, 0.70	3.56, 0.13	4.69, 0.04 *
Stationary	--	0.74, 0.95	2.16, 0.47	2.95, 0.24
8.00				
Exponential	1.57, 0.70	--	2.00, 0.53	3.13, 0.20
Stationary	0.74, 0.95	--	2.90, 0.25	3.69, 0.12
7.90				
Exponential	3.56, 0.13	2.00, 0.53	--	1.13, 0.85
Stationary	2.16, 0.47	2.90, 0.25	--	0.79, 0.94
7.80				
Exponential	4.69, 0.04 *	3.13, 0.20	1.13, 0.85	--
Stationary	2.95, 0.24	3.69, 0.12	0.79, 0.94	--

Table 20. Q and P-values calculated by comparing cellular C quotas, during exponential and stationary growth phases, using one-way ANOVAs with Tukey's HSD multiple comparisons test. An asterisk indicates a significant difference ($p < 0.05$) between treatments.

pH treatment (statistical value)	8.10 (q, p)	8.00 (q, p)	7.90 (q, p)	7.80 (q, p)
8.10				
Exponential	--	3.48, 0.14	5.51, 0.02 *	3.62, 0.12
Stationary	--	0.26, 0.99	0.57, 0.98	0.84, 0.93
8.00				
Exponential	3.48, 0.14	--	2.03, 0.51	0.14, 0.99
Stationary	0.26, 0.99	--	0.82, 0.94	1.10, 0.86
7.90				
Exponential	5.51, 0.02 *	2.03, 0.51	--	1.89, 0.57
Stationary	0.57, 0.98	0.82, 0.94	--	0.28, 0.99
7.80				
Exponential	3.62, 0.12	0.14, 0.99	1.89, 0.57	--
Stationary	0.84, 0.93	1.10, 0.86	0.28, 0.99	--

Discussion

I. *Preliminary Experiment*:

The saturating growth irradiance of *Pseudo-nitzschia australis* (HAB 327b) was ca. 140 µmol photons • m^{-2} • s^{-1}, when cultures were maintained at 13°C. This is in agreement with previous studies, which utilized different strains of this toxigenic diatom species (Cochlan et al. 2008; Bill et al. 2011; Thorel et al. 2014). However, Thorel et al. (2014), using a strain of *P. australis* isolated from the NW coast of France, reported a somewhat reciprocal relationship between irradiance and the optimum temperature to achieve maximal growth rates. In their study, at the lowest PPFD tested (35 µmol photons • m^{-2} • s^{-1}), the maximum growth rate ($\mu = 0.47 \pm 0.14$ d^{-1}) was found at 18.6 ± 3.3°C. At the highest PPFD tested (400 µmol photons • m^{-2} • s^{-1}), the maximum growth rate ($\mu = 0.66 \pm 0.07$ d^{-1}) was observed at 13.5 ± 0.7°C. Additionally, the highest growth rate reported ($\mu = 0.83 \pm 0.04$ d^{-1}) was achieved at an irradiance of 100 µmol photons • m^{-2} • s^{-1} and a temperature of 17.4 ± 0.7°C.

Using a strain isolated from the central California coast, Cochlan et al. (2008) found a maximal growth rate ($\mu = 1.81$ d^{-1}) at 100 µmol photons • m^{-2} • s^{-1} when cultures were maintained between 13 – 14°C. They also observed no change in specific growth rate at the highest PPFD tested (334 µmol photons • m^{-2} • s^{-1}) when a constant temperature was maintained. A study by Bill et al. (2011), which

utilized the same unialgal neritic strain from California, observed a maximum growth rate (μ =1.44 d^{-1}) at 334 µmol photons • m^{-2} • s^{-1} when cultures were maintained at 13°C, although growth rates saturated at an irradiance of ca. 200 µmol photons • m^{-2} • s^{-1}. In the present study, although the optimal temperature for growth was not determined, at the experimental temperature of 13°C the growth rates are in agreement with previous studies, which indicate that the saturating PPFD for growth of most tested neritic strains of *P. australis* ranges from 100 – 200 µmol photons • m^{-2} • s^{-1}.

II. *Primary Experiment—Exponential Growth Rates*

In the three highest pH treatments (pH = 8.1, 8.0, 7.9), the specific growth rates of the *P. australis* (HAB 200) cultures did not change significantly, despite differences in the concentration of dissolved CO_2 and seawater pH. Similarly, other laboratory studies have reported that changes in CO_2 availability and/or alterations in seawater pH do not affect the specific growth rate of other diatoms, including *Chaetoceros brevis* (Boelen et al. 2011), *C. muelleri* (Ihnken et al. 2011), and *Thalassiosira pseudonana* (Crawfurd et al. 2011; Yang and Gao 2012), as well as natural field assemblages of diatoms (Tortell et al. 2000; Hare et al. 2007; Gao et al. 2012).

Many marine phytoplankton, particularly bloom-forming species, have the ability to maintain rapid growth even under conditions of low CO_2 availability (elevated pH) and it has been proposed that their utilization of an efficient and well-regulated CCM reduces their likelihood of becoming C-limited (Reinfelder 2011; Mackey et al. 2015). Most diatoms are believed to possess CCMs, although it is possible that some species differ in how they acquire and retain the inorganic carbon required to saturate photosynthesis (e.g., C_3 versus C_4 pathway; Giordano et al. 2005; Reinfelder 2011; Matsuda and Kroth 2014; Mackey et al. 2015). Trimborn et al. (2008) examined inorganic carbon acquisition in a strain of *P. multiseries,* and found strong evidence that it operates an efficient CCM, a physiological trait which may be shared by other bloom-forming species of the *Pseudo-nitzschia* genus. However, growth would not have been limited by C-availability in the present study since the highest pH tested was only 8.1, and the cultures were enriched with dissolved CO_2 to maintain specific pH levels/DIC concentrations. Thus, it is not surprising that the specific growth rates did not significantly differ among the three higher pH (lower pCO_2) treatments, regardless if *P. australis* operates a CCM.

The growth rate of *P. australis* cultures maintained at the lowest pH tested (pH 7.8) was ca. 30% lower than the rate achieved in the other three pH treatments. This is surprising if one assumes that *P. australis* operates a CCM,

given that an increase in the bioavailability of dissolved CO_2 is generally predicted to benefit those species with a CCM, as increased dissolved CO_2 is thought to either relieve or down-regulate the energy required for maintaining CCM activity, thereby freeing additional energy for use in other cellular processes such as growth. Both, Sun et al. (2011) and Tatters et al. (2012) reported elevated growth rates for cultures of *Pseudo-nitzschia multiseries* (ca. 16% increase) and *P. fraudulenta* (ca. 33% increase), respectively, when maintained in semi-continuous, nutrient-replete cultures under conditions of increased pCO_2/low pH (ca. 750 µatm/pH 7.9). Others have also reported increased growth rates for different diatom genera when cultured under conditions of increased CO_2 availability and/or low pH, although it should be noted that there is little consistency among experimental conditions employed in these studies (Wu et al. 2010; Low-Décarie et al. 2011; Yang and Gao 2012; McCarthy et al. 2012).

Gao et al. (2012) observed that growth irradiance modulates the relationship between pCO_2 and the specific growth rate realized for cultures of *Phaeodactylum tricornutum*, *Skeletonema costatum*, and *Thalassiosira pseudonana*. These authors demonstrated that cells grown at high-CO_2 (1,000 µatm) experienced light stress when cultured at PPFDs above a particular 'threshold' (>125 – 178 µmol photons $\cdot$ m^{-2} $\cdot$ s^{-1}), whereas cultures grown at ambient-CO_2 (385 µatm) showed either an increase or no change in growth at the

same PPFDs. However, under lower PPFD (≤125 – 178 µmol photons • m^{-2} • s^{-1}), high-CO_2-grown cultures generally grew faster than those at ambient-CO_2 for all three species. Interestingly, at a PPFD of ca. 250 µmol photons • m^{-2} • s^{-1}, which is ca. the same PPFD used in the present study, the growth rate of *T. pseudonana* was ca. 20% lower in the high-CO_2 treatment compared to cultures at ambient-CO_2.

Heiden et al. (2016) reported somewhat similar results using cultures of the Antarctic diatoms, *Fragilariopsis curta* and *Odontella weisflogii*, where at an irradiance of 200 µmol photons • m^{-2} • s^{-1}, the growth rates were lower for cultures maintained at high (1,000 µatm) versus ambient (380 µatm) pCO_2. However, at an irradiance of 1,000 µmol photons • m^{-2} • s^{-1}, they found no significant differences in the growth rates of cultures maintained at different levels of pCO_2. Clearly, the specific growth rate of certain diatoms can be adversely affected by a synergistic relationship between PPFD and pCO_2 but this response is likely species-dependent and thus warrants further investigation.

In the present study, it is possible that the ca. 30% reduction in the specific growth rate of the *P. australis* cultures maintained at the highest CO_2 concentration (pH 7.8), was related to cells experiencing some degree of light stress, since the growth irradiance used here was 240 µmol photons • m^{-2} • s^{-1}, approximately the same as employed by Gao et al. (2012). The previous *Pseudo-nitzschia* studies of

Sun et. al (2011) and Tatters et al. (2012) used growth irradiances of only 120 and 90 µmol photons • m^{-2} • s^{-1} for *P. multiseries* and *P. fraudulenta*, respectively, both of which are below the 'threshold' PPFD range of 125 – 178 µmol photons • m^{-2} • s^{-1} reported by Gao et. al (2012). Their use of low growth PPFDs may partially account for their reported increases in specific growth rates with increasing pCO_2. Additionally, they used pCO_2 levels (equivalent to pH = 7.9) that were less than either the diatom studies of Gao et al. (2012), Heiden et al. (2016), or the present work with *P. australis*, which used greater pCO_2 levels to maintain pH as low as 7.8.

Decreasing pH can also affect cellular membrane potential, enzyme activity, and energy partitioning (e.g., Beardall and Raven 2004; Giordano et al. 2005), all of which may influence cell metabolism and growth rate. Altered transmembrane potential affects a wide range of cellular processes, such as nutrient uptake and excretion, that depend upon proton pumps. In the present study, both the average Si:N and Si:P drawdown ratios decreased with reduced pH/increased pCO_2 (Figure 6A-B), indicative of higher uptake rates of NO_3^- and PO_4^{3-}, relative to $Si(OH)_4$, in the more acidic (lower pH) treatments. Cell-normalized uptake rates confirm that $Si(OH)_4$ uptake decreased slightly with reduced pH, while the uptake of NO_3^- increased, although there was a slight drop at pH 7.8 (Figure 7A-B). However, it is important to note that cell-normalized

uptake rates of NO_3^- were always greater than the uptake rates for $Si(OH)_4$, regardless of pH treatment.

The cellular Si metabolism of the diatom *T. weissflogii* has been reported to change as a function of pCO_2 (Milligan et al. 2004). Although for nutrient-replete batch cultures, intracellular influx of Si was similar at both low (ca. 100 µatm) and high (ca. 750 µatm) pCO_2 conditions, Si efflux more than doubled in the high pCO_2 treatment. Additionally, Si dissolution rates were 6 to 7-fold greater at the low pH (7.7) versus high pH (8.4), and actual rates of Si incorporation into the frustules were reduced in the low pH/high pCO_2 treatment. Although less efficient retention and incorporation of Si taken up under acidified conditions did not result in decreased cellular division rates of *T. weissflogii*, it should not be discounted as a potential limiting factor in the present study that could help to explain the decreased growth rate reported for *P. australis* under the lowest pH treatment tested in the present study. The effects of seawater carbonate chemistry on the Si metabolism of diatoms are still not well understood, and further work is required, as taxon-specific differences are likely to occur.

The decline in growth rate of *P. australis* at pH 7.8 appears unrelated to photosynthesis and/or carbon acquisition since the P-E curves of exponentially growing cells clearly show that photosynthetic rates were not inhibited by differences in seawater pH and/or the increased availability of CO_2 (Figure 8).

The measured photosynthetic parameters were all very similar (and statistically indistinguishable) among treatments when normalized to either Chl *a* or PC (Figure 8B-C). More importantly, when photosynthetic rates are normalized to cell density, the maximum rate of photosynthesis per cell (P_m^{cell}) was significantly greater in cultures grown at pH 7.8 compared to pH 8.1 (Fig 8A; Table 11), suggesting that there was limited or no damage to the photosynthetic capacity of *P. australis* in the low pH treatments. Furthermore, the cellular fluorescence capacity (F_v/F_m) of the *P. australis* cultures were indicative of positive photophysiological health during nutrient-replete exponential growth, with relatively constant values (0.58 to 0.60) that did not vary as a function of pH (Table 8).

Iron (Fe) is another biologically important element, which is required by diatoms for growth and photosynthesis (e.g., Raven et al. 1999). However, the chemistry of Fe in seawater is complex, and its bioavailability to phytoplankton is pH sensitive (Millero et al. 2009; Shi et al. 2010). In Fe uptake experiments using three model diatoms (*T. weissflogii*, *T. oceanica*, and *P. tricornutum*), significant decreases in Fe uptake rates were observed in cultures at reduced seawater pH (Shi et al. 2010). This effect was particularly evident when the Fe enrichments were chelated by an excess of the organic chelating agent ethylenediaminetetraacetic acid (EDTA). The authors concluded that the decreased Fe uptake rates were not a physiological response by the diatoms, but rather the result of pH induced changes

in Fe chemistry – the dissociation of Fe from EDTA releases approximately 2.3 protons (H^+) at a pH of 8.1, and this reaction becomes increasingly less favorable as pH declines. They also showed that the Fe requirement of these diatoms did not change with alterations in seawater pH. In the present study, EDTA (6.6 μM) was also used to chelate the excess Fe added to the seawater culture medium, however, EDTA was not added in excess as in Shi et al. (2010). More importantly, their study was conducted under trace-metal clean conditions, and their diatom cultures were only enriched with nanomolar levels of Fe, in contrast to the micromolar enrichments used here. Although it is possible that reduced Fe uptake may be partially responsible for the observed decline in growth rate at pH 7.8, the high Fe enrichment, paired with the equal molar enrichments of EDTA used in the *P. australis* cultures, render this explanation as very unlikely.

III. *DA Quotas —Exponential Versus Stationary Growth*

Culture studies using toxigenic strains of *Pseudo-nitzschia* have demonstrated that DA production generally changes as a function of cellular growth phase (cf. reviews by Bates 1998; Pan et al 1998; Bates and Trainer 2006). However, the magnitude of these changes varies depending on the nutritional or physical limitation(s) that causes the transition from exponential to stationary growth (cf. reviews by Lelong et al. 2012; Trainer et al. 2012). Generally, DA

concentrations are low or non-detectable in exponentially-growing cells, but rapidly increase as division rates slow and the cells enter stationary phase. This trend was observed in the present study, where total DA cell quotas were 2-7 fold greater during stationary growth versus exponential growth, within the respective pH treatments (Figure 12; Table 7). Garrison et al. (1992) also detected DA during both the exponential and stationary growth phases of batch cultures of two *P. australis* isolates from Monterey Bay, CA. Here they found the greatest cellular quotas of pDA (12 and 37 pg pDA · $cell^{-1}$) after 2-3 days in stationary phase – although pDA declined in both isolates thereafter. Cusack et al. (2002) used a different strain *P. australis* isolated from the south coast of Ireland, and also found detectable levels of pDA during the late exponential phase, which increased steadily over several weeks of stationary growth in cultures under high PPFD (115 µmol photons · m^2 · s^{-1}). More recently, similar pDA quotas during the exponential growth phase (ranging from 0.50 to ca. 2.3 pg pDA · $cell^{-1}$) were reported for a *P. australis* isolate from northwestern Baja California, Mexico (Santiago-Morales and García-Mendoza, 2011) when cultured under high irradiance (200 µmol photons · m^2 · s^{-1}) and two Si:NO_3 ratios (0.5 and 2.5). However, the highest pDA quotas (2.9 and 3.3 pg pDA · $cell^{-1}$) were measured after several days in the stationary phase. Therefore, the results of the current study are in agreement with previous findings where lower, but detectable cellular

pDA quotas are found during the exponential growth phase of *P. australis*, with higher pDA quotas present during the stationary phase of growth.

At the present time, it is not completely understood what causes DA production in *Pseudo-nitzschia* to change over the course of the growth cycle. However, macronutrient-limitation has been shown to be correlated with increased DA production during the stationary phase, although the physiological basis for these observations remain elusive (e.g., Trainer et al. 2012). For example, several studies have shown that Si and/or P limitation are often linked to elevated DA production in *P. cuspidata* (Trainer et al. 2009), *P. multiseries* (Pan et al. 1996a, b, c; Kudela et al. 2004; Lundholm et al. 2004; Hagström et al. 2010; Sun et al. 2011), *P.* cf. *pseudodelicatissima* (Pan et al. 2001), and *P. seriata* (Fehling et al. 2004).

In the current study, the experiments were designed such that Si depletion would induce *P. australis* into stationary growth; however, the external concentrations of $Si(OH)_4$ and NO_3^- were depleted almost simultaneously from the culture media in all of the pH treatments (Figure 4 and 5). Internal nutrient pools were not measured, and thus their potential influence is unknown. Therefore, although it is clear that macronutrient limitation halted further biomass accumulation, it is not possible to conclude which nutrient ultimately was responsible for the initial induction of the stationary phase of growth. However, to

the author's knowledge, this is the first study to measure ambient macronutrient concentrations in batch cultures of *P. australis*, at this frequency, to determine if macronutrient limitation specifically caused the cells to transition from exponential to stationary growth.

Others, such as Cusack et al. (2002) only measured the initial macronutrient concentrations (760 μM NO_3^-, 250 μM $Si[OH]_4$, and 20 μM PO_4^{3-}) in their batch cultures, but based on these initial concentrations and the study length (30 days), it is much more likely that DIC became limited prior to depletion of either Si or P. Garrison et al. (1992) employed more ecologically realistic macronutrient concentrations (54 μM NO_3^-, 39 μM $Si[OH]_4$, and 3 μM PO_4^{3-}), and also measured macronutrients near the end (3.5 and 6.6 μM NO_3^-, 2.8 and 1.4 μM $Si[OH]_4$, and 0.1 and 0.1 μM PO_4^{3-}) of their 11 and 12 day experiments with *P. australis*. Although it is likely that nutrient limitation was responsible for inducing the stationary phase in their study, it is not clear which nutrient was depleted first, since the temporal relationship between nutrient drawdown and cell abundance was not determined. Therefore, even though the reported nutrient data alludes to the possibility that stationary growth may have been induced by nutrient limitation in Garrison et al. (1992), it cannot be assumed since other biochemical factors including carbon limitation or the associated increase in pH from photosynthetic activity (see below) may have prevented further biomass accumulation. Neither of

these factors would have impacted the present study since pH was rigorously monitored and controlled with CO_2 injection. Therefore, the current study demonstrates conclusively that macronutrient limitation ($Si[OH]_4$ and/or NO_3^-) initiated the stationary phase of cellular growth, and after ca. 2 days, total DA quotas (pDA + dDA) were 2-7 fold greater than in the late exponential growth phase.

Since DA is a secondary amino acid, N is required for its biosynthesis. The drawdown ratio of Si:N decreased linearly with decreasing pH (Figure 6), which indicates that NO_3^- was taken up relatively faster than $Si(OH)_4$ in cultures maintained at reduced pH. Cell-normalized drawdown rates (Figure 7A-B) confirm that NO_3^- was always taken up faster than $Si(OH)_4$, regardless of pH treatment (Figure 7A-B). Therefore, based on the initial macronutrient concentrations, calculated drawdown ratios, and cell-normalized drawdown rates, this would suggest almost simultaneous depletion of $Si(OH)_4$ and NO_3^- from the growth medium when cultured under the more acidic growth conditions. Thus, the intention to have Si-limitation alone induce the stationary growth phase was less likely realized in the cultures maintained at low pH. The result would be little to no ambient N available for continued DA synthesis once cellular division plateaued in these treatments. In spite of this, total DA $\cdot$ $cell^{-1}$ increased with decreasing pH after ca. two days of stationary growth and quotas were nearly 3-

fold greater at pH 7.8 compared to 8.1 (Figure 12; Table 7). However, it is quite possible that overall DA production may have been limited by NO_3^- availability in all of the pH treatments, since ambient concentrations in the media appear to have been depleted at or near the onset of the stationary phase, and any internal pools were likely utilized by the final sampling time (ca. two days into the stationary phase) although such measurements were not made. On the other hand, Cusack et al. (2002) observed a steady increase in cellular DA over several weeks of stationary growth in cultures of *P. australis*. However, their initially high NO_3^- concentrations (760 µM NO_3), compared to the much lower concentrations of 250 µM $Si[OH]_4$ and 20 µM PO_4^{3-} in their growth medium, presumably provided adequate N-substrate to facilitate the increase in total DA (pDA + dDA) measured over the course of the stationary phase. These authors reported a total DA quota of 0.65 pg DA · $cell^{-1}$ after ca. four days in the stationary phase and reached a maximum of 26.0 pg DA · $cell^{-1}$ after an additional 20 days. As in the present study, Garrison et al. (1992) used much more modest and ecologically realistic macronutrient concentrations which likely explains why they did not observe a similar increase in cellular DA quotas over time during the stationary phase.

In the present study, since DA production during stationary growth may have been limited by NO_3^- availability, the toxin results should be considered as conservative estimates of DA production, especially at the lower pH treatments.

Still the results clearly demonstrate a strong reciprocal relationship between DA production and seawater pH, with an approximate 3-fold increase in both pDA and total DA concentrations (pDA + dDA) normalized to cell abundance, as seawater pH decreased from pH 8.1 to 7.8

IV. *DA Quotas—Effects of pH/pCO_2*

During the nutrient-replete exponential growth phase, cell-normalized DA production did not significantly vary as a function of pH treatment, but both pDA and total DA quotas during the Si/NO_3-depleted stationary growth phase increased significantly by as much as 3-fold in the lowest pH treatment (pH 7.8) compared to the control (pH 8.1). However, within pH treatments, cellular quotas of pDA, dDA, and total DA during the stationary growth phase were 2 to 7-fold higher than the cellular quotas measured during the exponential growth phase. Relatively few studies have examined the effects of pH and/or pCO_2 on toxin production in *Pseudo-nitzschia*. Early work by Lundholm et al. (2004) found that DA production increased once growth became limited by elevated pH in batch cultures of *P. multiseries*. Similarly, Trimborn et al. (2008) observed a 70-fold increase in pDA concentrations of *P. multiseries* when maintained at pH 8.9 compared to 7.9. However, it should be noted that they employed semi-continuous culturing methodology where cultures are diluted once or twice per day (to maintain

constant pH conditions and exponential cellular growth), throughout the entire experiment (i.e., cultures never experienced stationary growth). Additionally, the pH of their growth medium was adjusted through additions of HCl or NaOH, and not by directly bubbling with CO_2, as in the present work. Sun et al. (2011) and Tatters et al. (2012) also employed similar semi-continuous culturing methods, but maintained pH by using CO_2 bubbling, and examined the interactive effects of OA and either P or Si-limitation with *P. multiseries* and *P. fraudulenta*. Sun et al. (2011) demonstrated that P-limitation, in conjunction with reduced pH/elevated pCO_2, increased total DA production (pDA +dDA) by >3-fold in *P. multiseries*. They also observed approximately a 2 to 3-fold increase in total DA production with P-replete cultures under the same conditions of pH/pCO_2, although these values were 30 to 50-fold lower than those reported for P-limited cultures at corresponding levels of pH/pCO_2. Tatters et al. (2012) reported a similar trend for *P. fraudulenta*, where total DA production in Si-limited cultures was 7 to18-fold higher than under Si-replete conditions at corresponding pCO_2 concentrations. Total DA production also increased with decreasing pH under Si-replete conditions, although statistically significant increases were only observed in the Si-limited treatments. The results of the current study support the findings of Sun et al. (2011) and Tatters et al. (2012), and clearly demonstrate that reduced

pH/elevated pCO_2 conditions, in conjunction with macronutrient limitation, leads to increased DA production in *Pseudo-nitzschia australis*.

It is still unclear why or how differences in pH/CO_2 availability affects DA production in *Pseudo-nitzschia*. It is possible that changes in seawater pH modifies the internal pH of cells, which would likely alter different enzymatic processes, including DA production. Lundholm et al. (2004) suggested that biosynthesis of DA may be optimized at a particular pH. However, this hypothesis requires further investigation since both elevated pH (Lundholm et al. 2004; Trimborn et al. 2008) and lower pH levels (Sun et al. 2011; Tatters et al. 2012; current study) have been linked to greater cellular DA concentrations. Additionally, until the physiological pathway of DA production has been fully mapped, it will be difficult to conclude any specific effects of extra- or intracellular pH changes on DA biosynthesis in *Pseudo-nitzschia*.

Although it has not been investigated, pH-induced shifts in the bacterial communities associated with *Pseudo-nitzschia* cells might also play an important role in the regulation of DA production. In the current work, microscopic analysis of live whole culture samples revealed that bacteria were present in the culture flasks of every pH treatment – most bacteria were observed moving freely in the media, but often they appeared to be associated/attached to the outside of *P. australis* cells. Bacteria are known to form complex relationships with various

species of *Pseudo-nitzschia,* and DA production is enhanced in xenic cultures compared axenic cultures (Douglas et al. 1993; Bates et al. 1995a, b; Kotaki et al. 2008; Kobayashi et al. 2003, 2009; reviewed in Lelong et al. 2012). However, the reasons for this are unknown, and there is currently no evidence that bacteria are capable of producing DA autonomously, although it has been suggested they may supply *Pseudo-nitzschia* cells with specific compounds necessary for DA synthesis or that function as cellular signals that elicit DA production (Bates et al. 1998, 2004). Regardless, further investigation into how bacterial associations may be affected by changes in pH/pCO_2 would provide valuable information on their potential role in DA synthesis.

In addition to their being affected by seawater pH, the availability and speciation of different trace metals, such as Fe and Cu, have also been linked to DA production (Maldonado et al. 2002; Ladizinsky 2003; Wells et al. 2005; Shi et al. 2010). It has been suggested that *Pseudo-nitzschia* may utilize DA as a means to alleviate Fe-limitation by chelating Fe that is otherwise biologically unavailable in the surrounding seawater, thus making it more accessible (Maldonado et al. 2002; Wells et al. 2005). On the other hand, high concentrations of Cu are known to be harmful to phytoplankton and it is thought that DA may function to chelate excess Cu as a defense against toxicity (Maldonado et al. 2002; Ladizinsky 2003). However, *P. australis* cultures in the present work were grown in seawater

medium where enrichments of Fe and Cu were added in concentrations that were neither limiting nor toxic (6.6 μM Fe; 0.08 μM Cu). Additionally, if pH-induced Fe-limitation or Cu-toxicity had occurred during the present experiments, relatively high concentrations of dissolved DA would be expected in the growth media. However, measured concentrations of dDA during both growth phases were relatively low (0.48– 23.70 ng mL^{-1}), and cell-normalized concentrations reported in this study were always less than particulate DA regardless of pH treatment (Figure 12; Table 7).

The availability of dissolved inorganic carbon (DIC) has also been suggested as a factor that may limit cellular DA production. It is possible that the increased concentrations of dissolved CO_2 in the low pH treatments allowed *P. australis* cells to down-regulate their CCM activity, preserving energy which could then be allocated to increase DA biosynthesis. However, cellular DA concentrations during the exponential growth phase did not significantly vary with pH, despite the increase in rates of carbon fixation per cell in the two lowest pH treatments (Figure 8A; Table 4). Although DA concentrations increased with decreasing pH during the stationary phase, the CO_2 injection and monitoring system maintained the cultures at the desired experimental pH/pCO_2 conditions, and thus eliminated the possibility of carbon limitation during these experiments.

V. *Photosynthesis Versus Irradiance (P-E) Curves and Cellular Carbon Quotas*

The photosynthetic response of *P. australis* to dissolved CO_2 enrichment differs slightly, depending on the parameter used to normalize the photosynthetic rates of ^{14}C uptake as a function of PPFD (Figure 8; Tables 4-6). When Chl *a* or PC is used, no significant differences were detected as a function of pH between any of the P-E parameters, indicating no measurable effects of CO_2 availability or pH on photosynthetic carbon fixation. The maximum rates of carbon fixation (P_m^{Chl} and P_m^C) for all pH treatments are similar to those reported by Pan et al. (1991) for a strain of exponentially growing *P. multiseries* maintained under continuous light at a PPFD of 105 µmol photons $\cdot$ m^{-2} $\cdot$ s^{-1} and a temperature of 10°C (Table 10). However these chlorophyll normalized rates of P_m^{Chl} were ca. 2-fold less than those reported for a different strain of exponentially growing *P. multiseries* maintained at a higher temperature (17°C) and different light cycle (12:12 L:D; 120 µmol photons $\cdot$ m^{-2} $\cdot$ s^{-1}; Sun et al. 2011; Table 10). P_m^{Chl} values for *P. australis* were observed to increase with decreasing pH (from pH 8.1 – 7.9), a trend that was similarly reported by Sun et al. (2011) for *P. multiseries* over their range of pH tested (Table 10). The values reported in the present study for the light-limited (initial) slope of the chlorophyll-normalized curves (α^{Chl} ; photosynthetic efficiency) are comparable to those reported by Sun et al. (2011), whereas the α^{Chl} values of Pan et al. (1991) and Pan et al. (1996) are ca. 2 to 5 fold lower (Table

10). The inconsistency of these previous results with those of the present work, may be related to the different experimental growth temperatures employed by each study, as Pan et al. (1993) showed that values of α^{Chl}, α^{C}, P_m^{Chl}, and P_m^{C} increased exponentially between maintenance temperatures of 0-15°C in cultures of *P. multiseries*. Additionally, because each study employed a unique diel light cycle in their culturing methodology (i.e. continuous versus non-continuous light), direct comparisons between the photosynthetic results is challenging.

When the P-E curves of *P. australis* are normalized to cell density, the maximum rate of carbon fixation (P_m^{cell}) increases with decreasing pH, and although there is a slight decrease (ca. 10%) at pH 7.8, the average rate is still greater than P_m^{cell} at pH 8.1 and 8.0 by ca. 14% and 24%, respectively (Figure 8A; Table 4). Since P_m^{cell} represents the maximum possible rate of photosynthesis that cells can achieve under saturating light, the increased values of P_m^{cell} in the reduced pH/elevated pCO_2 treatments, indicate that potential photosynthetic production by *P. australis* may be greater under conditions of ocean acidification. However, the average values of P_m^{cell} at pH 7.8 were ca. 10% lower than those measured at pH 7.9 and although this difference was not statistically significant, it's possible that under even greater pCO_2 conditions (not measured here), that the effects of acidification on photosynthetic performance may become less pronounced. In any case, for *P. australis*, the response of photosynthesis to increasing pCO_2 was not

linear in the present study. Using *P. multiseries* cultures, Pan et al. (1991) reported values of P_m^{cell} and α^{cell} that were ca. 3 to 4-fold and ca. 8 to 9-fold lower, respectively, than values for all of the pH treatments in the present work, however, these differences may be the result of the 4-fold greater content of Chl *a* · $cell^{-1}$ found in *P. australis* compared to *P. multiseries*. Furthermore, it is possible that part of the reason there were no significant variations in most of the photosynthetic parameters, regardless of which variable was used to normalize the P-E curves, was due to the relative constancy of Chl *a* · $cell^{-1}$ among the pH treatments (Pan et al. 1991; MacIntyre et al. 2002).

The average cellular quotas of PC (pmol C · $cell^{-1}$; Figure 11B) followed a trend similarly observed for the values of P_m^{cell} as a function of pH treatments, where values increased with decreasing pH but dropped slightly (ca. 9%) at pH 7.8, which suggests that cellular PC quotas may have been closely linked to the photosynthetic rates at the various pH treatments. Therefore, under conditions of increasing acidity predicted to occur by the end of the century, *P. australis* may produce increased quantities of cellular carbon, from elevated cellular photosynthetic rates during exponential growth that could have a potentially positive ecological effect by increasing C flux to the ocean floor. However, PC quotas during the stationary growth phase did not vary among pH treatments and it is possible that cells at the reduced pH levels released a greater proportion of their

fixed carbon as DOC, but this was not measured in the current work. A recent study by Taucher et al. (2015) found that cultures of the diatom *Thalassiosira weissflogii* produced greater quantities of DOC during the stationary growth phase when grown at low pH/high pCO_2.

In the present study flocculates of cells were observed in every culture vessel on the final sampling day and this appeared to be more pronounced at the reduced pH treatments, Diatoms often release transparent exopolymer particles (TEP) – sticky, carbon-rich compounds that capture cells and other organic material, forming aggregates that can sink and thus enhance carbon flux from the euphotic zone to the deep ocean. A recent study found that elevated pCO_2 significantly enhanced TEP accumulation during the stationary growth phase by 12% and 35% in cultures of the diatoms *T. weissflogii* and *D. fragilissimus*, respectively (Taucher et al. 2015). Therefore, it's possible that at reduced pH, a greater amount of mucus-like TEP was released by the *P. australis* cells, which would have contributed to the observed flocculation and help to account for why cellular PC quotas did not increase with decreasing pH during the stationary phase as observed during the exponential phase (Figure 10B).

VI. *Ecological Implications and Summary*

The results of this unialgal laboratory study of a ubiquitous and highly toxic diatom strongly suggest that natural blooms of *P. australis* in coastal regions will become more toxic in a more acidic future Ocean. The pH/pCO_2 values tested here, are not only representative of those predicted for most surface waters of the World Ocean by the end of the century, but are already found off the West coast of North America (e.g., Feely et al. 2008, 2016; Cochlan et al. unpublished results) and thus a greater understanding of the ecological implications of an increasingly acidified ocean are clearly warranted. The diatom *P. australis* is commonly found in temperate coastal areas, and often dominates the phytoplankton assemblages in upwelling regions off central and northern California, as seen during the massive toxic bloom along the U.S. West coast during 2015 (California Ocean Science Trust 2016; Du et al. 2016; McCabe et al. 2016;). In this eastern boundary upwelling system, the nutrient-replete waters that upwell to the surface are routinely found at pH levels not expected for the World Ocean until the year 2100 (Feely et al. 2008, 2016). Although this controlled culture study did not observe changes in cellular toxicity as a function of pH during nutrient-replete exponential growth, the cellular toxicity of *P. australis* increased almost 3-fold with decreasing pH during the nutrient-deplete stationary growth phase. Clearly, there is a complex interactive effect of seawater pH/pCO_2 and nutrient availability on DA

production in *P. australis*, a conclusion that supports the results of studies for two other species of this diatom genus.

Although the greatest cellular DA quotas during stationary growth were measured at pH 7.8, the average exponential growth rate of these cultures was 30% lower than the three higher pH treatments. This implies that *P. australis* experienced a reduction in biological fitness at the lowest pH, since its growth was clearly inhibited, although DA production by this diatom was not negatively affected. In fact, pDA and total DA quotas during the stationary growth phase increased as pH decreased with no noticeable impact on cellular growth, until the threshold pH of 7.8 was reached, where specific growth rate decreased substantially. In addition, there appeared to be no clear link between the exponential growth rates realized during nutrient-replete conditions and cellular toxicity in the nutrient-depleted stationary phase as a function of pH treatment. However, it is unclear whether the decline in the specific growth rate at pH 7.8 was the result of pH/pCO_2 directly impacting the physiology of *P. australis* cells or the indirect result of possible pH/pCO_2-induced changes in ambient nutrient availability/chemistry (i.e. Fe and/or $Si[OH]_4$), which could also have affected cell physiology and led the observed decline in growth rate.

In an ecological context, the reduction in specific growth rate could translate into a loss of competitive success for *P. australis* in a naturally mixed

species community, which would diminish its bloom-forming potential and thereby reduce the possible negative ecological/environmental consequences of elevated cellular toxicity at reduced pH. A recent long-term study examined the effects of acidification and warming on a southern California diatom community, which included *P. delicatissima*, and found that after 12 months of conditioning at low pH (~7.95), no *Pseudo-nitzchia* cells were detected despite the fact *P. delicatissima* initially composed 19% of the original community abundance (Tatters et al. 2013). Additional experiments assessing the long-term competitive success and evolutionary potential of *Pseudo-nitzschia* in mixed phytoplankton community experiments, to predicted future conditions of OA, would greatly contribute to our understanding of how these toxic organisms may impact marine ecosystems in the future.

Diatoms play a crucial role in the marine carbon cycle by exporting large quantities of fixed carbon to the ocean floor after large bloom events. The elevated values of P_m^{cell} and cellular PC observed at reduced pH during the exponential growth phase, suggest that in the future ocean, *P. australis* blooms may be capable of enhancing carbon flux from the atmosphere to the ocean interior, acting as a positive feedback mechanism for OA. However, the likelihood of this occurring will depend on the fate of the fixed organic carbon produced by *P. australis*, which was not investigated in the current study.

In summary, the knowledge gained from this controlled laboratory study clearly demonstrates that increasingly acidic seawater caused by elevated pCO_2, can affect the growth, photosynthesis, and toxic potential of *Pseudo-nitzschia australis*. However, more acidic conditions appear to affect measurable rates of growth and photosynthesis independent of their effects on DA production, or at least until a threshold pH value is reached. It is evident that the environmental factors that regulate growth and photosynthesis are not necessarily the same as those that regulate DA production and cellular toxicity. Future studies should investigate the interactive effects of OA and other environmental variables that are expected to respond to climate change, using other ecologically significant species of *Pseudo-nitzschia*. Longer-term experiments evaluating the evolutionary potential of these organisms to climate-induced perturbations of the marine environment would also be extremely valuable. Toxic blooms of *Pseudo-nitzschia* have major ecological and economic consequences, so it is imperative we continue to examine how these toxigenic diatoms respond to the ongoing climatic changes affecting the World Ocean and its inhabitants.

References

Anderson, D.M., Burkholder, J.M., Cochlan, W.P., Glibert, P.M., Gobler, C.J., Heil, C.A., Kudela, R.M., Parsons, M.L., Rensel, J.E., Townsend, D.W., Trainer, V.L., Vargo, G.A. 2008. Harmful algal blooms and eutrophication: examples of linkages from selected coastal regions of the United States. *Harmful Algae* 8: 39-53.

Auro, M.E. and Cochlan, W.P. 2013. Nitrogen utilization and toxin production by two diatoms of the *Pseudo-nitzschia pseudodelicatissima* complex: *P. cuspidata* and *P. fryxelliana. Journal of Phycology* 49: 156-169.

Bates, S.S., Bird, C.J., de Freitas, A.S.W., Foxall, R., Gilgan, M., Hanic, L.A., Johnson, G.R., McCulloch, A.W., Odense, P., Pocklington, R., Quilliam, M.A., Sim, P.G., Smith, J.C., Subba Rao, D.V., Todd, E.C.D., Walter, J.A., Wright, J.L.C. 1989. Pennate diatom *Nitzschia pungens* as the primary source of domoic acid, a toxin in shellfish from eastern Prince Edward Island, Canada. *Canadian Journal of Fisheries and Aquatic Sciences* 46: 1203– 1215.

Bates, S.S., de Freitas, A.S.W., Milley, J.E., Pocklington, R., Quilliam, M.A., Smith, J.C., Worms, J. 1991. Controls on domoic acid production by the diatom *Nitzschia pungens* f. *multiseries* in culture: nutrients and irradiance. *Canadian Journal of Fisheries and Aquatic Sciences* 48: 1136–1144.

Bates, S.S., Douglas, D.J., Doucette, G.J., Léger, C. 1995a. Effects of reintroducing bacteria on domoic acid production by axenic cultures of the diatom *Pseudo-nitzschia pungens* f. *multiseries*. In: Lassus, P., Arzul, G., Erard, E., Gentien, P., and Marcaillou, C. (Eds.). *Harmful Marine Algal Blooms*. Lavoisier Publishing, Paris: 401–406.

Bates, S.S., Douglas, D.J., Doucette, G.J., Léger, C. 1995b. Enhancement of domoic acid production by reintroducing bacteria to axenic cultures of the diatom *Pseudo-nitzschia multiseries*. *Natural Toxins* 3: 428–435.

Bates, S.S., Léger, C., Smith, K.M. 1996. Domoic acid production by the diatom Pseudo-nitzschia multiseries as a function of division rate in silicate-limited chemostat culture. In: Yasumoto, T., Oshima, Y., Fukuyo, Y. (Eds.). *Harmful and Toxic Algal Blooms*. Seventh International Conference on Toxic Phytoplankton, UNESCO. Sendai, Japan: 163–166.

Bates, S.S., Garrison, D.L., Horner, R.A. 1998. Bloom dynamics and physiology of domoic-acid-producing *Pseudo-nitzschia* species. In: Anderson, D.M., Cembella, A.D., Hallegraef, G.M. (Eds.). *Physiological Ecology of Harmful Algal Blooms*. Springer-Verlag, Berlin: 267–292.

Bates, S.S., Gaudet, J., Kaczmarska, I., Ehrman, J.M. 2004. Interaction between bacteria and the domoic-acid-producing diatom *Pseudo-nitzschia multiseries* (Hasle) Hasle; can bacteria produce domoic acid autonomously? *Harmful Algae* 3: 11–20.

Bates, S.S. and Trainer, V.L. 2006. The ecology of harmful diatoms. In: Granéli, E., Turner, J.T. (Eds.). *Ecology of Harmful Algae*. Springer-Verlag, Berlin: 81–88.

Beardall, J. and Raven, J.A. 2004. The potential effects of global climate change on microalgal photosynthesis, growth, and ecology. *Phycologia* 43: 26-40.

Berner, R.A. 2003. The long-term carbon cycle, fossil fuels, and atmospheric composition. *Nature* 426: 323-326.

Bill, B.D. 2011. Carbon and nitrogen uptake of toxigenic diatoms: *Pseudo-nitzschia australis* and *Pseudo-nitzschia turgidula*. Master of Science Thesis. San Francisco State University, San Francisco, CA, 118 pp.

Boelen, P., Van de Poll, W.H., Van der Strate, H.J., Neven, I.A., Beardall, J., Buma, A.G.J. 2011. Neither elevated nor reduced CO_2 affects the photophysiological performance of the marine Antarctic diatom *Chaetoceros brevis*. *Journal of Experimental Marine Biology and Ecology* 406: 38-45.

Brand, L.E. and Guillard, R.R.L. 1981. A method for the rapid and precise determination of acclimated phytoplankton reproduction rates. *Journal of Plankton Research* 3: 193-201.

Caldeira, K. and Wickett, M.E. 2003. Oceanography: anthropogenic carbon and ocean pH. *Nature* 425: 365. doi:10.1038/425365a.

California Ocean Science Trust. 2016. Frequently asked questions: harmful algal blooms and California fisheries, developed in response to the 2015-2016 domoic acid event. California Ocean Science Trust, Oakland, CA, 28 pp.

Chen, X. and Gao, K. 2003. Effect of CO_2 concentrations on the activity of photosynthetic CO_2 fixation and extracellular carbonic anhydrase in the marine diatom *Skeletonema costatum*. *Chinese Science Bulletin* 48: 2616-2620.

Cho, E.S., Kotaki, Y., Park, J.G. 2001. The comparison between toxic *Pseudo-nitzschia multiseries* (Hasle) Hasle and non-toxic *P. pungens* (Grunow) Hasle isolated from Jinhae Bay, Korea. *Algae* 16: 275–285.

Cochlan, W.P., Herndon, J., Kudela, R.M. 2008. Inorganic and organic nitrogen uptake by the toxigenic diatom *Pseudo-nitzschia australis* (Bacillariophyceae). *Harmful Algae* 8: 111-118.

Collins, S. 2012. Evolution on acid. *Nature Geoscience* 5: 310-311.

Crawfurd, K.J. Raven, J.A. Wheeler, G.L., Baxter, E.J., Joint, I. 2011. The response of *Thalassiosira pseudonana* to long-term exposure to increased CO_2 and decreased pH. *PLoS One* 6: e26695.

Cusack, C.K., Bates, S.S., Quilliam, M.A., Patching, J.W., Raine, R. 2002. Confirmation of domoic acid production by *Pseudo-nitzschia australis* (Bacillariophyceae) isolated from Irish waters. *Journal of Phycology* 38: 1106–1112.

Cushing, D.H. 1971. Upwelling and fish production. *Advances in Marine Biology* 9: 255-334.

Dickson, A.G. 1984. pH scales and proton-transfer reactions in saline media such as seawater. *Geochimica Et Cosmochimica Acta* 48: 2299-2308.

Dickson, A.G. and Millero, F.J. 1987. A comparison of the equilibrium constants for the dissociation of carbonic acid in seawater media. Deep Sea Research Part A: *Oceanography Research Papers* 34: 1733–1743.

Dickson, A.G. 1993. The measurement of seawater pH. *Marine Chemistry* 44: 131-142.

Dickson, A.G., Sabine, C.L., Christian, J.R. (Eds.). 2007. Guide to best practices for ocean CO_2 measurements. *PICES Special Publication* 3: 191 pp.

Doney, S.C., Fabry, V.J., Feely, R.A., Kleypas, J.A. 2009. Ocean acidification: The other CO_2 problem. *Annual Review of Marine Science* 1: 169-192.

Doney, S.C. 2010. The growing human footprint on coastal and open-ocean biogeochemistry. *Science* 328: 1512-1516.

Doney, S.C., Ruckelshaus, M., Emmett Duffy, J., Barry, J.P., Chan, F., English, C.A., Galindo, H.M., Grebmeier, J.M., Hollowed, A.B., Knowlton, N. and Polovina, J. 2012. Climate change impacts on marine ecosystems. *Annual Review of Marine Science* 4: 11-37.

Douglas, D.J., Bates, S.S., Bourque, L.A. Selvin, R.C. 1993. Domoic acid production by axenic and non-axenic cultures of the pennate diatom *Nitzschia pungens* f. *multiseries*. In: Smayda, T.J. and Shimizu, Y. (Eds.). *Toxic Phytoplankton Blooms in the Sea*. Elsevier Science Publishers B.V., Amsterdam: 595–600.

Du, X., Peterson, W., Fisher, J., Hunter, M. and Peterson, J. 2016. Initiation and development of a toxic and persistent *Pseudo-nitzschia* bloom off the Oregon coast in spring/summer 2015. *PloS One*: 11. p.e0163977.

Dugdale, R.C. and Goering, J.J. 1967. Uptake of new and regenerated forms of nitrogen in primary productivity. *Limnology and Oceanography* 12: 196-206.

Edler, L. and Elbrächter, M. 2010. The Utermöhl method for quantitative phytoplankton analysis, Chap. 2. In: Karlson, B., Cusack, C., and Bresnan, E. (Eds.). *Intergovernmental Oceanographic Commission of UNESCO: Microscopic and Molecular Methods for Quantitative Phytoplankton Analysis*. Paris, UNESCO. IOC Manuals and Guides, No. 55.

Eppley, R. W. and Peterson, B.J. 1979. Particulate organic matter flux and planktonic new production in the deep ocean. *Nature*, London 282: 677-680.

Feely, R.A., Sabine, C.L., Hernandez-Ayon, J.M., Lanson, D. Hales, B. 2008. Evidence for upwelling of corrosive "acidified" water onto the continental shelf. *Science* 320: 1490-1492.

Feely, R.A., Simone, R.A., Carter, B., Bednaršek, N., Hales, B., Chan, F., Hill, T.M., Gaylord, B., Sanford, E., Byrne, R.H., Sabine, C.L., Greeley, D., Juranek, L. 2016. Chemical and biological impacts of ocean acidification along the west coast of North America. *Estuarine Coastal and Shelf Science* 183: 260-270.

Fehling, J., Davidson, K., Bolch, C.J., Bates, S.S. 2004. Growth and domoic acid production by *Pseudo-nitzschia seriata* (Bacillariophyceae) under phosphate and silicate limitation. *Journal of Phycology* 40: 674–683.

Feng, Y., Hare, C.E., Leblanc, K., Rose, J., Zhang, Y., DiTullio, G.R., Lee, P.A., Wilhelm, S.W., Rowe, J.M., Sun, J. 2009. The effects of increased pCO_2 and temperature on the North Atlantic Spring Bloom. I. The phytoplankton community and biogeochemical response. *Marine Ecology Progress Series* 388: 13-25.

Fu, F.X., Tatters, A.O., Hutchins, D.A. 2012. Global change and the future of harmful algal blooms in the ocean. *Marine Ecology Progress Series* 470: 207-233.

Garrison, D.L., Conrad, S.M., Eilers, P.P., Waldron, E.M. 1992. Confirmation of domoic acid production by *Pseudo-nitzschia australis* (Bacillariophyceae) cultures. *Journal of Phycology* 28: 604–607.

Gao, K., Xu, J., Gao, G., Li, Y., Hutchins, D.A., Huang, B., Wang, L., Zheng, Y., Jin, P., Cai, X., Hader, D., Li, W., Xu, K., Liu, N., Riebesell ,U. 2012. Rising CO_2 and increased light exposure synergistically reduce marine primary productivity. *Nature Climate Change* 2: 519-523.

Garthwaite, I., Ross, K.M., Miles, C.O., Hansen, R.P., Foster, D., Wilkins, A.L., Towers, N.R. 1998. Polyclonal antibodies to domoic acid, and their use in immunoassays for domoic acid in seawater and shellfish. *Natural Toxins* 6: 93-104.

Giordano, M., Beardall, J., Raven, J.A. 2005. CO_2 concentrating mechanisms in algae: mechanisms, environmental modulation, and evolution. *Annual Review of Plant Biology* 56: 99-131.

Guillard, R.R.L. 1973. Division rates. In: *Handbook for Phycological Methods—Culture Methods and Growth measurements*. Cambridge University Press, Cambridge, UK: 289-311.

Guillard, R.R.L. and Sieracki, M.S. 2005. Counting cells in culture with the light microscope. In: Anderson, R.A. (Ed.). *Algal Culturing Techniques.* Academic Press, Elsevier: 117-132.

Hagström, J.A., Granéli, E., Moreira, M.O.P., Odebrecht, C. 2011. Domoic acid production and elemental composition of two *Pseudo-nitzschia multiseries* strains, from the NW and SW Atlantic Ocean, growing in phosphorus-or nitrogen-limited chemostat cultures. *Journal of Plankton Research* 33: 297–308.

Hallegraeff, G.M. 2010. Ocean climate change, phytoplankton community responses, and harmful algal blooms: a formidable predictive challenge. *Journal of Phycology* 46: 220-235.

Hare, C.E., Leblanc, K., DiTullio, G.R., Kudela, R.M., Zhang, Y., Lee, P.A., Riseman, S., Hutchins, D.A. 2007. Consequences of increased temperature and CO_2 for phytoplankton community structure in the Bering Sea. *Marine Ecology Progress Series* 352: 9–16.

Hauri, C., Gruber, N., Vogt, M., Doney, S.C., Feely, R.A., Lachkar, Z., Leinweber, A., McDonnell, A.M., Munnich, M., Plattner, G.-K. 2013. Spatiotemporal variability and long-term trends of ocean acidification in the California Current System. *Biogeosciences* 10: 193-216.

Heiden, J.P., Bischof, K., Trimborn, S. 2016. Light intensity modulates the response of two Antarctic diatom species to ocean acidification. *Frontiers in Marine Science* 3: 260. doi: 10.3389/fmars.2016.00260.

Hennon, G.M.M., Quay, P., Morales, R.L., Swanson, L.M., Armbrust, E.V. 2014. Acclimation conditions modify physiological response of the diatom *Thalassiosira pseudonana* to elevated CO_2 concentrations in a nitrate-limited chemostat. *Journal of Phycology* 50: 243-253.

Herve, V., Derr, J., Douady, S., Quinet, M., Moisan, L. 2012. Multiparametric Analyses reveal the pH-dependence of silicon biomineralization in diatoms. *PLoS One* 7: e46722. Dpo:10.1371/journal.pone.0046722.

Howard, M.D.A., Cochlan, W.P., Ladizinsky, N., Kudela, R.M. 2007. Nitrogenous preference of toxigenic *Pseudo-nitzschia australis* (Bacillariophyceae) from field and laboratory experiments. *Harmful Algae* 6: 206-217.

Ihnken, S., Roberts, S., Beardall, J. 2011. Differential responses of growth and photosynthesis in the marine diatom *Chaetoceros muelleri* to CO_2 and light availability. *Phycologia* 50: 182-193.

International Governmental Panel on Climate Change (IPCC). 2014. Climate change 2014: Synthesis Report. Contribution of Working Groups I, II, and III to the Fifth Assessment Report of the Intergovernmental Panel on Climate Change [Core Writing Team: Pachauri, R.K., Meyer, L.A. (eds.)]. IPCC, Geneva, Switzerland: 1-151. Available at: https://www.ipcc.ch/pdf/assessment-report/ar5/syr/SYR_AR5_FINAL_full.pdf.

Jackson, J.B.C. 2008. Ecological extinction and evolution in the brave new ocean. *Proceedings of the National Academy of Sciences of the United States* 105, Supplement 1: 11548-11465.

Kleypas, J.A., Feely, R.A., Fabry, V.J., Langdon, C., Sabine, C.L., Robbins, L.L. 2006. Impacts of ocean acidification on coral reefs and other marine calcifiers: a guide for future research. Workshop sponsored by NSF, NOAA & USGS.

Knepel, K. and Bogren, K. 2002. Determination of orthophosphate by flow injection analysis: QuickChem® Method 31-115-01-1-H. Lachat Instruments. Milwaukee,WI.

Kobayashi, K., Kobiyama, A., Kotaki, Y., Kodama, M. 2003. Possible occurrence of intracellular bacteria in *Pseudo-nitzschia multiseries*, a causative diatom of amnesic shellfish poisoning. *Fisheries Science* 69: 974–978.

Kobayashi, K., Takata, Y., Kodama, M. 2009. Direct contact between *Pseudo-nitzschia multiseries* and bacteria is necessary for the diatom to produce a high level of domoic acid. *Fisheries Science* 75: 771–776.

Kotaki, Y., Lundholm, N., Katayama, T., Furio, E.F., Romero, M.L., Relox, J.R., Yasumoto, T., Naoki, H., Hirose, M.Y., Thann, T.D., Thuoc, C.V. 2008. ASP toxins of pennate diatoms and bacterial effects on the variation in toxin composition. In: Moestrup, Ø. (Ed.). *Proceedings of the 12th International Conference on Harmful Algae.* International Society for the Study of Harmful Algae and Intergovernmental Oceanographic Commission of UNESCO, Copenhagen: 300–302.

Kudela, R., Roberts, A., Armstrong, M. 2004. Laboratory analysis of nutrient stress and toxin accumulation in *Pseudo-nitzschia* species from Monterey Bay, California. In: Steidinger, K., Landsberg, J.H., Tomas, C., Vargo, G. (Eds.). *Harmful Algae 2002, Florida Fish and Wildlife Conservation Commission.* Florida Institute of Oceanography, and Intergovernmental Oceanographic Commission of UNESCO, St. Petersburg, FL, USA: 136–138.

Ladizinsky, N. 2003. The influence of dissolved copper on the production of domoic acid by *Pseudo-nitzschia* species in Monterey Bay, California: laboratory experiments and field observations. Master of Science Thesis, California State University, Monterey Bay, CA, 68 pp.

Lelong, A., Hegaret, H., Soudant, P., Bates, S.S. 2012. *Pseudo-nitzschia* (Bacillariophyceae) species, domoic acid and amnesic shellfish poisoning: revisiting previous paradigms. *Phycologia* 51: 168-216.

Lewis, E. and Wallace, D.W.R. 1998. Program developed for CO_2 system calculations. ORNL/CDIAC-105. Carbon Dioxide Information Analysis Center, Oak Ridge National Laboratory, U.S. Department of Energy. Available at: http://cdiac.ornl.gov/oceans/co2rprt.html

Lohbeck, K.T., Riebesell, U., Reusch, T.B.H. 2012. Adaptive evolution of a key phytoplankton species to ocean acidification. *Nature Geoscience* 5: 346-351.

Low-Décarie, E., Fussmann, G.F., Bell, G. 2011. The effect of elevated CO_2 on growth and competition in experimental phytoplankton communities. *Global Change Biology* 17: 2525–2535.

Lundholm, N., Hansen, P.J., Kotaki, Y. 2004. Effect of pH on growth and domoic acid production by potentially toxic diatoms of the genera *Pseudo-nitzschia* and *Nitzschia*. *Marine Ecology Progress Series* 273: 1-15.

MacIntyre, H.L., Kana, T.M., Anning, T., Geider, R.J. 2002. Photoacclimation of photosynthesis irradiance response curves and photosynthetic pigments in microalgae and cyanobacteria. *Journal of Phycology* 38: 17-38.

Maldonado, M.T., Hughes, M.P., Rue, E.L., Wells, M.L. 2002. The effect of Fe and Cu on growth and domoic acid production by *Pseudo-nitzschia multiseries* and *Pseudo- nitzschia australis*. *Limnology and Oceanography* 47: 515–526.

Matsuda, Y. and Kroth, P.G. 2014. Carbon fixation in diatoms. In: Hohmann-Marriott, M.F. (Ed.). *The Structural Basis of Biological Energy Generation.* Springer Netherlands: 335-362.

McCabe, R.M., Hickey, B.M., Kudela, R.M., Lefebvre, K.A., Adams, N.G., Bill, B.D., Gulland, F.M.D., Thomson, R.E., Cochlan, W.P., Trainer, V.L. 2016. An unprecedented coastwide toxic algal bloom linked to anomalous ocean conditions. *Geophysical Research Letters* 43. doi:10.1002/2016GL070023.

McCarthy, A., Rogers, S.P., Duffy, S.J., Campbell, D.A. 2012. Elevated carbon dioxide differentially alters the photophysiology of *Thalassiosira pseudonana* (Bacillariophyceae) and *Emiliania huxleyi* (Haptophyta). *Journal of Phycology* 48: 635-646.

Millero, F.J., Woosley, R., Ditrolio, B., Waters J. 2009. Effect of ocean acidification on the speciation of metals in seawater. *Oceanography* 22: 72–85

Milligan, A.J., Varela, D.E., Brzezinski, M.A. Morel, F.M. 2004. Dynamics of silicon metabolism and silicon isotopic discrimination in a marine diatom as a function of pCO_2. *Limnology and Oceanography* 49: 322-329.

Milligan, A.J., Mioni, C.E., Morel, F.M.M. 2009. Response of cell surface pH to pCO_2 and iron limitation in the marine diatom *Thalassiosira weissflogii. Marine Chemistry* 114: 31-36.

Pan, Y., Rao, V.S., Warnock, R.E. 1991. Photosynthesis and growth of *Nitzschia pungens* f. *multiseries* Hasle, a neurotoxin producing diatom. *Journal of Experimental Marine Biology and Ecology* 154: 77-96.

Pan, Y., Rao, D.S., Mann, K.H., Li, W.K.W., Warnock, R.E. 1993. Temperature dependence of growth and carbon assimilation in *Nitzschia pungens* f. *multiseries*, the causative diatom of domoic acid poisoning. In: Smayda, T.J., Shimizu, Y. (Eds.). *Toxic Phytoplankton Blooms in the Sea*, Elsevier, Amsterdam: 619-624.

Pan, Y.L., Subba Rao, D.V., Mann, K.H. 1996a. Changes in domoic acid production and cellular chemical composition of the toxigenic diatom *Pseudo-nitzschia multiseries* under phosphate limitation. *Journal of Phycology* 32: 371–381.

Pan, Y.L., Subba Rao, D.V., Mann, K.H., Brown, R.G., Pocklington, R. 1996b. Effects of silicate limitation on production of domoic acid, a neurotoxin, by the diatom *Pseudo-nitzschia multiseries*: 1. Batch culture studies. *Marine Ecology Progress Series* 131: 225–233.

Pan, Y.L., Subba Rao, D.V., Mann, K.H., Li, W.K.W., Harrison, W.G. 1996c. Effects of silicate limitation on production of domoic acid, a neurotoxin, by the diatom *Pseudo-nitzschia multiseries*: 2. Continuous culture studies. *Marine Ecology Progress Series* 131: 235–243.

Pan, Y.L., Subba Rao, D.V., Mann, K.H. 1996d. Acclimation to low light intensity in photosynthesis and growth of *Pseudo-nitzschia multiseries* Hasle, a neurotoxigenic diatom. *Journal of Plankton Research* 18: 1427-1438.

Pan, Y.L., Bates, S.S., and Cembella, A.D. 1998. Environmental stress and domoic acid production by *Pseudo-nitzschia*: A physiological perspective. *Natural Toxins* 6: 127-135.

Pan, Y.L., Parsons, M.L., Busman, M., Moeller, P.D.R., Dortch, Q., Powell, C.L., Doucette, G.J. 2001. *Pseudo-nitzschia* sp. cf. *pseudodelicatissima* - a confirmed producer of domoic acid from the northern Gulf of Mexico. *Marine Ecology Progress Series* 220: 83–92.

Parkhill, J.P., Maillet, G., Cullen, J.J. 2001. Fluorescence-based maximal quantum yield for PSII as a diagnostic of nutrient stress. *Journal of Phycology* 37: 517-529.

Parsons, T.R., Takahashi, M., Hargrave, B. 1984. Biological oceanographic processes, 3rd edition. Pergamon Press, Oxford, UK: 330 pp.

Platt, T.P. and Gallegos, C.L. 1980. In: Falkowski P.G. (Ed.). *Primary Productivity in the Sea*. Plenum Press, New York: 339-351.

Raven, J.A. and Johnston, A.M. 1991. Mechanisms of inorganic carbon acquisition in marine phytoplankton and their implications for the use of other resources. *Limnology and Oceanography* 36: 1701-1714.

Raven, J.A., Evans, M.C., Korb, R.E. 1999. The role of trace metals in photosynthetic electron transport in O_2-evolving organisms. *Photosynthesis Research* 60: 111-150.

Reinfelder, J.R. 2011. Carbon Concentrating Mechanisms in Eukaryotic Marine Phytoplankton. *Annual Review of Marine Science* 3: 291-315.

Riebesell, U., Kortzinger, A., Oschlies, A. 2009. Sensitivities of marine carbon fluxes to ocean change. *Proceedings of the National Academy of Sciences of the United States* 106: 20602-20609.

Santiago-Morales, I.S. and García-Mendoza, E. 2011. Growth and domoic acid content of *Pseudo-nitzschia australis* isolated from northwestern Baja California, Mexico, cultured under batch conditions at different temperatures and two Si:NO_3 ratios. *Harmful Algae* 12: 82–94.

Shi, D., Xu, Y., Hopkinson, B.M., Morel, F.M.M. 2010. Effect of ocean acidification on iron availability to marine phytoplankton. *Science* 327: 676–679.

Smith, P. and Bogren, K. 2001. Determination of nitrate and/or nitrite in brackish or seawater by flow injection analysis colorimetry: QuickChem® Method 31-107-04-1-E. Lachat Instruments, Milwaukee, WI.

Sobrino, C., Ward, M.L., Neale, P.J. 2008. Acclimation to elevated carbon dioxide and ultraviolet radiation in the diatom *Thalassiosira pseudonana*: effects on growth, photosynthesis, and spectral sensitivity of photoinhibition. *Limnology and Oceanography* 53: 494-505.

Sun, J., Hutchins, D.A., Feng, Y., Seubert, E.L., Caron, D.A., Fu, F. 2011. Effects of changing pCO_2 and phosphate availability on domoic acid production and physiology of the marine harmful bloom diatom *Pseudo-nitzschia multiseries*. *Limnology and Oceanography* 56: 829–840.

Tatters, A.O., Fu, F-X, Hutchins, D.A. 2012. High CO_2 and silicate limitation synergistically increase the toxicity of *Pseudo-nitzschia fraudulenta*. *PLoS ONE* 7: e32116. doi:10.1371/journal.pone.0032116.

Tatters, A.O., Roleda, M.Y., Schnetzer, A., Fu, F., Hurd, C.L., Boyd, P.W., Caron, D.A., Lie, A.A.Y, Hoffmann, L.J., Hutchins, D.A. 2013. Short- and long-term conditioning of a temperate marine diatom community of acidification and warming. *Philosophical Transactions of the Royal Society B* 368: 20120437.

Taucher, J., Jones, J., James, A., Brzezinski, M.A., Carlson, C.A., Riebesell, U., Passow, U. 2015. Combined effects of CO_2 and temperature on carbon uptake and partitioning by the marine diatoms *Thalassiosira weissflogii* and *Dactyliosolen fragilissimus*. *Limnology and Oceanography* 60: 901-919.

Thorel, M., Fauchot, J., Morelle, J., Raimbault, V., Le Roy, B., Miossec, C., Kientz-Bouchart, V. Claquin, P. 2014. Interactive effects of irradiance and temperature on growth and domoic acid production of the toxic diatom *Pseudo-nitzschia australis* (Bacillariophyceae). *Harmful Algae* 39: 232-241.

Tortell, P.D. 2000. Evolutionary and ecological perspectives on carbon acquisition in phytoplankton. *Limnology and Oceanography* 45: 744-750.

Tortell, P.D., DiTullio, G.R., Sigman, D.M., Morel, F.M.M. 2002. CO_2 effects on taxonomic composition and nutrient utilization in an equatorial Pacific phytoplankton assemblage. *Marine Ecology Progress Series* 236: 37-43.

Tortell, P.D., Martin, C.L., Corkum, M.E. 2006. Inorganic carbon uptake and intracellular assimilation by subarctic Pacific phytoplankton assemblages. *Limnology and Oceanography* 51: 2102-2110.

Trainer, V.L., Wells, M.L., Cochlan, W.P., Trick, C.G., Bill, B.D., Baugh, K.A., Beall, B.F., Herndon, J., Lundholm, N. 2009. An ecological study of a massive bloom of toxigenic *Pseudo-nitzschia cuspidata* off the Washington State coast. *Limnology and Oceanography* 54: 1461-1474.

Trainer, V.L., Bates, S.S., Lundholm, N., Thessen, A.E., Cochlan, W.P., Adams, N.G., Trick, C.G. 2012. *Pseudo-nitzschia* physiological ecology, phylogeny, toxicity, monitoring, and impacts on ecosystem health. *Harmful Algae* 14: 271-300.

Trick, C.G., Bill, B.D., Cochlan, W.P., Wells, M.L., Trainer, V.L., Pickell, L.D. 2010. Iron enrichment stimulates toxic diatom production in high-nitrate, low-chlorophyll areas. *Proceedings of the National Academy of Science U.S.A.* 107: 5887–5892.

Trimborn, S., Lundholm, N., Thoms, S., Richter, K.W., Krock, B., Hansen, P., Rost, B. 2008. Inorganic carbon acquisition in potentially toxic and non-toxic diatoms: the effect of pH-induced changes in seawater carbonate chemistry. *Physiologia Plantarum* 133: 92-105.

Vincent, W.F. 1980. Mechanisms of rapid photosynthetic adaptation in natural phytoplankton communities. II. Changes in photochemical capacity as measured by DCMU-induced chlorophyll fluorescence. *Journal of Phycology* 16: 568-577.

Wells, M.L., Trick, C.G., Cochlan, W.P., Hughes, M.P., Trainer, V.L. 2005. Domoic acid: the synergy of iron, copper, and the toxicity of diatoms. *Limnology and Oceanography* 50: 1908-1917.

Wells, M.L., Trainer, V.L., Smayda, T.J., Karlson, B.S., Trick, C.G., Kudela, R.M., Ishikawa, A., Bernard, S., Wulff, A., Anderson, D.M., and Cochlan, W.P. 2015. Harmful algal blooms and climate change: Learning from the past and present to forecast the future. *Harmful Algae* 49: 68-93.

Welschmeyer, N.A. 1994. Fluorometric analysis of chlorophyll *a* in the presence of chlorophyll *b* and pheopigments. *Limnology and Oceanography* 39: 1985-1992.

Wright, J.L.C., Boyd, R.K., De Freitas, A.S.W., Falk, M., Foxall, R.A., Jamieson, W.D., Laycock, M.V., McCulloch, A.W., McInnes, A.G., Odense, P., Pathak, V.P., Quilliam, M.A., Ragan, M.A., Sim, P.G., Thibault, P., Walter, J.A., Gilgan, M., Richard, D.J.A., Dewar, D. 1989. Identification of domoic acid, a neuroexcitatory amino-acid, in toxic mussels from eastern Prince Edward Island. *Canadian Journal of Chemistry* 67: 481–490.

Wolters, M. 2002. Determination of silicate in brackish or seawater by flow injection analysis. QuikChem® Method 31-114-27-1-D. Lachat Instruments, Milwaukee, WI.

Wu, Y., Gao, K., Riebesell, U. 2010. CO_2-induced seawater acidification affects physiological performance of the marine diatom *Phaeodactylum tricornutum*. *Biogeosciences* 7: 2915-2923.

Yang, G. and Gao, K. 2012. Physiological responses of the marine diatom *Thalassiosira pseudonana* to increased pCO_2 and seawater acidity. *Marine Environmental Research* 79: 142-151.

Appendix I: Comparison of Microscopically Determined Cell Density Versus *In Vivo* Fluorescence During Exponential Growth of *Pseudo-nitzschia australis*

Background and Objective

In vivo fluorescence measurements of phytoplankton biomass are quick and simple to perform, however whole culture samples of the chain-forming diatom *Pseudo-nitzschia australis* produce relatively unstable *in vivo* fluorescence readings when grown under nutrient-replete conditions. Initially, this made it difficult to decide which numerical value of relative fluorescent unit (RFU) to record for any given sample of culture since the RFU value changed as a function of time while the sample was inserted into the fluorometer. This variability lead to inconsistencies in the RFUs recorded for a single sample by different lab personnel. Thus, it was questioned whether measuring RFU values over time were an appropriate measure for the determination of exponential growth rates of *P. australis* cultures. Given the obvious time advantage and simplicity in using RFUs compared to the more tedious and time-consuming approach of using a microscope to count cells, the following analysis was conducted to determine if RFUs measured over time could be used to monitor the growth of *P. australis* in batch cultures.

Methods

Three (n = 3) nutrient-replete replicate cultures of *P. australis* were grown at four different pH levels (8.1, 8.0, 7.9, 7.8), under the culturing conditions outlined on page 9 of the *Methods* section. At approximately the same time each day (12:00 h), whole culture samples were collected for determination of *in vivo* fluorescence, using a Turner Designs AU-10 fluorometer, and cell density using a 1-mL gridded Sedgewick-Rafter chamber and an inverted microscope equipped with a differential interference contrast (DIC) system (Olympus model IX83). When measuring RFUs, whole culture samples (8-9 mL) were collected from each treatment in 10-mL borosilicate disposable culture tubes (Fisher Scientific) and allowed to sit in the dark for ca. 2 minutes before being gently inverted 3-4 times and placed inside the fluorometer. For cell counts, whole culture samples (1.5 mL) from each treatment were preserved with acidic Lugol's solution (2.5% v/v final concentration) and stored in the dark at ca. 5°C until analyzed. A minimum of 1,000 cells per sample were counted to ensure reliable abundance estimates; 1,000 counts per sample yield estimates of total cell abundance with an accuracy (95% confidence limit) between ± 5% and ± 10% (Guillard and Sieracki 2005). Specific growth rates were calculated with the exponential growth equation (Guillard 1973) using a least-squares linear regression analysis of the exponential growth phase, determined from semi-log plots of the natural log of cell density and *in vivo* fluorescence versus time. Statistical differences between the growth rates

calculated using RFUs and cell density, within pH treatments, were determined using a paired sample *t*-test. The level of significance (α) was set to 0.05, and *t*-tests performed using KaleidaGraph© statistical software (Synergy Software, Reading, PA, USA).

Results and Conclusions

The daily increases in cell density and *in vivo* fluorescence of the *P. australis* cultures are shown in Figure A.1. On day 1, cell densities and RFUs were relatively low for all cultures (generally < 100 cells • mL^{-1} and < 1 RFU), and these data were not included in the growth rate calculations due to a lack of confidence in their accuracy and to account for any potential lag phase that may have occurred after culture transfers. The average (mean ± 1 SD) specific growth rates of the four pH treatments, determined using cell density and RFUs are listed in Table A.1. In the three lowest pH treatments (8.0, 7.9, 7.8), growth rates determined from RFUs resulted in slightly, but insignificantly ($p \geq 0.05$) greater specific growth rates compared to the rates calculated using cell densities over time. However, in the pH 8.1 treatment, RFUs resulted in a statistically significant higher growth rate ($p = 0.02$) compared to direct microscopic counts, although the average percent difference between the growth rates was small (5.2 ± 1.1%). Additionally, a strongly significant ($p < 0.0001$) linear relationship was observed

between RFUs and cell density when the data from all the pH treatments were combined ($r^2 = 0.9925$; Figure A.2). Therefore, it is clear that RFUs can be used to provide an accurate measure of the specific growth rate in cultures of *P. australis* during exponential growth, and offer a quick and practical alternative method for actively monitoring growth when cell counts cannot be conducted in a timely manner.

It should be noted that all RFU measurements in the present study were performed by a single investigator, due to the unstable RFU readings generated over time by the fluorometer for any sample of *P. australis* culture. Prior experience demonstrated that results often became highly variable when more than one investigator was responsible for conducting the *in vivo* measurements. Microscopic analysis of live whole culture samples of *P. australis* revealed that these cells were found both singularly and in a wide range of chain lengths, frequently as long as > 50 cells. The instability of RFUs provided by the fluorometer was likely due to variations in the number of cells per chain present in a given volume of water. This would result in a highly variable number of cells passing through the excitation beam of the fluorometer at any given time, contributing to the unstable RFU readings observed during this study.

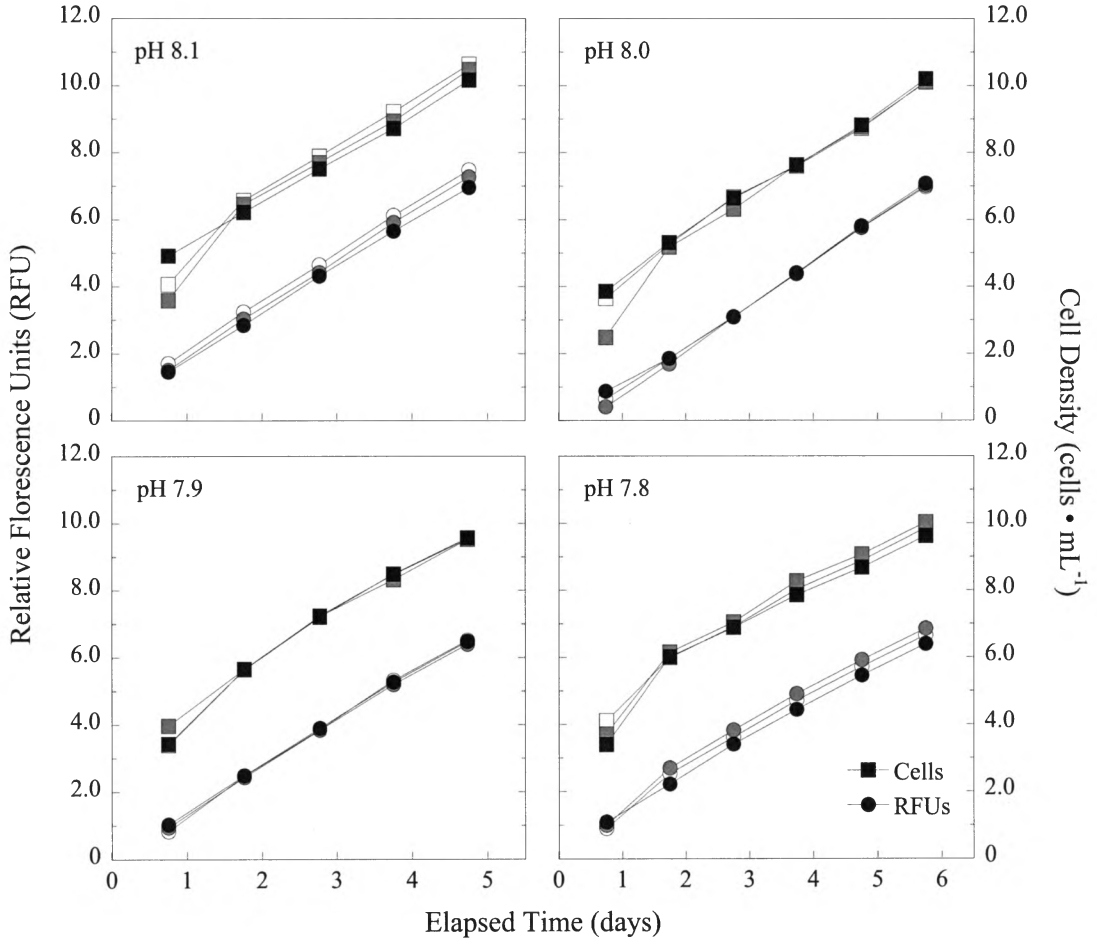

Figure A.1. Exponential growth curves of triplicate batch cultures of *P. australis* for the four pH treatments. Semi-log plots of cell density (■) and *in vivo* fluorescence (●) versus time. Note: all RFU values were multiplied by 10 before being log transformed (i.e., ln [RFU x 10]).

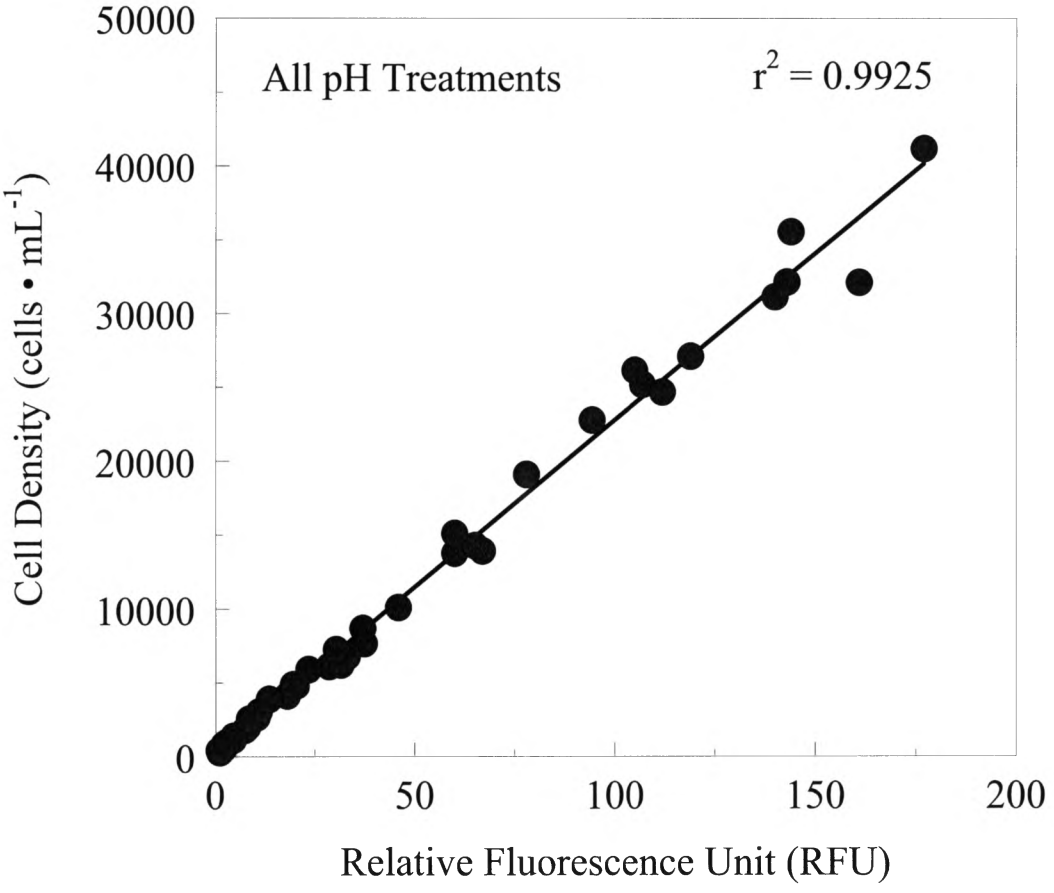

Figure A.2. Linear relationship between relative fluorescence units (RFU) and cell density (cells • mL^{-1}) combined from the triplicate *P. australis* cultures for all pH treatments (n = 12; i.e., 4 pH treatments x 3 cultures per treatment). Fifty-three (n = 53) values are plotted, and the data are the same values used to calculate the exponential growth rate for each culture (i.e., data from day 1 were excluded).

Table A.1. Exponential growth rates (μ; d^{-1}) calculated for *P. australis* cultures in the four pH treatments using cell density and relative fluorescence units (RFU). The percentage difference between these separate measurements and the *p*-value from a paired *t*-test comparing are listed. Reported values are the means of triplicate ($n = 3$) cultures and parenthesis indicate ± 1 SD.

pH Treatment	μ Cell Density	μ RFU	% Difference	*p*-value (paired *t*-test)
8.10	1.33 (± 0.02)	1.41 (± 0.03)	5.4 (± 1.1)	0.02
8.00	1.26 (± 0.03)	1.32 (± 0.02)	4.2 (± 3.5)	0.19
7.90	1.30 (± 0.02)	1.35 (± 0.02)	3.6 (± 1.5)	0.05
7.80	0.95 (± 0.04)	1.04 (± 0.01)	8.4 (± 4.1)	0.07

Appendix II: Comparison of pH Determination: Glass Electrodes Versus Spectrophotometer Readings.

Background and Objective

Phytoplankton culturing studies often measure pH using either a glass/reference electrode (pH probe) or a spectrophotometer with a 10-cm cell. However, the use of these two different approaches makes direct comparisons between studies problematic, as the pH values are reported on different pH scales depending on the method employed. For example, the pH probes used in this study were calibrated (see below) using National Bureau of Standards (NBS)/National Institute of Standards and Technology (NIST)-traceable buffers, which means that all pH measurements are reported on the NBS scale (mols $H^+ \cdot kg^{-1}$ of H_2O). However, the spectrophotometric method outlined by Dickson et al. (2007), determines the pH of seawater using the total hydrogen ion pH scale (mols $H^+ \cdot kg^{-1}$ of seawater). As a result, the pH of a given volume of seawater (temp 20°C; salinity 35) measured on the total pH scale can be ca. 0.13 units lower than the value measured on the NBS scale (Lewis and Wallace 1998). This discrepancy arises from the fact that measurements on the NBS scale are calibrated using calibration buffers that have a low ionic strength compared to seawater and thus are not the recommended scale for use with seawater pH measurements (Dickson 1984; Dickson 1993; Dickson et al. 2007). The following

analysis was conducted to determine the differences between pH values measured with glass pH probes (NBS scale) from those determined with a spectrophotometer (total pH scale).

Methods

Three (n = 3) nutrient-replete replicate cultures of *P. australis* were grown at four different pH levels (8.1, 8.0, 7.9, 7.8), under the culturing conditions outlined on page 9 of the *Methods* section. Additionally, a more detailed description of how the pH in each culture was monitored and controlled during the experiment can be found on pages 14-16 of the *Methods* section and on page 29 in Figure 1. The pH of each culture was continuously monitored using a glass pH probe (Sentix® 41-3; Wissenschaftlich-Technische Werkstatten [WTW]) connected to a pH meter (model 3310, WTW), which was connected to and monitored by a PC computer (equipped with CapCTRL software, version 1.3.2). Each pH probe was calibrated (3-point calibration) at the beginning of each batch cycle using National Bureau of Standards (NBS)/National Institute of Standards and Technology (NIST)-traceable buffers (Fisher color-coded certified standard buffer solutions; pH 4.00, 7.00, and 10.00; Catalog No. SB105). Thus, all pH measurements taken with these pH probes were determined on the NBS scale.

The pH of each culture was also determined spectrophotometrically (Agilent model 8453 UV/visible spectrophotometer) using the indicator dye (*m*-cresol purple) method (SOP 6b) as outlined by Dickson et al. (2007) in: *Guide to the best practices for ocean acidification CO_2 measurements*. All pH measurements using this method are reported on the total pH scale. However, preliminary measurements carried out at 25°C resulted in pH values (total scale) that were ca. 0.25-0.30 pH units lower than those recorded using the pH probes (NBS scale). pH of seawater is temperature sensitive, and since the pH probes are continuously immersed within each culture flask during the experiment, the pH values will be directly influenced by the temperature of each culture. Although the culture incubators were set to 13°C, the average temperature of each culture measured ca. 13.5°C. Therefore, it was decided to maintain the samples for the spectrophotometric pH method at a temperature of 13.5°C, in order to better compare these results with those of the pH probes. However, this was decided after running a preliminary test using the pH 8.1A and 8.0A cultures only (Table A.3), so results reported for these two pH treatments came from a single triplicate culture conducted at 13.5°C. The results for the pH 7.9 and 7.8 treatments were calculated using samples from each triplicate flask (Table A.3). Whole culture samples were collected in analytical duplicates (2 x 50 mL per triplicate culture) in acid-clean centrifuge tubes (Corning™, Tewksburty, MA, USA) without headspace

and centrifuged at 4,000 g for 5 min at the approximate same temperature of the culture media (13.5°C). The supernatant (seawater without *P. australis* cells) was then carefully poured into a separate centrifuge tube and immediately placed in a water bath at 13.5°C. These samples were then measured spectrophotometrically, equipped with a 10-cm path-length cell, using the indicator dye method outlined by Dickson et al. (2007).

Results and Conclusions

The results for both pH methods are listed in Table A.3. As predicted, the spectrophotometric method (total pH scale) consistently resulted in lower pH values compared to measurements made using the pH probes (NBS scale) and these differences ranged from 0.07 – 0.12 pH units (Table A.3). Numerically, this is not a large difference, however, because the pH scale is logarithmic, a change of 0.1 pH units is equivalent to an approximate 26% increase in acidity. Therefore, every pH treatment tested in this study was maintained at a slightly lower pH value than intended. However, the differences observed between the two pH measurements were generally very similar among treatments. This indicates that the general purpose of this study was still achieved, in that four distinct pH treatments of increasing acidity (reduced pH) were used. Thus, although the spectrophotometric pH measurements do show that pH was lower than intended,

the results of this study remain valid since the pH gradient among treatments was achieved.

Table A.4. Comparison of the pH values measured with a pH probe (NBS scale) versus those measured with a spectrophotometer (Total scale) at 13.5°C. An asterisk indicates that measurements were only made from a single culture ($n = 1$). All other reported values are the means of triplicate cultures ($n = 3$) ± 1 standard deviation (± SD).

pH Intended	pH Probe (NBS Scale)	pH Spec. (Total Scale)	Difference
8.10-8.15	8.15 *	8.08 *	0.07
8.00-8.05	8.04 *	7.92 *	0.12
7.90-7.95	7.94 (± 0.01)	7.83 (± 0.02)	0.11 (± 0.02)
7.80-7.85	7.83 (± 0.01)	7.72 (± 0.01)	0.11 (± 0.01)

Appendix III: Standard Operating Procedure for Performing Photosynthesis Versus Irradiance (P vs. E) Measurements using ^{14}C

Original: *circa* 2003 (W.P. Cochlan)
Revision: March 21, 2007 (J. Betts)
Latest Update: May 08, 2017 (C. Wingert)

Overview/Purpose:

The radioisotope ^{14}C is used to determine the rate of photosynthetic carbon fixation by phytoplankton cells during photosynthesis vs. irradiance (P vs E) experiments. Such experiments are short in duration (0.5 - 1 h), and are conducted within temperature-controlled photosynthetrons. They must only be performed within a radiation-designated region of the laboratory or within a radioisotope van when at sea. This method depends on the hypothesis that the rate of photosynthesis is proportional to the amount of ^{14}C-labeled inorganic carbon incorporated into particulate organic carbon within phytoplankton cells, over the incubation time (0.5 – 1 hour). The procedure requires that the experimentalist is trained and approved to handle radioisotopes, all appropriate PPE is worn by the experimentalist, and s/he, employs a functioning fume hood (to fume off excess unincorporated ^{14}C following the designated incubation period), and a liquid scintillation counter: 1) to analyze samples for incorporation of ^{14}C into particulate material – the phytoplankton, and 2) to ensure the working area is not

contaminated by accidental spillage of radioisotope by performing routine 'wipe tests'.

Personal Protective Equipment (PPE), Safety, and Waste Disposal:

Read MSDS for all listed chemicals and follow the recommendations for Personal Protective Equipment (PPE). Ensure safe handling and disposal of waste by adhering to all Federal, State, and University regulations.

1. Disposable lab coats must be worn at all times with appropriate footwear (closed-toed shoes, which should also be covered with "booties" while at sea).

2. Gloves (nitrile or neoprene; NOT latex) are to be worn at all times when handling radioisotopes; rings must be removed prior to donning gloves. Double gloving is advised when handling undiluted stocks of radioisotopes.

3. Safety glasses or goggles must be worn at all times and these should be used exclusively for radioactive work and labeled appropriately.

4. Bench tops in the radioactive-designated work-space should be covered with two layers of 'paper/plastic benchtop' covering (plastic, shiny side down), which needs to be taped down to the bench tops.

5. Any scintillation vials or sample bottles must be placed on benchtop-covered plastic trays used exclusively for radiation work.

6. Active Radiation area to be designated, "off-limits" to all except authorized users and this space should be appropriately labeled with "radioactive" signage and stickers.

7. There should be dedicated forceps, pipettors, tips, and glass-fiber filters (GF/F) filters for isotope use only, and these must be labeled with the appropriate radioactive stickers.

8. All venting on unincorporated ^{14}C in samples MUST be conducted within a running fume hood, in properly secured trays of scintillation vials.

9. Ensure there are properly secured (and labeled) bags and/or receptacles for all ^{14}C dry-waste. ANYTHING disposable that is potentially "hot," should always go into dry waste; however, it's important to keep in mind that radioactive dry waste is rather expensive to dispose of, so don't throw away non-hot items into your radioactive dry waste!

10. When at sea, it is important to have a designated notebook that stays in the rad van at all times, which will be considered "hot". At the end of each day, copy all your notes from this "hot" notebook to a "non-hot" notebook that you keep in your cabin or the main lab area. At the end of your time at sea, dispose of your "hot" notebook into dry-waste.

11. No foods or consumable liquids are permitted in radioactive work-spaces.

12. Liquid scintillation cocktail should be stored and secured within fume hood.

Supplies/Apparatus:

- Photosynthetrons (PS) including but not limited to: two (2) units, two (2) extra halogen bulbs, an assortment of tinted plastic tiles (1 in^2), screening, tape, glass plate and plexiglass plate, (7) gray L-joint supports

- Water circulation bath(s) including: four (4) tubes for circuit to PS, zip ties, two (2) electrical cords, at least four (4) spigot and closure ends [metal], and instrument manual

- Multiple, small 2x2 inch pieces of wood for properly securing all equipment, trays, etc. to tabletops within the rad van

- Sticky-back velcro (1-2 rolls) for properly securing sample bottles, HCl bottle, pipet tip box, etc

- Two (2) Light-green containment trays for work area

- Two (2) Plastic vial staging racks [left and right]

- Two (2) Repeator pipettors [one for ^{14}C dispensing and one for sample/HCL dispensing], including: Eppendorf canisters (2.5 mL and 25 mL), and appropriate adapters to connect canisters to pipettors

- One (1) P100 pipettor and One (1) P1000 pipettor (RAD USE ONLY) and corresponding tips

- One (1) Small white rectangular tray to house P-100 and ^{14}C repeator pipettor

- Several 50 mL low-density polyethylene (LDPE) centrifuge tubes ('Orange Tops' made by Corning) to be used as tip waste containers

- Five-ten (5-10) boxes of (500 each) of 25-mL glass scintillation vials (Fisher Scientific) with cone lids—overall quantity will depend on the estimated number of incubations to be performed while at sea

- Colored circular stickers for labeling caps of scintillation vials

- Light meter (for light calibration of PS), digital thermometer (to measure accuracy of temperature maintained by water circulation baths), and extra 9V batteries for both

- Scintillation fluid (Ecolume; MP Biomedical LLC) comes in 1 gal containers; 5-10 gal needed, depending on work load; including Dispenser for Ecolume (actual compartment, hard plastic tube and soft tubing, connector to Ecolume container)

- Three-four (3-4) Tripour beakers for HCL/Ecolume waste, office supply container for holding pens, pencils, etc

- "Radiation warning" stickers/labels for identifying "hot" equipment, containers, waste, etc

- 250 mL "10% HCL" clear bottle

- Wooden rack for separation of degassing ^{14}C samples in fume hood

- Two (2) files for opening ^{14}C ampules (stock isotope)

- One-two (1-2) concentrated ^{14}C in 5-mL ampules (sodium bicarbonate with 5μCi/mL ^{14}C)

- Two-four (2-4) 20-mL Teflon bottles filled with 20 g of ESAW (no enrichments, just salts!) used to create dilute working stock of ^{14}C stock for experimentation

- Appropriately thick bag(s) for dry-waste, and a receptacle for holding dry-waste bag(s) in place

- Three-four (3-4) Large necked darkened 250-mL bottles for samples

- Stopwatch/timer for recording incubation times

- Whatman GF/F filters and forceps (labeled as radiation use ONLY) for conducting routine wipe tests

A copy of this SOP should be kept in the rad van at all times, along with a condensed, single paged "Method Check List" (see the last page of this SOP), which should be placed on a wall in the rad van or workspace where ^{14}C incubations are being conducted.

Procedure:

A. Preparing ^{14}C working stock solutions:

1. When ^{14}C is initially received from a manufacturer (generally in 5.0 mL ampules), it is concentrated (1.0 mCi $\cdot$ mL^{-1}), and thus is EXTREMELY HOT (radioactive), and must be diluted into "working stock" solutions before P v E experiments can be conducted.

   This portion of the procedure poses the greatest hazard to the investigator, so extreme caution must be taken to ensure proper safety and therefore all appropriate PPE should to be worn at all times. If you have never opened a concentrated vial of ^{14}C, DO NOT attempt to open it yourself, and ask an experienced lab member/advisor for assistance.

2. As soon as ^{14}C is received from the manufacturer, a thorough wipe test must be conducted on all shipping materials, including the exterior and interior of the

various boxes, as well as the exterior of the white plastic containers that house each individual ampule of concentrated ^{14}C.

3. Each ampule contains a total volume of ~5.0 mL of ^{14}C, which needs to be split in half (2.5 mL) and diluted into two (2) separate "working stock" solutions.

4. These "working stocks" are created by diluting the concentrated ^{14}C with artificial seawater (ESAW—JUST SALTS, NO nutrient enrichment; for ESAW recipe, see pg. 494 in *Algal Culturing Techniques* ed. Anderson R.A. [2005]). Therefore, before opening any ^{14}C containers, ESAW must be made ahead of time.

5. Once ESAW has been made, fill two acid-cleaned 25-mL Teflon bottles with 20.0 g of ESAW each (using a balance). Immediately label these bottles as working stock #1 or #2; write the amount of concentrated ^{14}C to be added to each (2.5 mCi), date, and sign your initials. Also, apply radioactive stickers on both the cap and side of the bottle. Place these bottles into two (2) plastic bags and store them in the fridge if ^{14}C will not be added that day, and in a rad fridge once prepared.

6. Organize your radioactive work station before opening the ^{14}C ampule to ensure everything needed to conduct the dilutions is immediately available (labeled Teflon bottles filled with ESAW, pipettors, tips, metal file, waste containers, Kim Wipes (Kimberly-Clark), and an emergency clean-up kit in case of a spill).

7. Carefully remove an ampule of ^{14}C from its shipping container, and thoroughly inspect the glass to ensure that there are no cracks/leaks. Place the vial on its side within a 'Kay Dry' lined tray and grab a metal file.

8. With the metal file in one hand and the ampule of ^{14}C in the other, gently begin etching around the top of the ampule in a circular motion. This will help create a "perforation," which allows the top of the ampule to be broken off so you can remove the ^{14}C. It's important to keep in mind that you'll be extracting the ^{14}C with a P-1000 pipette, so create an etch on the ampule that will allow for a P-1000 tip to be inserted once the top is broken off.

9. When the ampule has been adequately etched, use two hands to snap the top of it off. This should snap easily if the glass has been etched appropriately, so if it doesn't break on the first attempt, continue etching the glass with the file

until it does. Again, do not attempt this step on your own if you have not done it before!

10. Using a P-1000, pipette a total 2.5 mL of ^{14}C from the ampule to each of the two (2) Teflon bottles filled with 20.0 g of ESAW. Remember, the total volume of ^{14}C within the ampule is only ~5.0 mL, so simply split it between the two Teflon bottles filled with ESAW, but record the exact volume added to each bottle. Cap each of the bottles and invert them several times to ensure they are well-mixed. Place each bottle into two (2) plastic bags and store them in an appropriate container within the radiation fridge.

11. There will likely be some residual ^{14}C remaining in the ampule, so transfer this to the fume hood (ensure it is turned on!), add 1.0 mL of 10% (v/v) HCl acid, gently swirl, and allow it to degas for 12-24 h before disposing of it in the appropriately labeled waste container.

12. Once finished, be sure to update the lab's radioactive work binder to indicate that new working stocks have been made. This is extremely important because the university and state of CA often send inspectors to check our records so ALWAYS log your radioactive work the day it was conducted.

B. Before beginning P v E incubations:

Prior to starting any P v E experiments, an investigator must first determine an appropriate range of light levels (PPFDs) to be used within the photosynthetron (PS) during the incubation. Each well within the PS is numbered (see diagram below) and the light intensity within each well can be adjusted using various shades of neutral density filters, to wrap the square plastic tiles that are situated at the bottom of each individual well. To measure the PPFD within a specific well, the spherical tip of a 4π quantum scalar irradiance collector (QSL-100 meter, Biospherical Instruments Inc.) must be immersed within a medium-filled scintillation vial and held as straight as possible (perpendicular to the light source). It's also important to make sure there are no overhead lights on in the room while measuring PPFDs within the PS because these will have an impact on your readings. Allow the PS to warm-up for ca. 30 minutes before taking any light measurements.

Wells #1 and #15 are always your "**dark**" wells, so these should have no light coming from below. Any of the remaining wells can then be used to create an

appropriate light curve for the incubations. Keep in mind, it's important to have a good "spread" of different PFFDs and ensure that no two light levels are too close together. For example, working with laboratory cultures of the diatom *Pseudo-nitzschia australis*, C. Wingert used PPFD's ranging from 0 -1,000 µmol photons • m^2 • s^{-1} (5.0, 14.0, 24.0, 53.0, 72.0, 84.0, 105, 145, 230, 360, 420, 540, 700, 1000). The location of these PPFDs within the various wells of the PS is depicted in the diagram below:

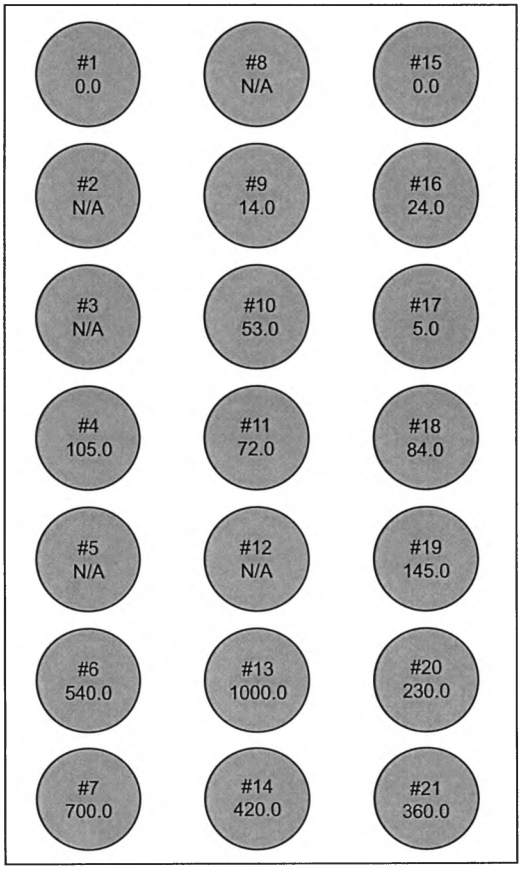

C. Preparing for a P v E incubation:

1. The photosynthetrons and water baths should be turned on at least 30 minutes prior to conducting any of the following procedures.

2. Verify correct temperature of the water baths and adjust accordingly. The temperature should be as close to the experimental or ambient sea temperature

as possible (check daily). Maintaining the correct temperature is very important, so ensure to record any temperature changes in your notebook.

3. The temperature displayed on the water baths is NOT the temperature within the photosynthetron! The temperature within the photosynthetrons tends to be ca. 2 °C warmer than the water baths due to the heat from the light source. Place a water-filled scintillation vial in an unused well and check the temperature using a digital thermometer.

4. Preliminary check for needed equipment/apparatus:

   PPE: googles/safety glasses, disposable lab coats, gloves

   Lab mat (Kay Dry) in work station(s)
   P-100 pipettor and tips

   Two repeater pipettors with:
   (a) 2.5-mL canisters (for ^{14}C inoculation; tip placed in 50-mL waste container)
   (b) 25-mL canisters (for sample and HCl acid distribution)

   Waste containers (50-mL orange top conicals and tri-pour beakers)

   250-mL bottle of 10% (v/v) HCl acid

   Kim Wipes

   Stop watch/timer

   Two plastic staging racks

   Staged glass scintillation vials (ensure they fit into the photosynthetron wells)

   Lab book.

5. The easiest way to keep track of samples is to set up a labeling system that includes: date, experiment name, treatment (if applicable), photosynthetron (left/right) and well number. Capping samples is the final step prior to beginning an incubation, so pre-labeling is key. Pre-staging vials and labels shortens the time between incubations. Make sure to stage two extra vials in addition to your sample amount for "Kills" or blanks.

D. To Begin the Incubation:

1. After inverting the sample bottle/rinsing the 25-mL canister with sample, aliquot exactly 5 mL of sample into each staged vial using a repeater pipettor

(setting #5, two shots of 2.5 mL).

Make sure to dispense the sample slowly and against the side of the vials to avoid breaking the cells.

2. Prepare two glass scintillation vials, pre-labeled and capped, with 20 mL of scintillation fluid (Ecolume) and place in the empty staging rack. These are "**Totals**" and will not be placed in the photosynthetron for incubation with samples.

3. After staged samples are placed in the work area, remove ^{14}C working stock solution from refrigerator and place in contained area in work station; isolate if possible. Before opening ^{14}C, place tip on the P-100 pipettor and loosen caps of waste containers to shorten exposure time to the isotope. Loosen cap of ^{14}C working stock solution, and attach a 2.5-mL canister to repeat pipettor.

   Remember that after the first use, this canister is extremely HOT, and should not touch anything but the inside of the waste container or the isotope. Handle with extreme caution.

4. With the 2.5-mL canister on the pipettor, remove the cap from ^{14}C and aliquot **50 uL** of ^{14}C into each sample (setting #1; one shot). Without tilting the pipettor, dispense ^{14}C directly into the vial to eliminate any fluid against the sides.

   Note: If trying to conserve the amount ^{14}C used, it's possible to add less isotope per vial provided that preliminary experiments are conducted first to determine if adding different isotope amounts significantly affects the calculated C uptake rates.. At sea, C. Wingert used the standard 50 µL volume addition, but in laboratory experiments with P. australis*, only 40 µL was added to each vial. However, it's also important to note that 5 mL of culture sample was always used, both at sea and in the laboratory experiments.*

5. RECORD INNOCULATION TIME (T_o)

6. Swirl vials (to mix sample with ^{14}C) now designated as "**Darks**" (placed in lowest light levels, well #1 and #15, in incubation). Using the P-100 pipettor, remove a 100-uL subsample from one vial and place it into a previously prepared "**Total**", place a 100-uL subsample from the remaining sample vial into the second "**Total**."

Each total should contain 100 uL of subsample from the corresponding "**Dark**," representing the total amount of ^{14}C added to each sample.

7. With the photosynthetron lamps shut off, cap and place the "**Darks**" into wells #1 and #15. Swirl, cap, and place each remaining sample into its designated well. Secure photosynthetron lid, turn on lamps.

8. RECORD INCUBATION START TIME ($T_{initial}$).

   Incubation times may vary; with low biomass it is suggested to incubate for one hour, rather than the standard 0.5 hour duration.

9. The two remaining vials containing sample and ^{14}C are now designated as "**Kills**." After beginning the incubation (above), take **"Kills"** along with the **"Totals"** and place them inside the fume hood in their designated rack.

10. Using a 25-mL canister (with the repeat pipettor used to dispense sample), add **0.5 mL** 10% HCl to each **"Kill"** [setting #1; one shot]. Adding HCl to the sample converts the ^{14}C to $^{14}CO_2$, potentially releasing all the ^{14}C from the sample, which, after degassing, represents any ^{14}C that might stick to the outside of the cells, or the blank.

11. At the end of the incubation, shut off the lamp.

12. RECORD END TIME (T_{final})

13. Transfer the sample vials from the photosynthetron to the staging rack, keeping in mind that the samples are now designated as their well number. <u>It is very important to keep track of the order</u>. Place the samples in their designated slots in the fume hood rack, remove caps and keeping track of their order/well number, place them into a plexiglass holder. Next, add 0.5 mL of 10% HCl acid to each sample (as done with **"Kills"**). Allow samples to degas for 12-24 hours within the fume hood (turned on at all time).

14. After the 12-24 hour period of degassing, add **15 mL** (two shots of 7.5mL) Ecolume scintillation fluid to the **"Kills"** and the sample vials, and cap accordingly with their designated well numbers. After the addition of scintillation fluid, it is advisable to wait ~12 hours before reading samples in a liquid scintillation counter.

15. Light levels should be checked each day to make sure there is little variation in the calculated range from previous recordings. This is done at the end of the day after all experiments have taken place. The recorded light levels for that day are used for each set of data analysis.

16. At the end of the day, be sure to update the lab's radioactive log binder with all the necessary information regarding the work that was done. Again, this is very important to do so if you have questions about how to properly record this information, don't be afraid to ask!

Calculations:

The results from the liquid scintillation counter will provide both CPMs and DPMs for each of your samples. However, only the DPM values are used for the calculation of photosynthetic carbon fixation rates using the following equations:

$$P = \frac{(DPM_{sample} - DPM_{darks}) * DIC * 1.05}{DPM_{added} * t} \quad (1)$$

$$DPM_{added} = \frac{(DPM_{totals} * \text{sample volume})}{\text{subsample volume}} \quad (2)$$

where: P = Photosynthetic carbon fixation rate ($\mu g\ C \cdot L^{-1} \cdot h^{-1}$)
DPM_{sample} = DPM of a particular sample vial
DPM_{darks} = Average DPM of your two "**Dark**" sample vials (wells #1 and #15)
DIC = Dissolved inorganic carbon concentration ($\mu g \cdot L^{-1}$)
1.05 = isotopic discrimination factor
t = Incubation time in hours (usually 0.5 – 1 h)
DPM_{totals} = average DPM of your two "**Total**" sample vials

(Note: 5 μCi = 1.11×10^7 dpm)

Sample volume (in mL) = volume of culture added to the vial (5.0 mL)
Subsample volume (in mL)= volume taken from "**Dark**" vials and pipetted into the "**Total**" vials (0.1 mL or 100 uL)

Using this equation, P is calculated for each sample vial, incubated at a specific irradiance, in the P v E experiment. The P data for every sample is then normalized to either, cell density, POC, or chlorophyll *a* concentration and graphed as a function of their incubation irradiance. C-uptake rates normalized to one of these biomass indices (P^B) should look similar to this:

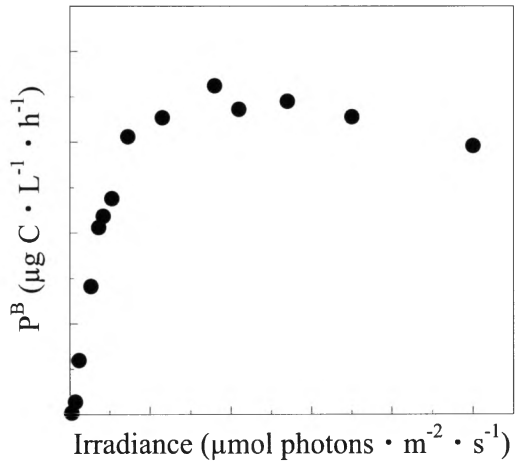

For curve fitting, use the 3-parameter P-E model of Platt and Gallegos (1980), which is described in detail on pg. 18. If done correctly, the curve should now look similar to this:

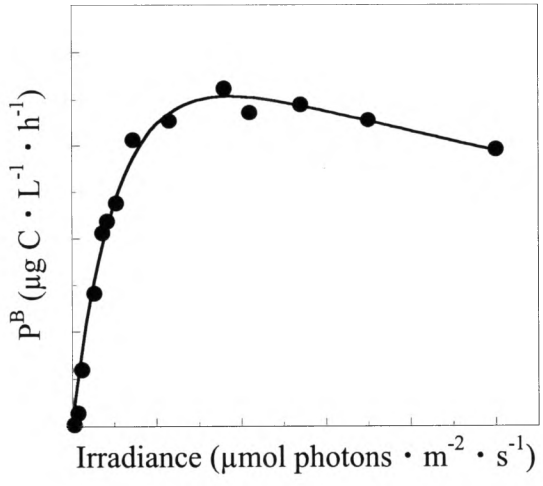

Values of P are always normalized to a specific biomass parameter, such as Chl *a* (μg Chl *a* · L^{-1}), cell density (cells · L^{-1}), or particulate carbon (μg C · L^{-1}). This is accomplished by simply dividing each of your calculated values of P (from equation 1) by one of these normalization parameters (chlorophyll, cell density or particulate carbon concentration to obtain either P^{chl}, P^{cell} or P^{C}, respectively prior to plotting the data as a function of irradiance).

P vs. E (Photosynthetron) Method Check List

- Preliminary check for: lab coats, goggles, gloves (double if hot, single if not), adequate waste receptacles, tips, water, HCl, etc
- Turn on water circulators and lamps, verify correct temp ^{o}C
- Get samples in darkened 250-mL polycarbonate bottles
- Lay down lab mat inside green tray at work station
- Aliquot **5.0 mL** of sample using Repeator Pipettor to 18 vials in rack; using 25 mL=V_{total} syringe, pipette two shots of 2.5 mL (**setting = 5**)
- Prepare two scintillation vials filled with 20-mL of EcoLume each, label these as "**totals**" and place in rack
- Remove ^{14}C from fridge and place in empty slot of rack
- Pipette (DIRECTLY into sample without touching the walls of scint vial) **50 µL** of ^{14}C into each of the 18 vials; using Repeator Pipettor with 2.5 mL=V_{total} syringe, pipette one shot of 50µL (**setting=1**), and **RECORD TIME OF INNOCULATION (T_{int})**
- Cap vials and invert to mix
- Take **100 µL** subsample from each "**dark**" vial, place into previously prepared "totals" (vials with 20-mL of scint fluor)
  - Cap and place in designated slots in fume hood (for 24 hr.)
- Turn off lamps before adding vials to incubator
- Place experimental vials + "**darks**" (16 vials total) into incubator
- Turn on lights and **RECORD TIME (T_0)**
- For the two (2) "**kill**s" vials, add **0.5 mL** of HCl (10%) (25 ml canister; one shot, **setting #1**) from 250 mL stock bottle to each of them (once moved to hood); uncap-degas (24 hr)
- Incubate vials in PS for appropriate time, turn off lights, and **RECORD TIME (T_{final})**
- Transfer vials to hood to correct slots; uncap
  - Add **0.5 mL** (10% v/v) HCl to vials in fume hood
  - Allow to degas for 24 hrs with fume hood ON
- Add scint fluor (15 mL) to degassed vials
  - Cap and store for transport (once container is full [100 vials] put in plastic bag, back in to original box)